UNIVERSIDADE DE SANTIAGO DE COMPOSTELA

FACULTADE DE FARMACIA

DEPARTAMENTO DE FARMACIA E TECNOLOXÍA FARMACÉUTICA

Tese de Doutoramento

NANOCÁPSULAS POLISACARÍDICAS COMO VEHÍCULOS ADYUVANTES DE VACUNAS

Sara Vicente Ozores

Santiago de Compostela, 2013

Diseño portada: Pepe Potel

DONA MARÍA JOSÉ ALONSO FERNÁNDEZ E DON ALEJANDRO SÁNCHEZ BARREIRO, CATEDRÁTICA E PROFESOR TITULAR, RESPECTIVAMENTE, DO DEPARTAMENTO DE FARMACIA E TECNOLOXÍA FARMACÉUTICA DA UNIVERSIDADE DE SANTIAGO DE COMPOSTELA,

INFORMAN:

Que a presente Memoria Experimental titulada: "Nanocápsulas polisacarídicas como vehículos adyuvantes de vacunas", elaborada por Sara Vicente Ozores, foi realizada baixo a súa dirección e no Departamento de Farmacia e Tecnoloxía Farmacéutica e, estando concluida, autorizan a súa presentación a fin de que poida ser xulgada polo tribunal correspondiente.

E para que conste, expiden e firman o presente certificado en Santiago de Compostela, o 30 de xaneiro de 2013.

Fdo. María José AlonsoFernández Fdo. Alejandro Sánchez Barreiro

Aos meus pais

Á miña familia

Looking beyond the embers of bridges glowing behind us
To a glimpse of how green it was on the other side
Steps taken forwards but sleepwalking back again
Dragged by the force of some inner tide

At a higher altitude with flag unfurled
We reached the dizzy heights of that dreamed of world

Encumbered forever by desire and ambition
There's a hunger still unsatisfied
Our weary eyes still stray to the horizon
Though down this road we've been so many times

The grass was greener
The light was brighter
The taste was sweeter
The nights of wonder
With friends surrounded
The dawn mist glowing
The water flowing
The endless river.

Forever and ever

"High Hopes" (extract) – Pink Floyd

AGRADECEMENTOS

E chegados a este punto quixera agradecer a todos os que chegaron a coloborar en esta tese, incluso aínda sen sabelo.

En primeiro lugar, moitísimas gracias aos meus directores de tese, María José Alonso e Alejandro Sánchez, por darme a oportunidade de descubrir esta área da investigación que realmente me apasiona, por confiar na miña capacidade para levar adiante este proxecto e dirixirme durante o camiño.

Neste senso quero tamén agradecer moi especialmente a Patrizia Paolicelli, por ser a persoa que me empezou a mostrar de que iba esto das vacunas, e a Cecilia Prego, porque con ela continuei aprendendo cada día. Ademáis gañei dúas boas amigas.

Quixera facer unha especial mención aos nosos colaboradores, xa que sen eles este traballo non sería posible. En primeiro lugar a Merce, a Belén e a África da Universidade de Vigo, nunca estarei suficientemente agradecida pola vosa colaboración. A Susana Martínez-Pulgarín e a José Ángel Escribano de Algenex pola súa colaboración na parte de influenza. A Jose Neissa do departamento de fisioloxía da USC, pola súa valiosa axuda nos experimentos de IVIS. Tamén aos nosos colaboradores dos Estados Unidos, David Pascual de Montana University, Herman Staats de Duke University, Robert Garcea da University of Colorado. E non quero olvidar aos técnicos que axudaron con tódolos experimentos en animales, a Rafa, a Andrea e a Christian.

I really want to thank my supervisors during my research internships in the University of Glasgow, Jim Brewer, and in the University of Texas Health Science Center at San Antonio, Bill Phillips and Beth Goins. I really appreciate your help and everything you taught me. Both were great experiences and made me grow as scientist, but also personally. Thank you.

Aos meus compañeiros de laboratorio, todos os que foron chegando e os que se foron marchando a longo de estos anos, unha longuísima lista, todos e cada un deles deixaron a súa impronta. Con todos aprendín e quédanme recordos inesquecibles e bos amigos. Pero aquí teño que agradecer especialmente ao "Equipo Nanovac". A Jorge e a José Vicente, e á última incorporación, a miña tocaia Sara, por facer que esos minutos antes de cada reunión fosen para botarnos unhas risas e liberar tensións, por apoiarnos mutuamente e sempre aprender os uns dos outros. Graciñas a todos.

Ás miñas amigas despojiles, Elena, Bea, Iria, Carolina, Isora e Rosalía, todas farmacéuticas, todas da misma fornada. A pesares da distancia, estar con vós é como si non pasara o tempo. A Maruxa, pola nosa amizade preparada mediante xelificación iónica e que se mantén estable durante tanto tempo. A Nuria e a tódolos meus amigos de Boiro. Pero sobre todo a David. O meu compañeiriño, que veu medrar esta tesis dende o seu inicio, que comparteu conmigo cada unha das súas etapas (en algún caso con bastantes kilómetros polo medio) e case case podería defendela. Moitas gracias por acompañarme.

E por suposto, a quen vai dedicado este libro. Aos meus pais. Porque sempre se mostraron orgullosos de min e confiaron nas miñas decisións e me deixaron facer, e parece que non saleu mal de todo. A Marcos, meu irmansiño. A tódolos primos, a toda a miña familia e aos avós que xa non están. É un privilexio medrar rodeada de vós.

ÍNDICE DE CONTENIDOS

Resumen/Abstract

RESUMEN

En la presente tesis doctoral se presenta el diseño y desarrollo de un sistema nanocapsular para la liberación simultánea de vacunas y agentes inmunoestimulantes. En particular, las nanocápsulas desarrolladas se componen de una cubierta de quitosano y un núcleo líquido oleoso (Miglyol® 812 o escualeno). El carácter multifuncional de estas nanoestructuras ha permitido la asociación de distintos tipos de antígenos, como el antígeno recombinante de la hepatitis B y la hemaglutinina del virus de influenza, sobre la superficie polimérica. Al mismo tiempo, el núcleo oleoso puede albergar moléculas con actividad inmunoestimulante, como el imiquimod, de forma que ambos componentes inmunoactivos se co-liberen una vez captadas por las células presentadoras de antígeno. Los estudios *in vitro* han demostrado que las nanocápsulas de quitosano son eficazmente internalizadas por células del sistema inmunológico (macrófagos), y además liberan adecuadamente el imiquimod asociado, dando lugar a una pronunciada secreción de citocinas. Se ha determinado además que mediante la adecuada combinación de los componentes del sistema se pueden llegar a generar respuestas inmunes mayores (niveles de IgG totales) que el adyuvante de referencia (álum), así como modular la cinética y el tipo de respuesta alcanzada (humoral ó celular). Así mismo, las nanocápsulas de quitosano han mostrado la capacidad de generar respuestas protectoras y prolongadas en el tiempo frente al antígeno asociado, tras una única inyección. Esta capacidad se ha relacionado con la biodistribución de las nanocápsulas y su acceso prolongado al sistema immune tras la formación de un depot en el lugar de injeción. Por otro lado, se ha evaluado su efectividad como sistema de liberación de vacunas sin agujas ("needle-free"). Más concretamente, utilizando la vía de administración nasal, se han conseguido generar respuestas inmunes sistémicas prolongadas, así como la inducción de memoria inmunológica.

Por tanto concluimos que con este trabajo de investigación se ha conseguido avanzar en el desarrollo de nuevos adyuvantes capaces de potenciar y modular la respuesta inmune frente a un antígeno específico, así como generar respuestas protectoras tras la administración por una vía no invasiva, como es la nasal.

ABSTRACT

The main goal of this thesis has been the design and development of a nanocapsular system for the co-delivery of vaccines and immunostimulant agents. In particular, such nanocapsules are composed of chitosan shell and a liquid oily core (Miglyol® 812 or squalene). The multifunctional character of these nanostructures enabled the association of different types of antigens, such as the recombinant hepatitis B surface antigen and the hemmaglutinin of influenza virus, onto the polymeric surface. The oily core can accommodate immunostimulant drugs, such as imiquimod, so that both immunoactive components can be co-delivered to antigen presenting cells. The *in vitro* studies showed that chitosan nanocapsules were effectively internalized by immune cells (macrophages), where they delivered the imiquimod cargo, thus resulting in a pronounced secretion of cytokines. We have also determined that an adequate combination of the components of the system led to an immune response (total IgG levels) that was more pronounced than that corresponding to the reference adjuvant (alum). In fact, upon a single injection the response achieved was comparable to that observed following the administration of two doses of alum. This high and prolonged response was related to the biodistribution patterns and the delayed access of the nanovaccine from the injection site to secondary lymphoid organs. Moreover, these multifunctional nanostructures enabled the modulation of the kinetics and type of immune response (humoral or cellular). On the other hand, we have also assessed the efficacy of chitosan nanocapsules as a needle-free vaccine delivery system. Namely, following nasal administration, some developed nanovaccines were able to generate systemic and prolonged immune responses, as well as inducing immunologic memory.

Overall, we can conclude that this research work contributed to advance on the development of new adjuvants able to potentiate and modulate the immune response against a specific antigen, as well as to generate protective responses upon administration through a non-invasive route, such as the intranasal.

Capítulo 1: INTRODUCCIÓN

NANOVACUNAS

Adaptado de:
Nanovacunas. S. Vicente, A. Sánchez, M.J. Alonso.
Monografía XXVIII: Nanotecnología Farmacéutica. Ed. Real Academia Nacional de Farmacia. Madrid, 2009

Las vacunas clásicas basadas en microorganismos atenuados o desactivados han sido utilizadas desde los tiempos de Jenner (s. XVIII) hasta nuestros días. Sin embargo, éstas pueden ir acompañadas de cierta problemática que compromete su seguridad y eficacia, como por ejemplo el riesgo a la reactivación del microorganismo atenuado, reacciones anafilácticas, etc. Sin embargo, la mayor purificación de las vacunas que se ha conseguido en los últimos años (desarrollo de antígenos subunidad) y que aumenta de forma importante la seguridad de las vacunas, suele conllevar, a cambio, una disminución en la inmunogenicidad. La menor potencia de la respuesta inmune lograda tanto con los antígenos recombinantes como con las vacunas ADN hace que sea necesario el apoyo con algún tipo de adyuvante, de forma que ayude a incrementar la respuesta inmunitaria frente el antígeno/material genético administrado.

Actualmente existen una amplia variedad de adyuvantes en estudio como son los toxoides bacterianos, las emulsiones, sustancias inmunoestimulantes y los sistemas de liberación de antígenos (1-3). Sin embargo el más ampliamente utilizado y todavía el único aprobado para su uso en la elaboración de vacunas en Estados Unidos, son las sales insolubles de aluminio, más conocidas como álum (4). Hasta el momento, el álum ha demostrado que puede ayudar a generar respuestas inmunológicas importantes al administrarse con el antígeno vía parenteral. Al mismo tiempo es considerado un adyuvante aceptablemente seguro desde el momento de su descubrimiento, en los años 20. A pesar de ello, el álum presenta ciertos inconvenientes relacionados principalmente con la aparición de síntomas locales tras la inyección, como hinchazón, eritemas o nódulos cutáneos, que pueden

durar incluso varias semanas. Otra importante desventaja de este adyuvante se relaciona con su inestabilidad tras la congelación debido a la destrucción del gel a 0ºC provocando una disminución en la potencia de la vacuna (5). Por otro lado, la respuesta inmunológica generada presenta un perfil bastante limitado al estimular la producción de citoquinas que favorecen principalmente la proliferación de linfocitos Th2 y la inducción de una respuesta humoral, además de promover la generación de IgE, inmunoglobulina que media en las respuestas alérgicas (6).

Sin embargo, a pesar de que el álum es el único adyuvante aprobado para su uso en humanos, actualmente se están invirtiendo grandes esfuerzos en la búsqueda de nuevos adyuvantes más eficaces y seguros, es decir, adyuvantes que permitan aumentar la respuesta inmune frente al antígeno que acompañan, modularla en función de las características del patógeno y que al mismo tiempo presenten un buen perfil de seguridad. Por ejemplo, nuevos adyuvantes han sido recientemente introducidos en el mercado europeo: las microemulsiones MF59™ (Aflunov®, Flocivia®, y Focetricia®) y AS03™ (Prepandrix®, Pandemrix® y Purmarix®) en vacunas frente a influenza, y AS04™ (Cervarix®) consistente en una combinación de álum y MPLA (monofosforil lípido A) que acompaña a antígenos recombinantes del virus del papiloma humano (7).

INTRODUCCIÓN DE LAS NANOTECNOLOGÍAS EN EL DESARROLLO DE VACUNAS.

Liposomas, micropartículas, emulsiones y más recientemente nanopartículas, han sido objeto de investigación como sistemas de liberación de vacunas que podrían mejorar la inmunogenicidad de los nuevos antígenos subunidad y, además, podrían permitir la administración a través de vías no invasivas, como la vía mucosa o la liberación transdérmica, ayudando a mejorar la cobertura inmunológica (8-11).

En general, los sistemas de liberación consisten en sistemas particulados que promueven la captación del antígeno por las células presentadoras de

antígeno (CPA) favoreciendo su reconocimiento para que, de este modo, el antígeno sea liberado al sistema inmune de una forma más eficiente (12, 13). Al mismo tiempo se puede aumentar la inmunogenicidad del antígeno asociado mediante la incorporación de algún tipo de adyuvante para ser liberado simultáneamente (14).

Ya a finales de los años 70, los sistemas poliméricos basados en microesferas comienzan a utilizarse como potenciales sistemas de liberación y transportadores de antígenos, con la finalidad de obtener un sistema de vacunación en dosis única (15). El importante desarrollo en la utilización de microesferas poliméricas biodegradables a partir de ese momento se debió en gran medida al interés mostrado por la industria química y farmacéutica en estos sistemas. De hecho, la Organización Mundial de la Salud (OMS) proponía las microsferas de PLGA (ácido poli-láctico-co-glicólico) como una nueva estrategia para mejorar la cobertura inmunológica, así como para reducir los costes asociados a la vacunación (16). A partir de ese momento, la utilización de microsferas elaboradas a partir de este biomaterial ha sido ampliamente estudiada para la liberación de vacunas y contribuir a la inducción de la respuesta inmune específica frente al antígeno asociado a través de diferentes vías de administración (17-22).

Más recientemente, el uso de las nanopartículas poliméricas para la liberación de vacunas ha comenzado a destacar como una posible estrategia para desarrollar nuevas vacunas (8, 10). Las características de estos nuevos nanosistemas poliméricos para la liberación de vacunas serán descritas en los siguientes apartados.

Nanopartículas poliméricas para la liberación de vacunas

Las nanopartículas son estructuras de tamaño nanométrico formadas a partir de diversos materiales capaces de asociar moléculas bioactivas. Una importante característica de estos sistemas es su mayor capacidad de captación por las células comparado con estructuras de mayor tamaño (23). Existen una amplia variedad de nanosistemas diferenciados por los materiales utilizados para su elaboración y/o método de preparación, de

forma que, de forma resumida, pueden distinguirse en nanosferas, nanocápsulas, liposomas, micelas poliméricas y dendrímeros (24). Dichos sistemas presentan propiedades que pueden ser empleadas para mejorar la liberación de fármacos, proteínas, genes y vacunas (**Tabla 1**). Son especialmente interesantes aquellos nanosistemas cuya composición se basa en biomateriales ó biopolímeros. La elaboración de nanopartículas a partir de este tipo de materiales garantiza el que se pueda llegar a desarrollar un vehículo biodegradable, biocompatible y potencialmente seguro para su administración en humanos.

Nanopartícula	Descripción	Aplicaciones recientes	Refs.
Dendrímeros	Compuesto macromolecular ramificado creado a partir de un núcleo interno	Conjugación al dendrímero PAMAM de una vacuna ADN y péptidos dirigidos a MHC II de las células dendríticas para la liberación selectiva.	(25)
Liposomas	Vesículas artificiales formadas a partir de fosfolípidos y colesterol	Liposomas catiónicos como sistema adyuvante de vacunas frente a tuberculosis y Chlamydia.	(26)
Nanocápsulas	Sistemas vesiculares de núcleo oleoso rodeados por una cubierta polimérica	Nanoemulsión recubierta de quitosano para potenciar y modular respuestas inmunes específicas frente a hepatitis B.	(27)
Micelas poliméricas	Compuestas por polímeros anfifílicos que se asocian en solución acuosa	Péptidos antigénicos anfifílicos autoensamblados formando micelas en soluciones acuosas.	(28)
Nanosferas	Sistemas matriciales en los cuales la molécula bioactiva se encuentra uniformemente dispersa.	Nanopartículas de PLGA-poloxamer para la liberación del antígeno recombinante de superficie de la hepatitis B.	(29)

Tabla 1: *Resumen de las diversas aplicaciones de los distintos tipos de sistemas coloidales para la liberación de vacunas.*

Las nanopartículas poliméricas diseñadas para la liberación de vacunas pueden actuar mediante un mecanismo depot, según el cual el antígeno asociado se va liberando gradualmente de manera sostenida, aunque su característica principal es la de promover la internalización del antígeno en las CPA y su posterior activación y maduración para iniciar la respuesta inmune adaptada (30). Además, este tipo de sistemas coloidales ofrecen grandes ventajas para la liberación de vacunas a través de las barreras mucosas, especialmente por la vía oral y nasal, siendo capaces de dar lugar a una respuesta inmunológica sistémica, pero al mismo tiempo, también a nivel de la mucosa debido a la importante presencia del sistema inmune en los tejidos asociados a las mucosas (MALT) (31), como por ejemplo, las placas de Peyer a nivel intestinal y el NALT a nivel de las vías respiratorias. Por un lado, las nanopartículas protegen al antígeno encapsulado frente a la degradación enzimática (especialmente tras su administración oral) y, por otro lado, pueden promover la captación por la células M del NALT y de las placas de Peyer (10).

El diseño de vehículos nanométricos basados en biomateriales puede ser una solución muy adecuada para superar las barreras biológicas y la baja inmunogenicidad de muchos antígenos, de forma que puedan contribuir en la inducción de la respuesta inmune específica deseada, ofreciendo al mismo tiempo importantes ventajas para aumentar la cobertura inmunológica. Por un lado, podrían contribuir enormemente en el diseño de un sistema de vacunación que evite las rutas de administración invasivas (9, 32) y, por otro lado, se podría mejorar la respuesta inmune en función de la aplicación final de la vacuna mediante la modificación de los distintos mecanismos de activación del sistema inmune innato, como el aumento en la captación o la activación directa de las CPA (p. ej. las células dendríticas) (33). Por tanto, mediante el diseño de un sistema coloidal polimérico se podrían intentar modular dichos mecanismos para conseguir una respuesta adecuada, como se resume a continuación:

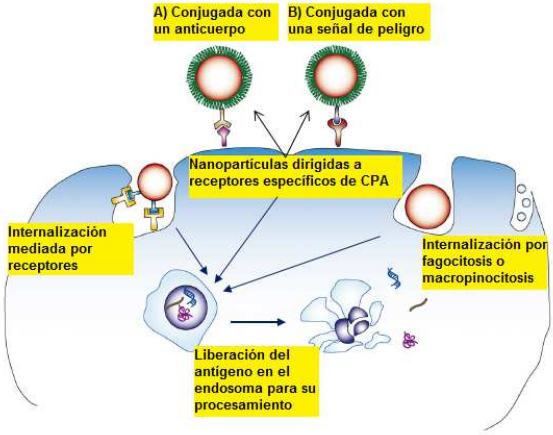

Figura 1: *Mecanismos de captación de nanopartículas por las células presentadoras de antígeno para la liberación intracelular del antígeno y posterior procesamiento. Adaptado de (33).*

1. La forma en que el antígeno es internalizado y luego liberado intracelularmente es un factor clave para que se llegue a generar una respuesta inmunitaria de células T, como se puede apreciar en la **Figura 1**. Por tanto, al aumentar la internalización y posterior liberación intracelular del antígeno con un sistema nanoparticulado, cabría esperar una mejora en el tipo de respuesta inmune generada.

2. Algunos biomateriales pueden incluso tener actividad adyuvante por si mismos y actuar como "señales de peligro" para activar los receptores TLR ("Toll-like receptors") de las CPA, como por ejemplo los polifosfacenos (34). Con lo cual un sistema de liberación de vacunas compuesto por este tipo de biomateriales, podría activar directamente estas células. También es importante destacar la capacidad de estos sistema para co-asociar antígenos y moléculas inmunoestimuladoras que actuarían como activadoras de las CPA (35).

3. Finalmente, mediante la modulación del tamaño de partícula, forma, carga y composición superficial, se puede facilitar el acceso directamente a las células dendríticas de los ganglios linfáticos en lugar de ser

previamente captadas y procesadas por las células dendríticas periféricas. De este modo, la respuesta inmune se generaría directamente en los órganos inductores (36).

El uso de nanopartículas poliméricas para la liberación de vacunas se ha ido incrementando en los últimos años. La importancia de estos nuevos vehículos para mejorar la inmunización se ve reflejada en el gran número de sistemas con diversas propiedades que han ido surgiendo, elaborados utilizando una amplia gama de biomateriales y técnicas de preparación, e ideados con la finalidad de generar vehículos de tamaño nanométrico capaces de acercar y liberar más fácil y eficazmente el antígeno al sistema inmune, al mismo tiempo que pudiese llegar a regular la respuesta inmunológica inducida. (11, 37).

Interacción de las nanopartículas poliméricas con el sistema inmune: captación por las células presentadoras de antígeno.

Las células dendríticas son unas potentes CPA que se encuentran en tejidos periféricos y órganos linfoides. Son capaces de activar a las células B y T e iniciar una respuesta inmune específica. El papel de las células dendríticas inmaduras que se encuentran en los tejidos periféricos es la de reconocer sustancias extrañas y patógenos. Presentan una alta capacidad para captar antígenos y procesarlos mediante la expresión abundante de los complejos mayores de histocompatibilidad tipo I y II (MHC I y II), moléculas co-estimuladoras (p. ej. CD80, CD86, CD40) y la secreción de otras moléculas accesorias necesarias, como citoquinas (p. ej. IL-12), quemoquinas (p. ej. CCL19 y CCL22) y la expresión de receptores de citoquinas (p. ej. CCR7), para una eficaz presentación del antígeno (38).

En el caso de los sistemas de liberación de vacunas, es especialmente interesante la capacidad de las nanopartículas poliméricas para ser más eficazmente captadas e internalizadas por las células dendríticas debido a su tamaño nanométrico (39).

Los antígenos particulados, y en concreto los sistemas coloidales poliméricos transportadores de antígeno, pueden ser captados por las células dendríticas a través de diversos mecanismos de endocitosis (**Figura**

1) (23): mediada por receptores (liberación selectiva), macropinocitosis, mediada por clatrina o caveolina, y fagocitosis. El que una nanopartícula polimérica se internalice de una u otra manera depende de forma importante de su tamaño, forma, carga y composición superficial (30). Una vez internalizada, se incluye en el compartimento endocítico para que el antígeno sea procesado en unidades peptídicas y posteriormente presentado en los MHC clase II a las células T $CD4^+$ en los órganos linfoides secundarios (**Figura 2**). De esta forma se inicia la inducción de una respuesta inmune específica frente al antígeno presentado. Alternativamente, puede producirse una presentación cruzada del antígeno exógeno mediante el uso de sistemas de liberación particulados a través de MHC clase I. Siguiendo esta ruta de procesamiento el antígeno es presentado a células T $CD8^+$ para finalmente conseguir una respuesta de linfocitos T citotóxicos (CTL) (40). Para el desarrollo de vacunas frente a patógenos intracelulares y vacunas terapéuticas este tipo de respuesta celular es especialmente interesante, ya que las CTL son capaces de eliminar patógenos intracelulares y células malignas o apoptóticas.

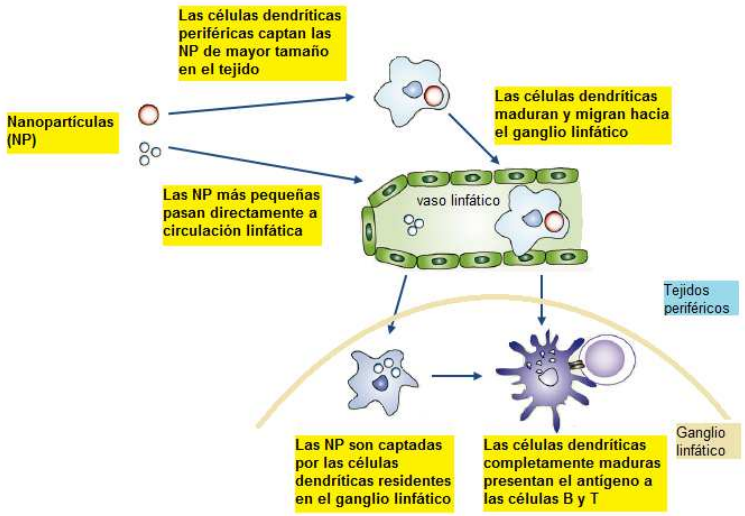

Figura 2: *Captación y procesamiento del antígeno transportado por nanopartículas por las células presentadoras de antígeno, para posteriormente iniciar una respuesta inmunológica específica en los ganglios linfáticos. Adaptado de (33).*

Una amplia variedad de biomateriales han sido utilizados para el desarrollo de nanopartículas para la liberación de vacunas, como poliésteres (PLGA y PLA), proteínas y poliaminoácidos (gelatina, protamina y ácido poli-γ-glutámico), y polisacáridos como el quitosano o el ácido hialurónico. En general, las nanopartículas poliméricas han demostrado una buena interacción con las células inmunitarias aumentando la captación de antígenos y sustancias inmunoestimulantes.

Las nanopartículas de PLGA han sido estudiadas ampliamente como sistemas de liberación de fármacos, proteínas y material genético (39), y por tanto pueden ser un excelente vehículo para ser captado eficazmente por las células dendríticas. Por ejemplo, nanopartículas de PLGA con un tamaño medio de 300 nm (41) son captadas por estas células de forma importante mediante fagocitosis. Así mismo, se ha determinado que las células dendríticas activadas por estas nanopartículas de PLGA presentan un importante potencial para activar a las células T. De hecho, en un estudio más reciente se ha corroborado que la internalización de un antígeno frente a células malignas de melanoma se ve favorecida al ser incluido en nanopartículas de PLGA (˜400nm) y que, además, se promueve la producción de interferón γ (IFN-γ) y la proliferación de CTLs frente al antígeno (42). A pesar de que las partículas de PLGA son altamente captadas por las células dendríticas, una posible estrategia para aumentar la interacción con células dendríticas ha sido descrita por Cruz y col. (43), la cual se basa en la conjugación de un anticuerpo específico frente a una lectina presente en la membrana celular de las células dendríticas (DC-SIGN). La conjugación del anticuerpo a las nanopartículas de PLGA se hace a través un espaciador de polietilenglicol (PEG), cuya longitud es crucial para la correcta interacción del anticuerpo con su ligando y la posterior internalización de la nanopartícula que lleva el antígeno encapsulado y, por tanto, influye de forma decisiva en la efectividad del sistema.

Al igual que el PLGA, para otros sistemas basados en proteínas o poliaminoácidos (como la gelatina (44), la protamina (45) y el poli-γ-

glutámico (46)) con tamaños de partícula entre 200 y 300nm, se ha observado una mayor interacción y posterior activación celular mediante el aumento en la expresión de moléculas co-estimuladoras y MHC clase II en la superficie celular. En un estudio donde se compara la internalización de ovalbúmina asociado a nanopartículas de poli-γ-glutámico o a álum (47), se comprueba que el antígeno es captado más eficientemente cuando se encuentra encapsulado en las nanopartículas mediante distintos mecanismos de internalización (endocitosis y/o pinocitosis) y que, además, son capaces de inducir respuestas mediadas por linfocitos Th1 y CTL, a diferencia del álum (preferentemente tipo Th2). La modificación del poli-γ-glutámico con aminoácidos hidrofóbicos para darle un carácter anfifílico al polímero, han demostrado que la mayor captación del antígeno (ovalbúmina) y posterior maduración de las células tiene lugar independientemente de que éste se encuentre encapsulado en las nanopartículas o como una mezcla física (46). Sin embargo, solamente las células dendríticas activadas con las nanopartículas cargadas con el antígeno han sido capaces de estimular una respuesta de células T específica, lo cual se ha atribuido a la prolongación de la vida media en el interior celular del antígeno encapsulado, pudiendo ser éste también un factor determinante en la generación de una respuesta inmune celular.

La incorporación de una sustancia inmunoestimulante en un sistema coloidal puede ver incrementada su propia capacidad estimuladora al ser reconocida y captada por las células dendríticas. Por ejemplo, la encapsulación de MPLA (derivado no tóxico del LPS) en nanopartículas de PLGA provocan una maduración de las células dendríticas mayor que el inmunoestimulante en solución (48). Por otro lado, estudios similares llevados a cabo con nanopartículas de gelatina y gelatina cationizada elaboradas mediante desolvatación (35), han demostrado incrementar la capacidad inmunoestimuladora del CpG ODN, un oligonucléotido capaz de estimular a las células dendríticas debido a su interacción con el receptor TLR4. De este modo se corrobora la eficacia de estos nanosistemas para ser internalizados por las células dendríticas mejorando

el efecto estimulante de MPLA ó CpG ODN. Se aprecia además, cómo diferencias en las propiedades superficiales del sistema afectan a la internalización y maduración de las células dendríticas, ya que las nanopartículas elaboradas a partir de gelatina cationizada, y por tanto con un potencial ζ positivo, han resultado ser más eficazmente captadas que las nanopartículas neutras. Esta observación ha sido descrita por otros autores, confirmando que el carácter catiónico de la superficie de las nanopartículas favorece la internalización por las células dendríticas y su posterior maduración (49-51). En esta línea, las nanopartículas basadas en polisacáridos catiónicos como el quitosano, también han demostrado una buena interacción con células dendríticas. Bal y col. (52) han descrito que la intensa captación de nanopartículas de trimetilquitosano (TMC) por las células dendríticas se debe a una interacción electrostática con la superficie celular que favorece el contacto de las nanoestructuras con las células. Esta hipótesis se confirma en el estudio de Zaki y col. (53) donde evalúan la interacción con macrófagos de nanopartículas quitosano, comparándolas con las mimas nanopartículas de quitosano recubiertas por un polisacárido aniónico, como es el ácido hialurónico. En este estudio se observa una mayor interacción de las nanopartículas de quitosano con la superficie celular, a diferencia de las nanopartículas recubiertas. Esta diferencia se traduce en una internalización más rápida y en mayor magnitud de las nanopartículas catiónicas a pesar de utilizar ambos prototipos un mecanismo endocítico probablemente mediado por clatrinas de la membrana celular.

En resumen, la liberación intracelular del antígeno a las células dendríticas (o CPA en general) es un factor especialmente importante a la hora de optimizar la respuesta inmune, siendo los sistemas de nanopartículas poliméricas una estrategia muy adecuada para conseguir este objetivo que, por otro lado, permitiría dirigir el antígeno hacia determinadas rutas de procesamiento intracelular, llegando incluso a modular la respuesta inmune (54). En general, independientemente de los diferentes tipos de biomateriales utilizados, estos vehículos de tamaño

nanométrico son capaces de interaccionar de forma importante con las células dendríticas, de forma que son eficazmente internalizadas dando lugar a su activación, provocando consecuentemente su maduración y migración a los órganos linfoides secundarios (ganglios linfáticos) para poder iniciar una respuesta inmunológica adaptada.

NANOVACUNAS PARA LA POTENCIACIÓN Y MODULACIÓN DE LA RESPUESTA INMUNE

Debido a la menor inmunogenicidad de los nuevos antígenos subunidad o plásmidos ADN codificadores de estos antígenos, suelen requerir una dosificación múltiple con dosis de recuerdo para asegurar la protección inmunológica, así como el apoyo de algún tipo de agente adyuvante de forma que ayude a la inducción y potenciación de la respuesta inmunitaria específica. Por lo tanto, se hace necesario el desarrollo de nuevos sistemas que sean menos tóxicos, más tolerables por el paciente, que permitan la potenciación y modulación de las respuestas inmunes frente a una amplia variedad de microorganismos patógenos, así como una reducción en el número de dosis necesaria para alcanzar protección frente a enfermedades infecciosas.

Como se ha descrito en la sección anterior, las nanovacunas basadas en biomateriales son capaces de interaccionar con las CPA de forma efectiva promoviendo la captación del antígeno asociado y su posterior activación y migración hacia los ganglios linfáticos. Esta característica se puede, por tanto, aprovechar para desarrollar un sistema adyuvante que potencie la respuesta inmune adaptada. El uso de biomateriales para la fabricación de nanostructuras liberadoras de antígeno (como polímeros biodegradables como el PLGA o el quitosano) garantiza la seguridad y la baja toxicidad de las mismas. Además, debido a la capacidad de las nanopartículas poliméricas para liberar la molécula bioactiva (ej. antígeno) de una manera controlada, otro objetivo ha sido el de reducir el número de dosis necesario para crear protección inmunológica prolongada en el tiempo.

Las nanopartículas poliméricas (polimetil-metacrilato) se utilizaron por primera vez en los años 70 como potenciadores de la respuesta inmune frente al toxoide tetánico e inmunoglobulina G (antígenos modelo) (55). Sin embargo, a partir de entonces se han utilizado diversos biomateriales con un mejor perfil de toxicidad y con propiedades biodegradables en el diseño de nanovehículos de vacunas para la potenciación y prolongación de la respuesta inmune. Por ejemplo, los poliésteres (PLGA, PLA) han sido ampliamente utilizados debido a sus propiedades de biodegradabilidad y biocompatilibidad (material GRAS reconocido por la FDA). Como se ha visto en el apartado anterior, las nanopartículas basadas en poliésteres presentan la capacidad de interaccionar y ser captadas por las células del sistema inmune innato (CPA). Sin embargo, en general se ha visto que la potenciación de la respuesta inmune *in vivo* con estos nanosistemas precisan de un agente adyuvante que se libere junto al antígeno. Así por ejemplo, nanosistemas basados en estos biomateriales fueron diseñados para la liberación del toxoide tetánico de forma gradual una vez inyectados y así prolongar la respuesta inmune. No obstante, la combinación con álum fue necesaria para llegar a aumentar la respuesta inmune de forma significativa (56, 57). Por otro lado, las nanopartículas de PLA preparadas sin la utilización de surfactantes mediante un método de diálisis, han sido la base para el diseño de una vacuna multivalente frente a VIH (58). Dos antígenos subunidad de la cápside del virus (gp120 y p24) se han podido asociar de forma simultánea a la superficie de las nanopartículas manteniendo la antigenicidad de ambos. Tras la administración subcutánea se llega a generar una respuesta inmune humoral elevada frente a ambos antígenos. Sin embargo, los autores concluyen que sería necesario incluir una molécula inmunoestimulodora al sistema para poder inducir niveles de protección mayores. Esta estrategia se ha seguido, por ejemplo, funcionalizando la superficie de nanopartículas de PLGA con LPS (59). Las nanopartículas con LPS interaccionan y son mejor captadas por las células dendríticas que las nanopartículas sin LPS *in vitro*. De hecho, tras la administración

subcutánea del sistema encapsulando ovalbúmina, se observa que los títulos de IgG específicos son equivalentes a álum y FCA y, además, son significativamente mayores que los conseguidos por las nanopartículas sin recubrimiento de LPS, lo cual se atribuye a su mayor capacidad para activar el inflamasoma en las células dendríticas. También la co-encapsulación de una molécula inmunoestimulante como el 7-acyl lipid A (nuevo adyuvante agonista de los receptores TLR) con un antígeno propio de células cancerígenas de melanoma en nanopartículas de PLGA, logró incrementar la respuesta de células T $CD8^+$ específicas en ganglios linfáticos y bazo con respecto a las nanopartículas sin el inmunoestimulante tras la administración subcutánea. En un modelo animal de melanoma la mayor efectividad del sistema conteniendo el adyuvante y el antígeno fue muy sutil ya que ambos son capaces de inhibir el crecimiento del tumor rompiendo la autotolerancia frente al antígeno. Sin embargo, el correspondiente sistema combinado dio lugar una mayor inmunoestimulación a nivel del tumor (activación de citoquinas pro-inflamatorias) que disminuiría la aparición de células T reguladoras y aumentaría la respuesta de células T efectivas frente al tumor (60).

Otro tipo de nanopartículas biodegradables ampliamente estudiadas son las basadas en ácido poli-γ-glutámico (61). Estas nanoestructuras han demostrado poseer propiedades inmunoadyuvantes capaces de potenciar la respuesta inmune frente al antígeno asociado, especialmente la respuesta de tipo Th1 (62) sin la adición de una molécula inmunomoduladora en su composición. Por esta razón, se han aplicado principalmente para la inmunoterapia del cáncer (63) y para vacunas frente a patógenos intracelulares como el VIH (64).

El quitosano se ha aplicado principalmente en el diseño de nanopartículas para la liberación de antígenos a través de las vías mucosas (ver siguiente sección) (65). Sin embargo, debido a las propiedades inmunoestimulantes de este polímero recientemente descritas (66, 67), las nanopartículas de quitosano también se están estudiando como potenciadores de la respuesta

inmune. Probablemente debido a la intensa interacción y captación por las CPA, como se ha descrito en el apartado anterior, se ha comprobado que estos nanosistemas polisacarídicos poseen un gran poder adyuvante cuando se administran *in vivo* por vía subcutánea o intramuscular. De hecho, en un trabajo previo hemos podido comprobar en nuestro laboratorio la capacidad de las nanopartículas formadas por quitosano y polaxamer (utilizado como estabilizador de la proteína) y preparadas por gelificación iónica (~ 200 nm), para potenciar la respuesta inmune frente al HBsAg encapsulado tras su administración intramuscular (68). En este estudio, los niveles de IgG totales en suero generados por las nanopartículas fueron mayores que los proporcionados por la vacuna convencional con álum a la misma dosis, apuntando un efecto inmunestimulador mayor que el adyuvante de referencia. Por otro lado, en un estudio realizado por Wen y col. (69), se ha determinado que las nanopartículas de quitosano administradas por vía subcutánea en dos dosis, además de potenciar la respuesta inmune con respecto al antígeno solo (ovalbúmina) o mezclado con quitosano libre, dan lugar a una respuesta mixta mediada por linfocitos Th1 y Th2, lo que sugiere que no solo se está produciendo una respuesta humoral, sino también de tipo celular, sin haber incluido un agente inmunomodulador en la composición de las nanopartículas.

El carácter catiónico del quitosano permite, además, la formación de nanopartículas híbridas en asociación con otros polianiones, como por ejemplo con sulfato de dextrano (70). En este estudio, el antígeno p24 del VIH se adsorbió a la superficie de estos complejos de polielectrolitos (PECs) que dan lugar a nanopartículas en torno a 500 nm. La respuesta inmune frente a p24 tras la administración subcutánea de las PECs fue similar al control positivo utilizado, en este caso nanopartículas de PLA con la misma dosis de antígeno y el mismo contenido en sólidos (los autores afirman que las nanopartículas de PLA dan lugar a títulos de anticuerpos mayores que el álum con el p24). Además, el análisis de citocinas liberadas por esplenocitos de los ratones inmunizados con las

PECs (IL-4 e IFN-γ) revela que son capaces de inducir una respuesta mixta Th1/Th2. Otro tipo de nanosistema híbrido para la liberación de vacunas fue descrito por Borges y col. (14). En este caso las nanopartículas de quitosano se recubren con alginato para proteger el antígeno previamente asociado a la superficie catiónica. Además, para conseguir polarizar la respuesta hacia el tipo celular (Th1), co-administran una molécula CpG ODN. Con este sistema, logran respuestas elevadas de IgG y una mayor producción del subitipo IgG2a, que determina el tipo de respuesta Th1. Sin embargo, el comportamiento más satisfactorio se ha atribuido a las nanopartículas de quitosano asociando el HBsAg y el CpG ODN sobre la superficie catiónica y sin recubrimiento de alginato, ya que se trata de un sistema más sencillo y genera mayores niveles de IgG totales manteniendo un buen balance Th1/Th2 (IgG2a > IgG1). Por lo tanto, en general, las nanoestructuras basadas en quitosano son capaces de potenciar la respuesta inmune adaptada frente al antígeno asociado y, a la vez, modular la respuesta inmune hacia un tipo mixto Th1/Th2.

APLICACIÓN DE LAS NANOVACUNAS A LA INMUNIZACIÓN POR VÍAS MUCOSAS

El gran éxito alcanzado con la vacunación oral frente a la poliomielitis, utilizando una vacuna basada en el microorganismo atenuado, ha llevado a considerar la vacunación a través de las vías mucosas una posible alternativa para desarrollar sistemas de liberación sin agujas. Las posibles consecuencias de implementar un sistema de este tipo serían, entre otras, la posibilidad de mejorar la cobertura inmunológica global e incrementar el perfil de seguridad de las vacunas al evitar el uso de agujas y jeringas. Igualmente importante, al introducir una forma de vacunación que no requiere inyección, se mejora la aceptación por parte del paciente, incrementado su confianza en las campañas y calendarios de vacunación de forma que se podría mejorar el cumplimiento en las pautas de inmunización (71).

Los antígenos administrados en las vacunas para inmunización están compuestos principalmente por proteínas propias del patógeno, ó por plásmidos ADN codificadores de proteínas antigénicas, como se ha descrito previamente. Sin embargo, debido a la baja estabilidad de estas biomoléculas, especialmente en zonas de alto contenido enzimático como el sistema digestivo, su administración se ve restringida a las vías parenterales (subcutánea e intramuscular) para evitar su posible degradación previa al efecto terapéutico. Además, al tratarse principalmente de moléculas de elevado peso molecular y carácter hidrofílico, presentan una limitada capacidad para ser transportadas a través de las barreras biológicas.

Uno de los principales objetivos en el desarrollo de nuevas tecnologías basadas en sistemas coloidales a base de biomateriales, ha sido el de mejorar la estabilidad de macromoléculas terapéuticas (péptidos, proteínas ó material genético) en los medios biológicos, así como para mejorar su transporte a través de las barreras biológicas que imponen las diferentes vías de administración no parenterales (72). Principalmente, el tamaño nanométrico de estos sistemas favorece enormemente su capacidad para superar las barreras biológicas y transportar la molécula bioactiva hacia el tejido diana donde llevará a cabo su acción farmacológica. Sin embargo, no solo el tamaño de partícula es un factor relevante a la hora de diseñar un nanovehículo para el transporte de macromoléculas a través de vías no invasivas, sino que otras propiedades como la bioadhesividad, la estabilidad en medios biológicos, su composición y propiedades superficiales, influyen de forma crucial en el éxito del nanosistema para hacer llegar la molécula terapéutica a su diana.

Una amplia variedad de nanosistemas elaborados a partir de diversos biomateriales, tanto de carácter hidrofóbico (PLGA, PLA, PECL) como hidrófilo (quitosano, ácido hialurónico, alginato, glucomanano) han sido utilizados como vehículos de macromoléculas terapéuticas a través de diferentes vías mucosas (72). Sin embargo, aquellos sistemas basados en polímeros hidrofílicos de origen natural, como por ejemplo el quitosano

(73-75), ofrecen otro tipo de ventajas a mayores, ya que permiten la encapsulación de macromoléculas terapéuticas mediante técnicas muy sencillas y en condiciones no agresivas que no requieren del uso de solventes orgánicos ni de la aplicación de elevada energía (p. ej. sonicación, ultrasonidos, etc.), además de presentar una aceptable estabilidad en fluidos biológicos y mayor afinidad por las superficies mucosas.

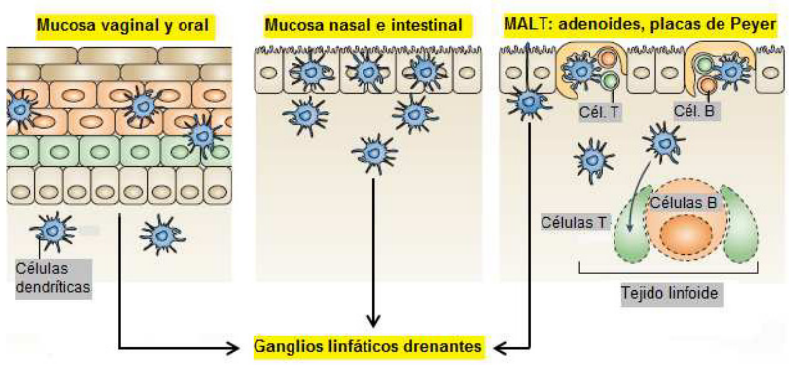

Figura 3: *Representación esquemática de la presencia del sistema inmune en las diferentes superficies mucosas. Adaptado de* (31)

La vacunación a través de las vías mucosas ha atraído gran interés en los últimos años, debido además a la posibilidad generar respuestas inmunes específicas a nivel de la superficie mucosa. Esta característica es de especial interés debido fundamentalmente a la gran ventaja que ofrece al proporcionar protección frente a patógenos que accedan al organismo utilizando esta vía de entrada, ya que con la administración parenteral del antígeno no se llega conseguir este tipo de respuesta. Las superficies mucosas son altamente ricas en tejidos linfoides (MALT), además de contar con la importante presencia de CPA en la zona submucosa, como se puede apreciar en la **Figura 3**. De esta forma, cualquier antígeno liberado y captado por las CPA del MALT y la submucosa, sería capaz de iniciar una respuesta inmune específica tanto a nivel de la mucosa, mediante la secreción de IgA, como a nivel sistémico, con la aparición de

IgG en sangre (31). Con lo cual, en primer lugar se crearía una barrera defensiva en dicha zona para minimizar la entrada de microorganismos, al tiempo que se podría llegar inducir una respuesta inmune sistémica duradera.

Por tanto, la elección de un sistema coloidal para mejorar el transporte de antígenos a través de las superficies mucosas para llegar a los tejidos donde se encuentran las CPA puede ser una buena alternativa a la liberación por inyección y para conseguir respuestas inmunitarias a nivel de la mucosa. En general, la vía oral y la vía nasal son las más comúnmente aceptadas debido a su buena aceptación por parte de los pacientes y a sus características favorables para la liberación de antígenos.

Administración de nanovacunas por vía oral

La captación de fármacos y antígenos transportados en sistemas de liberación particulados en el tracto gastrointestinal puede producirse por diversos mecanismos: a través de las microvellosidades, de los macrófagos intestinales, de los propios enterocitos ó del epitelio de las placas de Peyer a través de las células M. Sin embargo, la mayoría de las evidencias indican que la absorción, tanto de micropartículas como nanopartículas, se produce principalmente a través de las placas de Peyer. Los principales parámetros que afectan a la captación de sistemas particulados a través del epitelio de las placas de Peyer son el tamaño de partícula, la dosis de partículas administrada, y las características superficiales del sistema como la hidrofobicidad, la carga superficial, y la adición de ligandos dirigidos hacia una diana concreta del epitelio gastrointestinal (76). De esta forma, la modulación de estas características puede favorecer la captación de los sistemas desarrollados por las placas de Peyer.

A día de hoy, los sistemas mejor estudiados para la liberación de vacunas por vía oral han sido las micropartículas poliméricas, en concreto, las compuestas por PLA o PLGA. Es mucho menor la información que se maneja en cuanto al uso de nanopartículas poliméricas para inducir respuestas inmunológicas tras la administración oral (32). Sin embargo,

trataremos de resumir las características de los sistemas nanoparticulados estudiados a día de hoy para la inmunización oral.

El hecho de que este tipo de sistemas interaccionen principalmente con los órganos linfoides asociados a la mucosa intestinal es una de las principales ventajas de la administración de vacunas a través de la vía oral, ya que el antígeno podrá ser liberado directamente al sistema inmune presente en la mucosa intestinal, al mismo tiempo que se protege frente a la degradación enzimática. Aparte, existen otras posibilidades como la liberación selectiva con ligandos dirigidos a las células M y la incorporación de sustancias adyuvantes para mejorar la respuesta inmune a través de esta vía. Sin embargo, en general, se necesita de una mayor dosis de antígeno para generar una respuesta humoral similar a la conseguida con dosis más bajas a través de otras vías como la nasal, utilizando el mismo vehículo, como se observa en el estudio realizado por Jung y col. (77) con nanopartículas de PLGA modificado con PVA (polivinilalcohol). En este mismo estudio se comprueba además, el efecto del tamaño de partícula tras la administración oral. Coincidiendo con las hipótesis de que el tamaño de partícula llevado al rango nanométrico mejora el paso a través de las barreras mucosas, las nanopartículas de menor tamaño, en este caso de 100 nm, han sido mejor captadas en el tracto gastrointestinal que los prototipos de mayor tamaño (500 nm y >1 μm) y, consecuentemente, la respuesta inmune alcanzada ha sido superior en el caso de las partículas de menor tamaño. Por otro lado, la mejora de la estabilidad en fluidos gástrico e intestinal de los nanosistemas basados en poliésteres ha servido para mejorar la absorción del antígeno asociado a través de la mucosa gastrointestinal. Por ejemplo, las nanopartículas formadas a partir de un polímero di-bloque PEG-PLA-PEG mejora la estabilidad, prolonga el tiempo de liberación del antígeno (antígeno de superficie de la hepatitis B - HBsAg) y se consigue una respuesta sistémica equivalente al control con álum (parenteral) y una mejor respuesta mucosa con respecto a las nanopartículas de PLA (oral) y al álum (78).

Una posible estrategia para optimizar la interacción de los sistemas coloidales con la mucosa gastrointestinal se basa en la incorporación de un ligando específico que interaccione directamente con las células M de las placas de Peyer. Por ejemplo, nanopartículas de PLGA encapsulando el HBsAg han sido modificadas en su superficie con lectina, un ligando específico de las células M. Mediante microscopía confocal, Gupta y col. (79) han demostrado la intensa interacción entre los nanosistemas y las células M, lo que se ve reflejado en una mayor respuesta inmune humoral frente a la hepatitis B cuando se compara con el mismo sistema de nanopartículas que no presenta el ligando específico. Otros nanosistemas dirigidos a células M han sido recientemente descritos, por ejemplo, utilizando un ligando peptídico de la claudina 4 (proteína de las uniones íntimas entre las células epiteliales), el cual se ha conjugado al antígeno de influenza (HA) y posteriormente encapsulado en nanopartículas de PLGA (80). Aunque se determina una interacción importante con las placas de Peyer y el NALT, los autores concluyen que la exposición del antígeno sobre la superficie de la nanopartícula podría mejorar la interacción con las células diana. Por otro lado, Fievez y col. (81) postulan que la conjugación de un ligando no peptídico mejoraría la interacción con el epitelio gastrointestinal ya que se evitaría la degradación del mismo durante el tránsito digestivo al estar expuesto en la superficie de la nanopartícula. De este modo, conjugan el RGD peptidomimético (RGDp) (un ligando de la integrina β1 de las células M) a nanopartículas de PLGA a través de una cadena de PEG. El transporte a través de monocapas celulares *in vitro* (co-cultivos de Caco-2 y Raji) fue mayor para las nanopartículas con ligando, pero no se observaron diferencias entre el peptídico y el peptidomimético. Sin embargo, *in vivo*, la respuesta inmune sistémica frente a ovalbúmina (antígeno modelo) fue mayor en el caso de las nanopartículas con RGDp administradas intraduodenalmente, confirmando así la hipótesis de partida.

Otra interesante estrategia para mejorar la respuesta inmune tras la inmunización oral ha sido la co-encapsulación del antígeno con un

inmunoestimulante. En este caso, nanopartículas de quitosano recubiertas por alginato han demostrado su capacidad para ser captadas por las placas de Peyer sin mostrar signos de toxicidad (82) pudiendo ser *a priori* un buen sistema candidato para la inmunización oral. Sin embargo, ha sido necesaria la co-encapsulación del inmunoestimulador CpG ODN con el HBsAg para incrementar la respuesta inmune humoral y celular a través de esta vía (83). De hecho, se observa que es un factor fundamental el que se produzca una co-liberación simultánea del antígeno con el agente inmunoestimulante, ya que la administración del CpG ODN en solución con las nanopartículas no es capaz de ejercer una acción inmunoestimuladora suficiente para mejorar la respuesta inmune. La necesidad de la co-liberación con otra molécula inmunoestimulante (MPLA) también se ha visto con nanopartículas de PLGA (84). En este caso, el MPLA ayuda significativamente a aumentar los títulos de IgG específicos frente a ovalbúmina en suero con respecto a las nanopartículas sin MPLA. Además, a nivel de la mucosa gastrointestinal, la co-liberación de ovalbúmina y MPLA en nanopartículas de PLGA da lugar a una mayor secreción de IgA.

Por lo tanto, la incorporación del antígeno a un sistema de nanopartículas poliméricas podría ser una estrategia adecuada para su liberación a nivel intestinal. Sin embargo, como hemos descrito en este apartado, todavía es necesario optimizar los sistemas desarrollados hasta ahora.

Administración de nanovacunas por vía nasal

Entre las diferentes posibilidades para la vacunación a través de las superficies mucosas, además de la inmunización oral descrita previamente, la vía nasal es sin duda la opción más prometedora (85). El principal factor a tener en cuenta durante el desarrollo de una vacuna nasal es que el antígeno administrado pueda llegar a los órganos linfoides inductores que forman parte del NALT (adenoides) y a las células dendríticas que circulan en el área submucosa (**Figura 4**). Para ello, se deben superar las diversas barreras biológicas impuestas por la vía nasal: la

degradación enzimática, la presencia de mucus que recubre la cavidad nasal, la capa de células epiteliales y el aclaramiento mucociliar asociado. Teniendo esto en cuenta, mediante el diseño de un sistema de liberación adecuado se podría inducir y mejorar la respuesta inmune alcanzada a través de esta vía promoviendo la captación del antígeno por las células del sistema inmune innato de la zona (86).

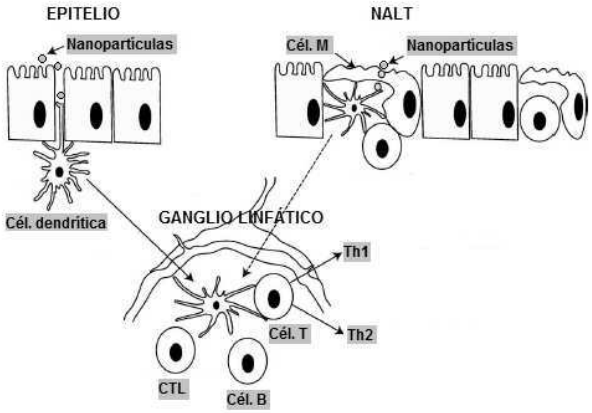

Figura 4: *Representación esquemática de como se produce la cascada de activación de la respuesta inmune específica tras la administración nasal de nanopartículas para la liberación de antígenos. Adaptado de (9).*

Entre las múltiples posibilidades para la liberación del antígeno a través de la vía nasal, diversos tipos de nanosistemas han sido estudiados para conseguir una respuesta inmunológica a través de esta vía (9). Sin embargo, es de especial interés el uso de sistemas nanoparticulados basados en biopolímeros como transportadores de antígenos. En concreto, aquellos basados en poliésteres (PLGA y PLA) y quitosano han sido los más ampliamente estudiados. Estos sistemas son especialmente prometedores debido a su demostrada capacidad para proteger las biomacromoléculas asociadas, promover la interacción y penetración a través de la mucosa nasal para finalmente conseguir el efecto terapéutico sistémico (72).

Las nanopartículas basadas en poliésteres han sido uno de los más prometedores candidatos para la liberación de vacunas a través de la vía nasal. Por ejemplo, resultados obtenidos por Jung y col. (77) indican que la aplicación nasal de nanopartículas de PLGA modificado con PVA reduce la dosis de toxoide tetánico necesario para alcanzar una respuesta inmune, comparando en este caso con la vía digestiva. Sin embargo, importantes problemas relativos a la inestabilidad del antígeno encapsulado en la matriz polimérica de PLGA y el limitado transporte a través de las superficies mucosas, ha dado lugar a una serie de modificaciones en la estructura de estos vehículos con el fin de solventar dichos inconvenientes. Las principales modificaciones que se han llevado a cabo se relacionan con la adición de sustancias estabilizadoras del antígeno y componentes hidrófilos que mejoren la estabilidad del sistema en los fluidos biológicos y permitan una mejor interacción con la mucosa nasal.

En nuestro laboratorio hemos podido comprobar que, con la introducción de un polímero anfifílico como el poloxamer en la estructura matricial de las nanopartículas de PLGA, se consigue preservar la antigenicidad del toxoide tetánico (87) ó del HBsAg encapsulado (29). Siguiendo esta estrategia se ha podido además asociar en nanopartículas formadas por mezclas de PLGA con poloxamer ó poloxamina, otro tipo de biomacromoléculas como plásmidos ADN codificadores de antígeno (88). Con estos sistemas se logra que el antígeno (β-galactosidasa) se exprese a partir del material genético encapsulado, tanto *in vitro* como *in vivo.* La inducción de una respuesta inmunológica específica frente a la β-galactosidasa indica que la molécula de ADN ha sido eficazmente transportada a través de la mucosa nasal, lo que verifica que se haya expresado el antígeno y consecuentemente, se ha logrado una respuesta inmune específica sistémica.

Por otro lado, se han desarrollado un tipo de nanopartículas que presentan una estructura núcleo-corona, compuestas por un núcleo hidrofóbico de PLA donde se encuentra el antígeno encapsulado, y una

cubierta hidrofílica de polietilenglicol (PEG), con el fin de mejorar la estabilidad del sistema en los fluidos biológicos al mismo tiempo que se mejora la interacción con el epitelio nasal (89). Este tipo de sistema ha demostrado ser un vehículo muy adecuado para la liberación tanto de antígenos como de plásmidos ADN codificadores de antígeno a través de la mucosa nasal y llegar a conseguir niveles importantes de IgG específica frente al toxoide tetánico y la β-galactosidasa, respectivamente (90). Una característica interesante de este sistema es que mediante la modificación del tamaño de partícula y la densidad de la cubierta hidrofílica de PEG, se puede optimizar la interacción con la mucosa nasal para incrementar el transporte de la molécula asociada a través de esta vía de administración (91).

La modificación de la superficie de nanopartículas de PLGA con un polímero hidrófilico, como el quitosano, también se ha llevado cabo con la finalidad de incrementar la interacción con la mucosa nasal debido fundamentalmente a las propiedades bioadhesivas de este polisacárido. En los estudios de biodistribución (92) que se han llevado a cabo tras el marcaje del toxoide tetánico con un radioisótopo, se puede observar una mayor presencia del toxoide en circulación sistémica cuando se administran las nanopartículas recubiertas con quitosano por la vía nasal comparadas con las nanopartículas sin cubierta. Este resultado indica la eficacia de la modificación superficial de las nanopartículas de PLGA con un polímero bioadhesivo para incrementar la interacción del sistema con la mucosa nasal. Sin embargo, en un estudio reciente donde se comparan nanopartículas de TMC, de PLGA y de PLGA recubiertas con TMC, se determina que solo las nanopartículas compuestas por TMC son capaces de generar respuestas humorales significativas (con respecto a los otros dos sistemas con PLGA), tanto a nivel sistémico como en la mucosa (93). Este resultado se atribuye a la mayor capacidad de las nanopartículas de TMC para estimular las células dendríticas inmaduras (comprobado *in vitro*) y a la prolongación del tiempo de residencia en la mucosa nasal, lo cual favorece una captación más eficiente del antígeno encapsulado por

parte de las células B locales. En un estudio posterior, se evaluó el mecanismo de inducción de la respuesta inmune por parte de estos sistemas administrados por vía nasal (94). En general, se pudo concluir que la composición del nanosistema afecta al tipo de inmunidad generada. Por ejemplo, las nanopartículas de TMC son capaces de generar una respuesta humoral importante debido a la mayor proliferación de células B en los ganglios linfáticos drenantes y en el bazo. Sin embargo, las nanopartículas basadas en PLGA dan lugar principalmente a una respuesta inmunosupresora, confirmada por la presencia de células T reguladoras en los ganglios linfáticos drenantes y en el bazo, así como la secreción de elevados niveles de IL-10, lo cual se podría ser beneficioso para el tratamiento de enfermedades autoinmunes. Por ejemplo, en un modelo animal de artritis se ha comprobado que las nanopartículas de PLGA y PLGA-TMC administradas por vía nasal son capaces de incrementar el efecto inmunosupresor del péptido Hsp70-peptide mB29 encapsulado, reduciendo notablemente la progresión de la enfermedad (94).

La trimetilación de los grupos amino del quitosano llevada a cabo en la molécula de TMC se ha realizado con la idea de mantener la solubilidad del polímero original (quitosano) en un amplio rango de pH manteniendo sus propiedades bioadhesivas, al mismo tiempo que permite la preparación de nanopartículas mediante gelificación iónica. Las nanopartículas elaboradas a partir de este derivado del quitosano, han sido también evaluadas como vehículos para la inmunización nasal frente a distintos antígenos, por ejemplo la hemaglutinina del virus de la influenza (95). Se han conseguido con este sistema, niveles importantes de IgG sérica y una fuerte inhibición de la hemaglutinación, junto con niveles significativos de IgA detectados en los lavados nasales, comparados con los alcanzados con el antígeno solo ó mezclado en una solución de polímero. Estos resultados se han atribuido principalmente a las propiedades mucoadhesivas del polímero que permiten una exposición más prolongada del antígeno, así como a la naturaleza particulada del sistema que mejora

el acceso al NALT y a los ganglios linfáticos. En un sistema más sencillo constituido por partículas del HBsAg (22 nm) cubiertas por TMC o quitosano, se ha determinado la superioridad del recubrimiento con TMC para estimular las células dendríticas *in vitro* (sobreexpresión de MHC clase II y CD86). Sin embargo, tras la administración nasal, el recubrimiento con quitosano favorece la inducción de una mayor respuesta inmune sistémica y mucosa, comparado con el TMC o el HBsAg solo, lo cual se atribuye principalmente a un transporte más efectivo de los sistemas recubiertos con quitosano a través de la mucosa nasal (96).

Con la idea de evaluar los posibles factores que afectan a la eficacia de las nanopartículas de quitosano como sistemas de liberación de antígeno, se ha estudiado el comportamiento de diversos sistemas elaborados mediante gelificación iónica a partir de quitosano de diferente peso molecular (97). Con los diferentes sistemas evaluados, se consigue una respuesta inmune prolongada frente al toxoide tetánico que se incrementa con el tiempo, lo que demuestra que las nanopartículas de quitosano son capaces de facilitar la liberación del antígeno a las CPA a través de la mucosa nasal y generar una importante respuesta inmune específica. Al mismo tiempo se aprecian ciertas diferencias relacionadas con el peso molecular del quitosano que se ha utilizado en cada formulación testada, de forma que tanto los niveles de IgG e IgA han sido significativamente mayores cuando el quitosano presenta un peso molecular superior. Nanopartículas formuladas con quitosano de alto peso molecular también se han utilizado para encapsular el HBsAg para su liberación intranasal (68). Con este sistema se han conseguido niveles moderados de anticuerpos específicos en suero que no dependen de la dosis administrada (10 ó 20 μg). La menor efectividad de estas nanopartículas en contraste con las nanopartículas encapsulando el toxoide tetánico, por ejemplo (97), se ha atribuido principalmente a la mayor complejidad del HBsAg (comparado con el toxoide, que es una proteína soluble) y a las diferentes interacciones con el polímero que dan lugar a una importante reducción del potencial ζ del sistema, lo cual podría afectar a la interacción con el epitelio de la mucosa nasal y, en

consecuencia, al transporte del antígeno. Para mejorar la respuesta inmune frente a HBsAg, Borges y col. (98) desarrollaron un sistema basado en nanopartículas de quitosano que asocian HBsAg en su superficie y posteriormente son recubiertas con alginato con el objetivo de mejorar la estabilidad del mismo y modular su liberación. Este sistema fue capaz de aumentar la respuesta inmune sistémica con respecto al antígeno solo tras la administración nasal. Sin embargo a pesar de ello, para potenciar la inducción de una respuesta sistémica significativa fue necesaria la co-administración de un inmunoestimulante, como es el CpG ODN, en solución.

Por lo tanto, el uso de sistemas de liberación nanométricos basados en biomateriales, han demostrado que pueden mejorar la respuesta inmune frente al antígeno que transportan cuando se administran a través de una vía no invasiva, como es la vía nasal. Los resultados obtenidos hasta hoy con los diferentes nanosistemas evaluados han sido muy prometedores, y se ha demostrado que modificaciones en la estructura de los nanosistemas que lleven a incrementar su estabilidad y/o la interacción con la mucosa nasal, facilitan de forma importante el éxito del sistema para alcanzar respuestas inmunes específicas importantes, tanto sistémicas como a nivel de la mucosa.

Por lo tanto, en los últimos años las nanovacunas han contribuido de forma importante al desarrollo de vacunas, ofreciendo un gran potencial no solo en el diseño de nuevos adyuvantes, sino también para vacunas de dosis única y "needle-free" (administración sin agujas), debido principalmente a la versatilidad de estos sistemas (por ejemplo, uso de una amplia variedad biomateriales, capacidad de asociación de distintas moléculas antigénicas e inmunoestimulantes, etc.), a su capacidad para prolongar la liberación del antígeno en el tiempo y a sus propiedades de penetración a través de barreras mucosas.

REFERENCIAS

1. Ryan EJ, Daly LM & Mills KHG (2001) Immunomodulators and delivery systems for vaccination by mucosal routes. *Trends Biotechnol* 19: 293-303.

2. O'Hagan DT & Rappuoli R (2004) Novel approaches to vaccine delivery. *Pharm Research* 21: 1519-1529.

3. Wilson-Welder JH, *et al* (2009) Vaccine adjuvants: Current challenges and future approaches. *J Pharm Sci* 98: 1278-1316.

4. Clements CJ & Griffiths E (2002) The global impact of vaccines containing aluminium adjuvants. *Vaccine* 20: S24-S33.

5. Zapata MI, Peck GE, Hem SL, White JL & Feldkamp JR (1984) Mechanism of freeze-thaw instability of aluminum hydroxycarbonate and magnesium hydroxide gels. *J Pharm Sci* 73: 3-9.

6. Brewer JM (2006) (How) do alumiun adjuvants work? *Immunol Lett* 102: 10-15.

7. EMA (2012) European medicines agency (science, medicine, health). *www ema europa eu*

8. Peek LJ, Middaugh CR & Berkland C (2008) Nanotechnology in vaccine delivery. *Adv Drug Deliver Rev* 60: 915-928.

9. Csaba N, Garcia-Fuentes M & Alonso MJ (2009) Nanoparticles for nasal vaccination. *Adv Drug Deliv Rev* 61: 140-157.

10. Vicente S, Prego C, Csaba N & Alonso MJ (2010) From single-dose vaccine delivery systems to nanovaccines. *J Drug Deliv Sci Technol* 20: 267-276.

11. Correia-Pinto JF, Csaba N & Alonso MJ (2013) Vaccine delivery carriers: Insights and future perspectives. *Int J Pharm 440*: 27-38.

12. Storni T, Kündig TM, Senti G & Johansen P (2005) Immunity in response to particulate antigen-delivery systems. *Adv Drug Deliver Rev* 57: 333-355.

13. De Temmerman M, *et al* (2011) Particulate vaccines: On the quest for optimal delivery and immune response. *Drug Discov Today* 16: 569-582.

14. Borges O, *et al* (2008) Alginate coated chitosan nanoparticles are an effective subcutaneous adjuvant for hepatitis B surface antigen. *Int Immunopharmacol* 8: 1773-1780.

15. Preis I & Langer R (1979) A single-step immunization by sustained antigen release. *J Immunol Methods* 28: 193-197.

16. Aguado MT (1993) Future approaches for vaccine development - single-dose vaccines using controlled-release delivery systems. *Vaccine* 11: 596-597.

17. Tobio M, *et al* (1999) Improved immunogenicity of a core-coated tetanus toxoid delivery system. *Vaccine* 18: 618-622.

18. Jaganathan KS & Vyas SP (2006) Strong systemic and mucosal immune responses to surface-modified PLGA microspheres containing recombinant hepatitis B antigen administered intranasally. *Vaccine* 24: 4201-4211.

19. Feng L, *et al* (2006) Pharmaceutical and immunological evaluation of a single-dose hepatitis B vaccine using PLGA microspheres. *J Control Release* 112: 35-42.

20. Davis SS (2006) The use of soluble polymers and polymer microparticles to provide improved vaccine reponses after parenteral and mucosal delivery. *Vaccine* 24: 7-10.

21. Alonso MJ, *et al* (1993) Determinants of release rate or tetanus vaccine from polyester microspheres. *Pharm Research* 10: 945-953.

22. Sánchez A, Gupta RK, Alonso MJ, Siber GR & Langer R (1996) Pulsed controlled-release system for potential use in vaccine delivery. *J Pharm Sci* 85: 547-552.

23. Xiang SD, *et al* (2006) Pathogen recognition and development of particulate vaccines: Does size matter? *Methods* 40: 1-9.

24. Orive G, Gascón AR, Hernández RM, Domínguez-Gil RA & Pedraz JR (2004) Techniques: New approaches to the delivery of biopharmaceuticals. *Trends Pharmacol Sci* 25: 382-387.

25. Daftarian P, *et al* (2011) Peptide-conjugated PAMAM dendrimer as a universal DNA vaccine platform to target antigen-presenting cells. *Cancer Res* 71: 7452-7462.

26. Henriksen-Lacey M, *et al* (2010) Liposomal cationic charge and antigen adsorption are important properties for the efficient deposition of antigen at the injection site and ability of the vaccine to induce a CMI response. *J Control Release* 145: 102-108.

27. Vicente S, *et al* (In press) A polymer/oil based nanovaccine as a single-dose immunization approach

28. Black M, *et al* (2012) Self-assembled peptide amphiphile micelles containing a cytotoxic T-cell epitope promote a protective immune response *in vivo*. *Adv Mater* 24: 3845-3849.

29. Paolicelli P, Prego C, Sanchez A & Alonso MJ (2010) Surface-modified PLGA-based nanoparticles that can efficiently associate and deliver virus-like particles. *Nanomed* 5: 843-853.

30. Bachmann MF & Jennings GT (2010) Vaccine delivery: A matter of size, geometry, kinetics and molecular patterns. *Nat Rev Immunol* 10: 787-796.

31. Neutra MR & Kozlowski PA (2006) Mucosal vaccines: The promise and the challenge. *Nat Rev Immunol* 6: 148-158.

32. Des Rieux A, Fievez V, Garinot M, Schneider YJ & Préat V (2006) Nanoparticles as potential oral delivery systems of proteins and vaccines: A mechanistic approach. *J Control Release* 116: 1-26.

33. Reddy ST, Swartz MA & Hubbell JA (2006) Targeting dendritic cells with biomaterials: Developing the next generation of vaccines. *Trends Immunol* 27: 573-579.

34. Mutwiri G, *et al* (2007) Poly[di(sodium carboxylatoethylphenoxy)phosphazene] (PCEP) is a potent enhancer of mixed Th1/Th2 immune responses in mice immunized with influenza virus antigens. *Vaccine* 25: 1204-1213.

35. Zwiorek K, *et al* (2008) Delivery of cationic gelatin nanoparticles strongly increases the immunostimulatory effects of CpG oligonucleotides. *Pharm Research* 25: 551-562.

36. Manolova V*, et al* (2008) Nanoparticles target distinct dendritic cell populations according to their size*. J Immunol* 38: 1404-1413.

37. Zolnik BS, Gonzalez-Fernandez A, Sadrieh N & Dobrovolskaia MA (2010) Minireview: Nanoparticles and the immune system*. Endocrinology* 151: 458-465.

38. Banchereau J & Steinman RM (1998) Dendritic cells and the control of immunity*. Nature* 392: 245-252.

39. Panyam J & Labhasetwar V (2003) Biodegradable nanoparticles for drug and gene delivery to cell and tissue*. Adv Drug Deliver Rev* 55: 329-347.

40. Kovacsovics-Bankowski M & Rock KL (1995) A phagosome-to-cytosol pathway or exogenous antigens presented on MHC class I molecules*. Science* 267: 243-246.

41. Elemanchili P, Diwan M, Cao M & Samuel J (2004) Characterization of poly(d,l-lactic-co-glycolic acid) based nanoparticulate system for enhanced delivery of antigens to dendritic cells*. Vaccine* 22: 2406-2412.

42. Ma W*, et al* (2012) PLGA nanoparticle-mediated delivery of tumor antigenic peptides elicits effective immune responses*. Int J Nanomed* 7: 1475-1487.

43. Cruz LJ, Tacken PJ, Fokkink R & Figdor CG (2011) The influence of PEG chain length and targeting moiety on antibody-mediated delivery of nanoparticle vaccines to human dendritic cells*. Biomaterials* 32: 6791-6803.

44. Coester C, Nayyar P & Samuel J (2006) *In vitro* uptake of gelatin nanoparticles by murine dendritic cells and their intracellular localisation*. Eu J Pharm Biopharm* 62: 306-314.

45. Kerkmann M*, et al* (2006) Immunostimulatory properties of CpG-oligonucleotides are enhanced by the use of protamine nanoparticles*. Oligonucleotides* 26: 313-322.

46. Akagi T, Wang X, Uto T, Baba M & Akashi M (2007) Protein direct delivery to dendritic cells using nanoparticles based on amphiphilic poly(amino acid) derivatives*. Biomaterials* 28: 3427-3426.

47. Uto T*, et al* (2011) Comparative activity of biodegradable nanoparticles with aluminum adjuvants: Antigen uptake by dendritic cells and induction of immune response in mice*. Immunol Lett* 140: 36-43.

48. Elemanchili P, Lutsiak CM, Hamdy S, Diwan M & Samuel J (2007) "Pathogen-mimicking" nanoparticles for vaccine delivery to dendritic cells*. J Immunother* 30: 378-395.

49. Ma Y*, et al* (2011) The role of surface charge density in cationic liposome promoted dendritic cell maturation and vaccine-induced immune responses*. Nanoscale* 3: 2307-2314.

50. Foged C, Brodin B, Frokjaer S & Sundblad A (2005) Particle size and surface charge affect particle uptake by human dendritic cells in an in vitro model*. Int J Pharm* 298: 315-322.

51. Han R, Zhu J, Yang X & Xu H (2011) Surface modification of poly(D,L-lactic-co-glycolic acid) nanoparticles with protamine enhanced cross-presentation of encapsulated ovalbumin by bone marrow-derived dendritic cells*. J Biomed Mater Res Part A* 96A: 142-149.

52. Bal SM*, et al* (2010) Efficient induction of immune responses through intradermal vaccination with N-trimethyl chitosan containing antigen formulations*. J Control Release* 142: 374-383.

53. Zaki NM, Nasti A & Tirelli N (2011) Nanocarriers for cytoplasmic delivery: Cellular uptake and intracellular fate of chitosan and hyaluronic acid-coated chitosan nanoparticles in a phagocytic cell model*. Macromol Biosci* 11: 1747-1760.

54. Dobrovolskaia MA & Mcneil SE (2007) Immunological properties of engineered nanomaterials*. Nat Nanotechnol* 2: 469-478.

55. Birrenbach G & Speiser PP (1976) Polymerized micelles and their use as adjuvants in immunology*. J Pharm Sci* 65: 1763-1766.

56. Katare YK, Panda AK, Lalwani K, Haque IU & Ali MM (2003) Potentiation of immune response from polymer-entrapped antigen: Toward development of single dose tetanus toxoid vaccine*. Drug Deliv* 10: 231-238.

57. Raghuvanshi RS, *et al* (2002) Improved immune response from biodegradable polymer particles entrapping tetanus toxoid by use of different immunization protocol and adjuvants. *Int J Pharm* 245: 109-121.

58. Lamalle-Bernard D, *et al* (2006) Coadsorption of HIV-1 p24 and gp120 proteins to surfactant-free anionic PLA nanoparticles preserves antigenicity and immunogenicity. *J Control Release* 115: 57-67.

59. Demento SL, *et al* (2009) Inflammasome-activating nanoparticles as modular systems for optimizing vaccine efficacy. *Vaccine* 27: 3013-3021.

60. Hamdy S, *et al* (2008) Co-delivery of cancer-associated antigen and toll-like receptor 4 ligand in PLGA nanoparticles induces potent CD8(+) T cell-mediated anti-tumor immunity. *Vaccine* 26: 5046-5057.

61. Akagi T, Baba M & Akashi M (2012) Biodegradable nanoparticles as vaccine adjuvants and delivery systems: Regulation of immune responses by nanoparticle-based vaccine. *Adv Polym Sci* 247: 31-64.

62. Uto T, *et al* (2009) Improvement of adaptive immunity by antigen-carrying biodegradable nanoparticles. *Biochem Biophys Res Commun* 379: 600-604.

63. Yamaguchi S, *et al* (2010) EphA2-derived peptide vaccine with amphiphilic poly(gamma-glutamic acid) nanoparticles elicits an anti-tumor effect against mouse liver tumor. *Cancer Immunol Immunother* 59: 759-767.

64. Wang X, Uto T, Akagi T, Akashi M & Baba M (2008) Poly(gamma-glutamic acid) nanoparticles as an efficient antigen delivery and adjuvant system: Potential for an AIDS vaccine. *J Med Virol* 80: 11-19.

65. Jabbal-Gill I, Watts P & Smith A (2012) Chitosan-based delivery systems for mucosal vaccines. *Expert Opin Drug Deliv* 9: 1051-1067.

66. Zaharoff DA, Rogers CJ, Hance KW, Schlom J & Greiner JW (2007) Chitosan solution enhances both humoral and cell-mediated immune responses to subcutaneous vaccination. *Vaccine* 25: 2085-2094.

67. Villiers C, *et al* (2009) From secretome analysis to immunology. Chitosan induces major alterations in the activation of dendritic cells via a TLR4-dependent mechanism. *Mol Cell Proteomics* 8: 1252-1264.

68. Prego C, *et al* (2010) Chitosan-based nanoparticles for improving immunization against hepatitis B infection. *Vaccine* 28: 2607-2614.

69. Wen Z, Xu Y, Zou X & Xu Z (2011) Chitosan nanoparticles act as an adjuvant to promote both Th1 and Th2 immune responses induced by ovalbumin in mice. *Marine Drugs* 9: 1038-1055.

70. Weber C, *et al* (2010) Polysaccharide-based vaccine delivery systems: Macromolecular assembly, interactions with antigen presenting cells, and *in vivo* immunomonitoring. *J Biomed Mater Res Part A* 93A: 1322-1334.

71. Guidice EL & Campbell JD (2006) Needle-free vaccine delivery. *Adv Drug Deliver Rev* 58: 68-89.

72. De la Fuente M, Csaba N, Garcia-Fuentes M & Alonso MJ (2008) Nanoparticles as protein and gene carriers to mucosal surfaces. *Nanomed* 3: 845-857.

73. Prego C, García M, Torres D & Alonso MJ (2005) Transmucosal macromolecular drug delivery. *J Control Release* 101: 151-162.

74. Oyarzun-Ampuero FA, Garcia-Fuentes M, Torres D & Alonso MJ (2010) Chitosan-coated lipid nanocarriers for therapeutic applications. *J Drug Deliv Sci Tec* 20: 259-265.

75. Garcia-Fuentes M & Alonso MJ (2012) Chitosan-based drug nanocarriers: Where do we stand? *J Control Release* 161: 496-504.

76. O'Hagan DT (1996) The intestinal uptake and the implications for drug and antigen delivery. *J Anat* 189: 447-482.

77. Jung T, *et al* (2001) Tetanus toxoid loaded nanoparticles from sulfobutylated poly(vinyl alcohol)-graft-poly(lactide-co-glycolide): Evaluation of antibody response after oral and nasal application in mice. *Pharm Research* 18: 352-360.

78. Jain AK, *et al* (2010) PEG–PLA–PEG block copolymeric nanoparticles for oral immunization against hepatitis B. *Int J Pharm* 387: 253-262.

79. Gupta PN, Khatri K, Goyal AK, Mishra N & Vyas SP (2007) M-cell targeted biodegradable PLGA nanoparticles for oral immunization agains hepatitis B. *J Drug Target* 15: 701-713.

80. Rajapaksa TE, Stover-Hamer M, Fernandez X, Eckelhoefer HA & Lo DD (2010) Claudin 4-targeted protein incorporated into PLGA nanoparticles can mediate M cell targeted delivery. *J Control Release* 142: 196-205.

81. Fievez V, *et al* (2009) Targeting nanoparticles to M cells with non-peptidic ligands for oral vaccination. *Eur J Pharm Biopharm* 73: 16-24.

82. Borges O, *et al* (2006) Uptake studies in rat Peyer's patches, cytotoxicity and release studies of alginate coated chitosan nanoparticles for mucosal vaccination. *J Control Release* 114: 348-358.

83. Borges O, *et al* (2007) Evaluation of the immune response following a short oral vaccination schedule with hepatitis B antigen encapsulated into alginate-coated chitosan nanoparticles. *Eur J Pharm Sci* 32: 278-290.

84. Sarti F, *et al* (2011) *In vivo* evidence of oral vaccination with PLGA nanoparticles containing the immunostimulant monophosphoryl lipid A. *Biomaterials* 32: 4052-4057.

85. Davis SS (2001) Nasal vaccines. *Adv Drug Deliver Rev* 51: 21-42.

86. Slutter B, Hagenaars N & Jiskoot W (2008) Rational design of nasal vaccines. *J Drug Target* 16: 1-17.

87. Tobio M, Nolley J, Guo Y, McIver J & Alonso MJ (1999) A novel system based on a poloxamer/PLGA blend as a tetanus toxoid delivery vehicle. *Pharm Research* 16: 682-688.

88. Csaba N, Sánchez A & Alonso MJ (2006) PLGA:Poloxamer and PLGA:Poloxamine blend nanostructrues as carriers for nasal gene delivery. *J Control Release* 113: 164-172.

89. Tobio M, Gref R, Sánchez A, Langer R & Alonso MJ (1998) Stealth PLA-PEG nanoparticles as nasal protein delivery systems. *Pharm Research* 15: 275.

90. Vila A, Sánchez A, Pérez C & Alonso MJ (2002) PLA-PEG nanospheres: New carriers for transmucosal delivery of proteins and plasmid DNA. *Polym Advan Technol* 13: 851-858.

91. Vila A, Gill H, McCallion O & Alonso MJ (2004) Transport of PLA-PEG particles across the nasal mucosa: Effect of particle size and PEG coating density. *J Control Release* 98: 231-244.

92. Vila A, Sánchez A, Tobío M, Calvo P & Alonso MJ (2002) Design of biodegradable particles for protein delivery. *J Control Release* 78: 15-24.

93. Slutter B, *et al* (2010) Nasal vaccination with N-trimethyl chitosan and PLGA based nanoparticles: Nanoparticle characteristics determine quality and strength of the antibody response in mice against the encapsulated antigen. *Vaccine* 28: 6282-6291.

94. Keijzer C, *et al* (2011) PLGA, PLGA-TMC and TMC-TPP nanoparticles differentially modulate the outcome of nasal vaccination by inducing tolerance or enhancing humoral immunity. *PLOS One* 6: e26684.

95. Amidi M, *et al* (2007) N-trimethyl chitosan (TMC) nanoparticles loaded with influenza subunit antigen for intranasal vaccination: Biological properties and immunogenicity in mouse model. *Vaccine* 25: 144-153.

96. Tafaghodi M, *et al* (2012) Hepatitis B surface antigen nanoparticles coated with chitosan and trimethyl chitosan: Impact of formulation on physicochemical and immunological characteristics. *Vaccine* 30: 5341-5348.

97. Vila A, *et al* (2004) Low molecular weight chitosan nanoparticles as new carriers for nasal vaccine delivery in mice. *Eur J Pharm Biopharm* 57: 123-131.

98. Borges O, *et al* (2008) Immune response by nasal delivery of hepatitis B surface antigen and codelivery of a CpG ODN in alginate coated chitosan nanoparticles. *Eur J Pharm Biopharm* 69: 405-416.

Antecedentes, hipótesis y objetivos

ANTECEDENTES

1. La nanotecnolgía se ha perfilado como una estrategia prometedora en el diseño de nuevas formulaciones de vacunas (nanovacunas) o para mejorar las vacunas ya existentes[1], ofreciendo interesantes ventajas como: (i) mejorando la interacción del antígeno con las células del sistema inmune y promoviendo su migración hacia los órganos linfoides secundarios [2] y (ii) mejorando el transporte del antígeno a través de barreras mucosas, protegiéndolo frente a la degradación enzimática y facilitando su acercamiento a las células inmunes del tejido submucoso[3].

2. La estructura versátil de las nanocápsulas, constituidas por una cubierta polimérica hidrofílica y un núcleo oleoso hidrofóbico, permite la co-asociación de antígenos y moléculas inmunoestimuladoras en el mismo vehículo.

3. El quitosano es un polisacárido natural de carácter catiónico capaz formar nanostructuras mediante procedimientos sencillos[4], además de conferirles propiedades biofarmacéuticas tales como la bioadhesividad, la promoción de la penetración de las moléculas asociadas[5] y la estimulación del sistema immune[6,7].

---

[1] **Vicente S et al.** (2010) From single-dose vaccine delivery systems to nanovaccines. *J Drug Deliv Sci Technol* 20: 267-276.

[2] **Bachmann MF & Jennings GT** (2010) Vaccine delivery: A matter of size, geometry, kinetics and molecular patterns. *Nat Rev Immunol* 10: 787-796.

[3] **Csaba N et al.** (2009) Nanoparticles for nasal vaccination. *Adv Drug Deliv Rev* 61: 140-157

[4] **Calvo et al.** (1996) Polyester nanocapsules as new topical ocular delivery systems for cyclosporin A. *Pharm Research* 13: 311-315

[5] **Garcia-Fuentes M & Alonso MJ** (2012) Chitosan-based drug nanocarriers: Where do we stand? *J Control Release* 161: 496-504.

[6] **Zaharoff DA et al.** (2007) Chitosan solution enhances both humoral and cell-mediated immune responses to subcutaneous vaccination. *Vaccine* 25: 2085-2094.

[7] **Bal SM et al.** (2010) Efficient induction of immune responses through intradermal vaccination with N-trimethyl chitosan containing antigen formulations. *J Control Release* 142: 374-383

4. Las emulsiones basadas en escualeno han sido la primera formulación adyuvante aprobada para su uso en humanos (solo en Europa) después de las sales de aluminio. Sin embargo, en estas nanoemulsiones el antígeno se encuentra disperso en la fase acuosa sin darse ningún tipo de interacción con los glóbulos oleosos[8].

[8] **O'Hagan DT et al.** (2012) The mechanism of action of MF59 - an innately attractive adjuvant formulation. *Vaccine* 30: 4341-4348.

HIPÓTESIS

1. Las nanocápsulas constituidas por un núcleo oleoso y una cubierta de quitosano pueden resultar una estrategia adecuada para la presentación del antígeno en la superficie del sistema al mismo tiempo que permiten la encapsulación de moléculas inmunoestimulantes.

2. Las nanocápsulas de quitosano pueden facilitar la captación del antígeno por las células presentadoras de antígeno, al mismo tiempo que se puede producir una co-liberación del antígeno con la molécula inmunoestimulante asociada en el mismo vehículo, pudiendo dar lugar a una potenciación de la respuesta inmune.

3. La mejor interacción con las células presentadoras de antígeno puede dar lugar a una mayor migración hacia los órganos linfoides secundarios (ganglios linfáticos) para iniciar la respuesta inmune adaptada. Por tanto, la biodistribución de las nanocápsulas de quitosano puede influir en la generación y duración de la respuesta inmune.

4. Las nanocápsulas de quitosano pueden también favorecer el transporte del antígeno a través de las barreras mucosas para llegar a los lugares de inducción situados en el tejido submucoso ó en los tejidos linfoides asociados a mucosas (NALT) y así dar lugar a respuestas inmunológicas sistémicas.

OBJETIVOS

Teniendo en cuenta los antecedentes expuestos y las hipótesis planteadas, el objetivo global de la presente memoria ha sido el desarrollo de un sistema adyuvante de vacunas basado en nanocápsulas de quitosano, capaz de potenciar y modular respuestas inmunes específicas tras su administración por vía parenteral ó a través de una vía no invasiva, como es la nasal. Para lograr este objetivo se han planteado las siguientes etapas:

Desarrollo de las nanocápsulas de quitosano como sistema adyuvante de antígenos subunidad y como sistema de vacunación en dosis única.

1. Estudio del efecto de las propiedades superficiales del sistema cuando se asocia el antígeno modelo (antígeno recombinante de la hepatitis B) a la superficie de las nanocápsulas de quitosano, sobre la potenciación y duración de la respuesta inmune incluso cuando se administran en una sola dosis. Estos resultados aparecen recogidos en el capítulo 2 de la memoria.

2. Estudio de la versatilidad del sistema mediante la asociación de diversos tipos de antígenos y estudio de la co-liberación con un inmunoestimulante, como es el imiquimod, encapsulado en el núcleo oleoso del sistema.Estos resultados aparecen recogidos en el capítulo 4 de la memoria.

3. Evaluación del mecanismo de acción de las nanocápsulas de quitosano mediante el uso de técnicas de imagen gammagráficas. Estos resultados aparecen recogidos en el capítulo 5 de la memoria.

Desarrollo de las nanocápsulas de quitosano como sistemas transportadores de antígenos subunidad a través de las barreras mucosas

4. Evaluación de la capacidad de nanocápsulas quitosano para generar y modular respuestas inmunes sistémicas tras la administración nasal. Estos resultados aparecen recogidos en el capítulo 3 de la memoria.

CAPÍTULO 2

CAPÍTULO 2

A polymer/oil based nanovaccine as a single-dose immunization approach

Este trabajo ha sido realizado en colaboración con: Belén Díaz-Freitas[1], Mercedes Peleteiro[1], David W. Pascual[2,3] y África González-Fernández[1].

[1]Immunology, Biomedical Research Center (CINBIO), University of Vigo, 36310 Campus Lagoas de Marcosende, Vigo, Spain.

[2]Department of Immunology & Infectious Diseases, Montana State University, Bozeman, MT 59717-3610, USA.

[3]Department of Infectious Diseases & Pathology, University of Florida, Gainesville, FL 32608, USA.

ABSTRACT

The recognized necessity for new antigen delivery carriers with the capacity to boost, modulate and prolong neutralizing immune responses prompted our approach, in which we describe a multifunctional nanocarrier consisting of an oily nanocontainer protected by a polymeric shell made of chitosan (CS), named CS nanocapsules (CSNC). The CS shell can associate the antigen on its surface, whereas the oily core might provide additional immunostimulating properties. In this first characterization of the system, we intended to study the influence of different antigen organizations on the nanocarrier's surface (using the recombinant hepatitis B surface antigen –rHBsAg- as a model antigen) on their immune-potentiating effect, without any additional immunostimulant. Thus, two prototypes of antigen-loaded CSNC (CSNC+ and CSNC-), exhibiting similar particle size (200 nm) and high antigen association efficiency (>80%), were developed with different surface composition (polymer/antigen ratios) and surface charge (positive/negative, respectively). The biological evaluation of these nanovaccines evidenced the superiority of the CSNC+ as compared to CSNC- and alum-rHBsAg in terms of neutralizing antibody responses, following intramuscular vaccination. Moreover, a single dose of CSNC+ led to similar IgG levels to the positive control. The IgG1/IgG2a ratio suggested a mixed Th1/Th2 response elicited by CSNC+, in contrast to the typical Th2-biased response of alum. Finally, CSNC+ could be freeze-dried without altering its physicochemical properties and adjuvant effect *in vivo*. In conclusion, the evaluation of CSNC+ confirms its interesting features for enhancing, prolonging and modulating the type of immune response against subunit antigens, such as rHBsAg.

INTRODUCTION

Aluminum salts (alum), mainly in the form of aluminum hydroxide ($Al(OH)_3$) or aluminum phosphate ($AlPO_4$), have been traditionally used worldwide (since 1930s) as adjuvants in many vaccines (1). Unfortunately, despite their wide use, these adjuvants exhibit important drawbacks, such as inflammatory reactions at the injection site, irreversible loss of potency upon freezing and induction of strong biased Th2-type immune responses (2). Consequently, many efforts have been oriented to the search of new adjuvants and delivery carriers, which could help induce, strengthen, and simultaneously prolong the immune response. Ideally, the delivery carrier could also contribute to the development of single-dose vaccines capable of generating protective immunity upon only one antigenic exposure. This is especially relevant for subunit antigens, characterized by their improved safety profile, but low immunogenicity, which usually require multiple doses to assure immunological protection (3).

A promising strategy towards this goal relies in the design of polymeric nanocarriers, which are known to protect the associated antigen from degradation, facilitate antigen uptake by antigen-presenting cells (APCs), and control antigen release (4). Within this frame, the increasing understanding of the influence of the nanocarrier characteristics (composition, size, charge) on their effectiveness is gradually paving the way to the rational design of nanovaccines (5). For instance, both size and surface properties of polymeric nanocarriers are known to have a critical influence on the uptake and activation of APCs (6) and, ultimately, on the type of immune response generated (preferentially cellular vs. humoral) (7, 8).

Chitosan (CS) is one of the most commonly used biomaterials in vaccine delivery. So far its use has been found particularly promising for mucosal immunization because of its mucoadhesive and penetration enhancing properties (9). In fact, chitosan itself, as a dry powder mixed with monophosphoryl lipid A (MPLA) and the antigen, is currently ongoing

phase I of clinical evaluation for intranasal vaccination against norovirus (10, 11). On the other hand, our group, among others, has developed CS nanoparticles specifically adapted for the protection and delivery of antigens (12). In particular, CS nanoparticles have demonstrated great potential for nasal vaccination (13-17). Recently, their application as vaccine adjuvants has also been investigated against a variety of protein and DNA-encoded antigens (14, 18-21), suggesting additional immunological properties of these CS-based nanocarriers.

Taking this background information into account, the aim of our work has been to design a new CS-based nanocarrier that might offer advanced properties in terms of antigen localization and the possibility to incorporate additional immunomodulating agents. This new nanocarrier, named CS nanocapsules (CSNC), has a core-corona architecture, which enables the surface presentation of different types of antigens, while co-delivering immunoactive molecules included in the oily core. However, in the present work, we intended to study the effect of the organization of the antigen molecules on the nanocarrier's surface, without including any additional immunostimulant, on their ability to promote antigen specific immune responses. For this purpose, we have selected the recombinant hepatitis B surface antigen (rHBsAg, since now HB in the text) as a model antigen, which could benefit from this technology. Therefore, in our aim to explore the potential of CSNC as adjuvant and single-dose vaccine formulation, we have developed and evaluated different HB-surface assembled CSNC exhibiting different surface characteristics (both surface charge and composition) Overall, we have designed a formulation able to elicit long-lasting and protective immune responses against subunit antigens, such as the HB, in order to offer an alternative to alum as adjuvant agent, as well as possibly reduce the number of doses to elicit immune protection.

MATERIALS AND METHODS

Ethics statement

Immunization studies involving fresh formulations of CSNC prototypes were conducted in the University of Vigo (Spain), and all protocols were adapted to the guidelines of the Spanish regulations (Royal Decree 1201/2005) regarding the use of animals in scientific research and under ried CSNC+ (trehalose 5%), the dried formulation was properly arranged and the approval of the ethical committee of the University of Vigo. In the case of freeze-dipped to Montana State University (Bozeman, MT) where the biological evaluation was performed. All animal care and procedures were in accordance with institutional policies for animal health and well-being and approved by Montana State University Institutional Animal Care and Use Committee.

Female BALB/c mice (4-5 weeks old) were housed in filter-top cages in a 12 h light/12 h dark cycle with constant temperature environment of 22º C and provided with food and water *ad libitum*.

Materials

Ultrapure chitosan (CS) hydrochloride salt (Protasan UP CL 113, MW 125 kDa, acetylation degree of 14%) was purchased from Novamatrix (Sandvika, Norway). Miglyol® 812 (M812) is a neutral oil composed of triglycerides of medium chain fatty acids (6-8 C) and was donated by Sasol Germany GmbH (Witten, Germany). The emulsifier soybean L-α-lecithin Epikuron 145V was a gift from Cargill (Barcelona, Spain). The recombinant hepatitis B surface antigen (rHBsAg or HB) (MW 24 kDa) was kindly donated by Shantha Biotechnics Ltd (Hyderabad, India) as an aqueous suspension in PBS containing a protein concentration of 0.16 mg/ml.

Preparation of HB-surface-assembled chitosan nanocapsules and physicochemical characterization.

Blank chitosan nanocapsules (CSNC) were prepared by the solvent displacement technique, as previously reported (22). The formation of

HB-surface-assembled CSNC was achieved by the strong electrostatic interaction between the cationic polysaccharidic surface of CSNC and the negatively charged particle antigen (-20 mV in water). For this purpose, HB stock solution was desalted and concentrated to 0.5 mg/mL by ultrafiltration (Amicon Ultra4, Millipore; Cork, Ireland). The resulting HB aqueous solution was immediately mixed with blank CSNC (CS concentration 1 mg/mL) and incubated for 1 hour at room temperature. Several nanosystems were prepared following two different strategies: 1) increasing the antigen amount (25, 50, 100, 250 μg) in the formulation or 2) maintaining constant the antigen amount (25 μg), but changing the CSNC concentration. Following these two methods, it was possible to prepare a series of nanosystems defined by their CSNC:HB ratio, ranging from 1:0.025 to 1:0.25.

The particle size and polydispersity index were measured by photon correlation spectroscopy (PCS) and ζ potential by laser doppler anemometry (LDA).

Quantification of HB association to CSNC

The amount of HB associated to CSNC surface was indirectly quantified by measuring the concentration of free antigen remaining in supernatant after ultracentrifugation (42000xg, 1h, 15ºC) of the nanostructures. An ELISA commercial kit (Murex HBsAg Version 3, Murex Biotech Ltd; Dartford, UK), was used to quantify HB concentration in the samples. The analysis protocol was conducted as specified by the manufacturer. The association rate for HB (A.R. %) was then calculated by the difference between the concentration of free antigen detected in the supernatant and the total concentration in the initial suspension.

Stability of cationic HB-surface-assembled CSNC

Storage at 4ºC of CSNC+ aqueous suspension

The stability of the CSNC+ suspension was assessed during storage at 4ºC. Samples were collected each week during one month. Particle size and

HB association to CSNC were analyzed according to the techniques already described.

Freeze-drying of CSNC+

The freeze-drying technique, or lyophilization, was used to enhance stability of CSNC+ by converting the aqueous suspension into a dry powder. For this purpose, prototype CSNC+ was freeze-dried in the presence of different sugar cryoprotectants (sucrose and trehalose) at concentrations 0, 1, 2.5, and 5%. CSNC+ suspension and cryoprotectant solution were mixed 1:1 (v:v) in 5 ml freeze-drying glass vials. Vials were slowly frozen at -20ºC and then placed on the stainless-steel shelf plates of the Labconco Freeze Dry System (Kansas City, MI), operating at -35ºC. The primary drying (sublimation) was carried out at this temperature under high vacuum (10^{-3} mBar) for approximately 40 h. The second drying step (moisture desorption) lasted 8 hours, during which the temperature gradually rose until +20ºC under vacuum. The final freeze-dried product was reconstituted with ultrapure water by gentle pipette mixing and analyzed for its physicochemical properties.

Vaccination studies

HB-alum preparation

HB adsorbed to aluminum hydroxide (HB-alum) was used as positive control. HB and aluminum hydroxide (AlhydrogelTM; Sigma-Aldrich, St. Louis, MO) solutions were incubated in a volumetric ratio 3:1 (HB:alum) for 30 minutes at 4° C under moderate agitation. Then, the suspension was centrifuged (10000xg, 10 minutes, 4° C), and the pellet was resuspended in adequate volume of isotonic saline solution.

Immunizations and sample collection

The adjuvant capacity of CSNC was evaluated either in their fresh or freeze-dried forms. Groups of 10 female BALB/c mice were immunized with 10 μg of HB incorporated in the selected fresh CSNC:HB prototypes (CSNC- and CSNC+) or adsorbed to alum, at weeks 0 and 4 (two doses) or in a single dose. Formulations of CSNC and HB-alum were injected i.m.

on the posterior leg of mice while animals were conscious. Subsequent sampling was performed monthly, post-primary immunization during a total period of 27 weeks. Blood samples were collected from the maxillary vein without anesthesia.

For the biological evaluation of freeze-dried formulation, mice were randomly distributed in two groups of 10 animals and then immunized i.m. with reconstituted freeze-dried formulation or HB-alum as control following a boost-dose schedule (0 and 4 weeks). For reconstitution of freeze-dried formulations, 0.5 mL of ultrapure water was added, and gentle pipette mixing was applied in order to properly disperse the nanocapsules. Blood samples were collected at selected time points post-immunization (days 28, 56, 84, 112) and specific serum anti-HB IgG titers were analyzed by ELISA.

Measurement of specific immunoglobulin responses

Serum anti-HB IgG endpoint titers were measured by ELISA. Maxisorp microtiter wells were coated with 5 μg/mL of HB in carbonate buffer (pH 9.6) overnight at 4ºC. Plates were then blocked with BSA 1% in PBS for 1 hour at 37º C in order to minimize non-specific interactions. Serum samples and a mouse IgG monoclonal antibody directed against HB (Biokit; Barcelona, Spain) (used as control in the calibration curve) were serially diluted and incubated for 2 hours at 37º C. All serum samples were tested at least twice and in duplicate. Control rabbit antiserum of known concentration (mIU/mL) (Acris Antibodies GmbH; Hiddenhausen, Germany) was used in order to transform serum titers into international units. Goat anti-mouse and anti-rabbit IgG conjugated with horseradish peroxidase (Southern Biotech; Birmingham, AL) were added to each well and incubated for 1 hour at 37º C. Bound antibodies were revealed with ABTS and the titers were expressed in μg/ml or in mIU/mL.

Antigen specific IgG subclasses (G1 and G2a) were also quantified in mouse serum in order to know the IgG1/IgG2a ratio. For this study, pooled sera from all mice from each group were prepared and analyzed

following a similar ELISA protocol described for total anti-HB specific IgG. In this case, polyclonal goat anti-mouse IgG1 and IgG2a antibodies, both conjugated with horseradish peroxidase (Southern Biotech; Birmingham, AL), were used as secondary antibodies. Then, a ratio between IgG1/IgG2a was calculated in relation to the optical density levels.

Statistical analysis

The analysis of variance (ANOVA) was performed using Statgraphics Plus 5.1. Tukey post-hoc analysis was employed to establish significant differences between groups. Differences were considered significant at a level of $p < 0.05$.

RESULTS

Development and characterization of HB-surface-assembled chitosan nanocapsules

For the purpose of loading HB onto CS nanocapsules (CSNC), we first prepared blank nanocapsules, and then the antigen was associated to their polymeric surface. Blank CSNC composed of an oily core of Miglyol® 812 (M812) and lecithin and a CS shell were obtained by the solvent displacement technique. The resulting CSNC exhibited a particle size in the nanometer range (around 200 nm) with spherical shape and high positive ξ potential provided by the CS coating (**Table 1** and **Figure 1**).

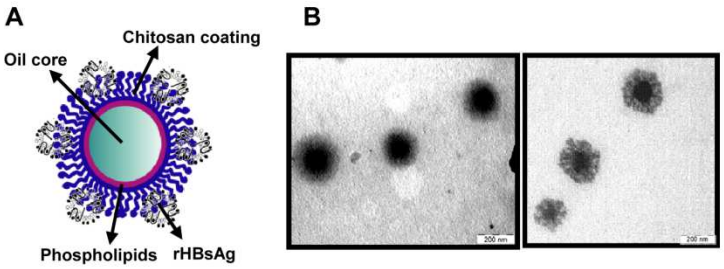

Figure 1: Morphology of CSNC. (A) Structure of HB-surface assembled CSNC showing the different components of the system. (B) TEM micrographs of blank CSNC (left) and HB-surface assembled CSNC (right).

Table 1: Physicochemical characterization of positively charged CSNC:HB prototypes. Results are presented as mean ± SD.

CSNC:HB ratio	HB (μg)	Size (nm)	PdI	ζ potential (mV)	A.R. (%)
Blank	---	196 ± 12	< 0.2	+45 ± 1	-
1:0.025	25	253 ± 11	< 0.2	n.d.	60 ± 3
1:0.05	50	254 ± 17	< 0.2	n.d.	55 ± 2
1:0.1	100	226 ± 5	< 0.2	n.d.	63 ± 2
1:0.25	250	245 ± 53	< 0.2	+41 ± 7	78 ± 3

CSNC: chitosan nanocapsules; HB: recombinant hepatitis B surface antigen; Pdl: polydispersity index; A.R.: association efficiency; n.d.: not determined.

Because of the cationic nature of the polymeric coating, it was possible to associate negatively charged particulated viral proteins, such as the HB (22 nm size and ζ potential of -20mV), to the surface of the CSNC. In order to identify the most adequate association conditions, we prepared different prototypes displaying different surface properties by associating the antigen at different ratios CSNC:HB.

Incubating increased amounts of HB (25, 50, 100, 250 μg) in a 1 mL suspension of blank CSNC (CS concentration of 1mg/mL) resulted in a series of nanosystems with CSNC:HB ratios between 1:0.025 and 1:0.25. The particle size of all formulations was around 250 nm, regardless the amount of antigen initially included, although slightly larger if compared to blank CSNC (**Table 1**). Additionally, it was observed that the association efficiency increased with the amount of HB added, reaching a value of around 80% of HB for the ratio CSNC:HB 1:0.25. Despite this high association rate, the ξ potential of the nanocapsules remained highly positive (+40 mV), thus, indicating the prevalence of the cationic polysaccharide on the surface of the nanostructure. On the other hand, increments in the antigen concentration beyond 0.25 mg/mL led to unstable nanosystems.

In order to further explore the association of the antigen to CSNC, we chose an alternative incubation protocol. A suspension of blank CSNC

was sequentially diluted and then incubated with constant antigen amount (25 μg). Using this method, we observed an inversion of the surface charge of the nanosystem for the ratio CSNC:HB, 1:3.2. Although, as shown in **Figure 2**, this inversion was initially accompanied by a significant size increment (larger than 1μm), it was possible to preserve the nanometric size by reducing the concentration of CSNC. Indeed, for the CSNC:HB ratio of 1:12.8, we obtained nanostructures of a size around 310 nm, a negative surface charge (-20 mV) and high association efficiency (83%).

Therefore, two different prototypes were obtained with similar particle size, but opposite surface characteristics in terms of composition and ζ potential: CSNC:HB with ratios of 1:0.25 (CSNC+) and 1:12.8 (CSNC-).

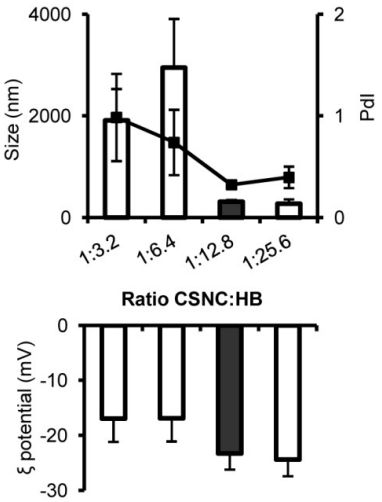

Figure 2: Physicochemical characterization of anionic HB-surface assembled CSNC prototypes. Particle size, polydispersion (Pdl) and ξ potential evolution of CSNC:HB when CSNC suspension was sequentially diluted. The ratio CSNC:HB which exhibited the most adequate physicochemical properties (black column) was: particle size 310 nm ± 34; polydispersity index 0.33 ± 0.04; ξ potential -23 mV ± 3. Mean ± SD.

Influence of surface charge in the adjuvant capacity of HB-surface-assembled CSNC prototypes

In order to assess the adjuvant capacity of CSNC+ and CSNC-, we administered the anionic and cationic prototypes by intramuscular (i.m.) injection to female BALB/c mice. Briefly, prime and boost doses of 10μg

of HB associated to CSNC, as well as to the conventional vaccine (HB-alum) at the same dose, were given in a 4 week interval.

As observed in **Figure 3A**, CSNC- was not able to induce a significant response against HB as compared to the vaccine containing alum, although anti-HB IgG levels remained over seroprotective levels (>10mUI/mL for humans (23)) during the 27-week study. In contrast, the cationic formulation (CSNC+) was able to generate a more potent antibody response quicker than that elicited by the HB-alum at the same dose ($p < 0.05$), thus, proving the immune potentiating effect of CSNC+. These results represent the proof-of-concept of the adjuvant capacity of HB-surface assembled CSNC+ prototype.

Induction of immune protection after a single injection of cationic HB-surface- assembled CSNC prototype

Taking into account the adjuvant effect observed for the CSNC+, we decided to evaluate the immune response elicited by this prototype after a single administration (10 μg) and compare it to two doses of HB-alum (10 μg at 0 and 4 weeks). As noticed in **Figure 3B,** although slightly lower, the antibody levels induced by only one shot of CSNC+ were similar to those elicited upon vaccination with two doses of 10 μg of HB-alum. In fact, no significant differences were observed between the vaccination regimens, except for two time-points (at 5 and 19 weeks post-immunization) ($p < 0.05$). Additionally, a single dose of CSNC+ induced protective anti-HB IgG levels (>10 mU/ml in humans), which remained around 200 mIU/mL until the end of the study (week 27). IgG levels higher than 100 mIU/mL are considered to provide proper immune protection against HB, suggesting that no additional boosters are further required (23).

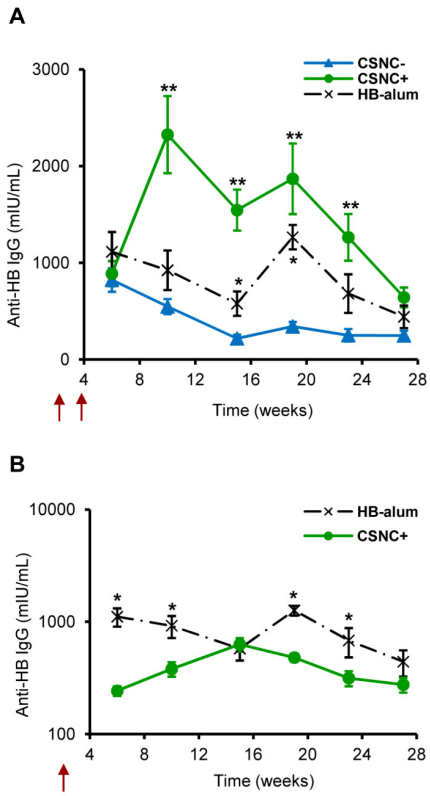

Figure 3: Efficacy evaluation of HB-surface assembled CSNC prototypes. Immune response induced by the nanovaccine prototypes (CSNC- and CSNC+) and the positive control (HB-alum) administered i.m. following different vaccination protocols. **(A)** IgG anti-HB levels generated after prime-boost immunization (arrows, weeks 0-4) with both prototypes: CSNC- (blue –▲); CSNC+ (green –●–) and HB-alum (black –·X·–) at the same dose (10 µg). Results are presented as mean ± SEM.*Alum or CSNC+ vs. CSNC- ($p < 0.05$). ** CSNC+ vs. Alum and CSNC- ($p < 0.05$). **(B)** IgG anti-HB (mIU/ml) levels elicited after a single dose (arrow) of CSNC+ (10 µg; green –●–) compared to alum-HB administered twice (10 µg, weeks 0 and 4) (black –·X·–). Results are presented as mean ± SEM.*($p < 0.05$).

Effect of cationic HB-surface assembled CSNC on the modulation of the elicited immune response

The effect of CSNC+ on the type of T helper (Th1 or Th2) responses preferentially involved was evaluated by measuring the serum anti-HB IgG subtypes (IgG1 and IgG2a) and calculating the ratio between both. While higher levels of antigen specific IgG1 in mice are associated to a

predominant humoral-Th2 type response, the presence of IgG2a is mostly related to a cellular-Th1 type.

IgG1/IgG2a ratios represented in **Figure 4** indicate that HB-alum vaccine induced a predominant humoral Th2-type response (higher levels of IgG1 with IgG1/IgG2a ratios ranging from 2 to 5), as expected (24). Higher production of IgG1 than IgG2a was also found after a single immunization with CSNC+. However, a second administration of this nanovaccine lessened the IgG1/IgG2a ratio, suggesting a cellular immune response (Th1 type) was also induced. These results show the impact of the nanovaccine booster upon the modulation of the immune response by CSNC+.

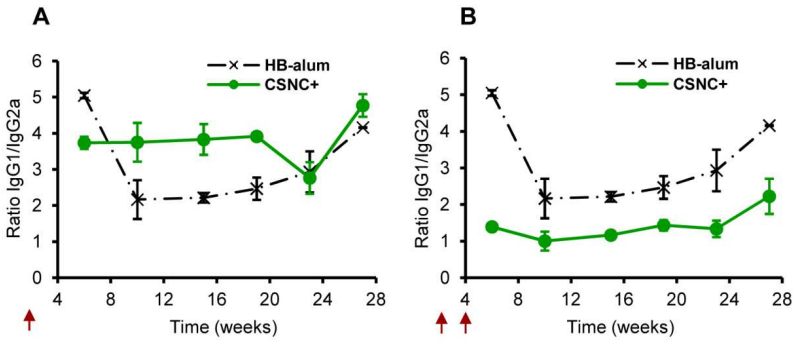

Figure 4: Modulation of the immune response by CSNC+. Ratio of IgG1/IgG2a anti-HB for prototype CSNC+ (10 μg; green –●–) after single **(A)** or double immunization separated 4 weeks **(B)** (indicated in arrows) compared to HB-alum (10 μg) administered in two doses (0, 4 weeks) (black –·X·–). Results are presented as mean ± SD.

Stability of the aqueous suspension of cationic HB-surface-assembled CSNC prototype

The stability of the prototype CSNC+ as aqueous suspension was assessed during its storage at 4ºC. The particle size, polydispersity index and HB association were analyzed each week during one month. The nanosystem maintained its original particle size and homogeneous distribution during at least one month of storage under refrigerated conditions **(Figure 5)**. Similarly, the antigen remained associated to CSNC during this period.

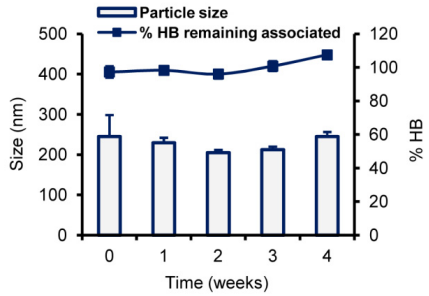

Figure 5: Stability of CSNC+. Both particle size (blue columns) and percentage of associated HB to CSNC (dark blue line) are shown at different time points (0-4 weeks) during storage at 4º C. Results are presented as mean ± SD.

Freeze-drying of cationic HB-surface-assembled CSNC prototype

The aqueous suspension of CSNC+ was transformed into a dried powder using standard freeze-drying techniques. Two different cryoprotectants, sucrose and trehalose, at increasing concentrations were added to the CSNC+ suspension to achieve a final concentration of 1, 2.5 or 5%. Subsequent freeze-drying, the resulting dried cakes had an overall good appearance without signs of collapse. Samples were rehydrated and redispersed without appreciable macroscopic aggregates. Particle size of the reconstituted suspension was then analyzed. On those samples without cryoprotectant or with low sugar concentration (1 and 2.5%), the particle size was found to be much larger compared to their sizes before freeze-drying (**Figure 6**). At 5% sucrose or trehalose, the original particle size of the fresh suspension was properly recovered.

Trehalose is usually preferred for cryoprotection of biomacromolecules because of its lower hygroscopicity, capacity of formation of more flexible hydrogen bonds and very low reactivity (25). Because the HB was associated to the CSNC surface and therefore more exposed to freezing stress, this disaccharide was selected as the most adequate cryoprotectant to produce a freeze-dried product from this nanosystem suspension when included in a concentration of 5%.

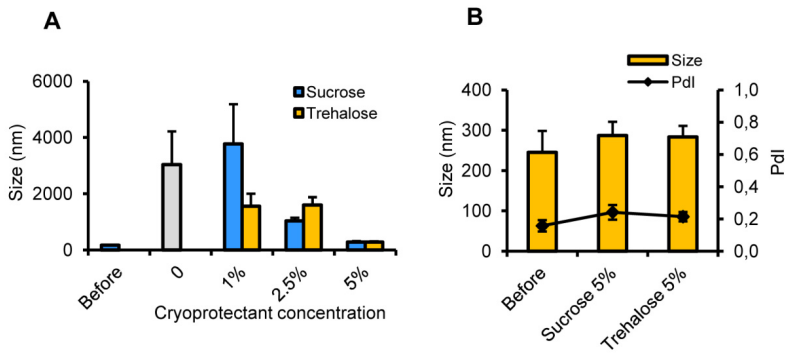

Figure 6: Physicochemical characterization of reconstituted CSNC+ freeze dried under different conditions. Particle size recovery after freeze-drying and reconstitution of CSNC+ using different cryoprotectants. **(A)** Particle size after reconstitution of freeze-dried formulation using sucrose (blue columns) and trehalose (yellow columns) as cryoprotectants at different concentrations. **(B)** Detailed physicochemical characterization of dried formulations in the absence (before) or in the presence of sucrose or trehalose (both at 5%). Size is shown in yellow columns and polydispersity index (PdI) in black line. Results are presented as mean ± SD.

Immunization with freeze-dried cationic HB-surface-assembled CSNC

To assess the preservation of the adjuvant properties of CSNC and immunogenicity of associated antigen after freeze-drying, dried CSNC+ with trehalose 5% was properly reconstituted and administered to BALB/c mice. Animals were i.m. vaccinated at 0 and 4 weeks with either the reconstituted CSNC+ prototype or freshly prepared HB-alum (as positive control), both containing 10 μg of HB. Dried CSNC+ was able to induce IgG titers similar to those achieved by standard alum-based vaccine (**Figure 7**). This result indicates that the freeze-dried product preserved a marked adjuvant capacity after the freeze-drying process and during transportation and storage with no cold chain restrictions.

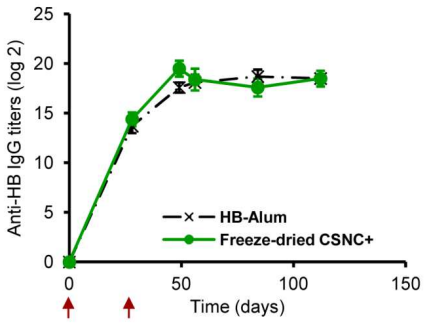

Figure 7: Efficacy of freeze-dried CSNC+ upon storage and reconstitution. Humoral immune response (IgG titers) after two i.m. administrations of reconstituted freeze-dried CSNC+ (green –●–) and compared to HB-alum (black –·X·–) at the same dose (10 µg, weeks 0 and 4). Results are presented as mean ± SEM.

DISCUSSION

Nanocapsules are colloidal structures showing a characteristic core-corona architecture, consisting of an oily liquid core surrounded by a polymeric shell. Until now, this type of structure has been used for the encapsulation of drugs with the idea of improving their solubility, as well as their transporting through mucosal barriers (26). Herein, the technology of chitosan nanocapsules (CSNC) was adapted to explore its potential for antigen delivery. Particularly, we studied the possibility to entrap and present the antigen molecules onto the surface of the nanocarrier and the influence of the physicochemical properties of the resulting nanovaccine on the generation of specific immune responses. Given the multifunctional character of these nanocarriers, the results of this work are expected to lead the way for their rational optimization based on the association of different immunostimulants and antigens.

Two different HB-surface-assembled CSNC prototypes were developed by modifying the proportions between CSNC and the antigen. CSNC:HB with ratios of 1:0.25 (CSNC+) and 1:12.8 (CSNC-) were obtained with similar particle size, but opposite surface characteristics in terms of composition and ζ potential (**Table 1** and **Figure 2**). The cationic surface charge of CSNC+ indicated the prevalence of CS on the surface of the nanostructure despite the high antigen association rate. In contrast, the negative charge of CSNC- indicated the exposure of the antigen molecules entrapped in the CS shell towards the external medium. This surface antigen display approach has been proposed as a way to mimic the

natural structure of pathogens (27). In fact, the exposure of repetitive copies of the antigenic epitope on the surface of nanoparticles has been demonstrated to enhance the immune response against weakly immunogenic antigens (28). In addition, the surface charge of the nanocarriers has been shown to affect their adjuvant properties, and in particular, the cationic surface charge has been determined to enhance the immune responses (29). Therefore, the influence of the antigen exposure and the surface properties (charge and composition) of the nanocarriers on the immune response was then investigated.

The immune response observed for CSNC+, CSNC- and the control HB-alum administered following a boost-dose immunization schedule evidenced clear differences between both CSNC prototypes. Namely, CSNC-, which contained a high proportion of antigen molecules on the surface of the nanostructure, was not efficient at improving the immune response elicited by HB-alum, suggesting that the presentation of repetitive copies of HB molecules onto a particulate carrier is not enough to trigger a potent immune response and other characteristics of the nanostructure are more crucial. In contrast, the prototype exhibiting an excess of CS on their surface (CSNC+), was able to stimulate the generation of a pronounced IgG response against HB, which was even higher than for the HB-alum (**Figure 3A**). This positive effect of the CS coating being exposed on the surface is in agreement with the promising results recently reported by our group for nanogelled CS encapsulating HB (14). The intense humoral immune response achieved with both CS-based nanocarriers provides additional evidence of the immunostimulatory properties of nanostructured CS (14, 18-21).

The adjuvant properties of CS itself have been previously studied *in vivo* with other model antigens, such as β-galactosidase (30). The adjuvant effect of CS was mainly attributed to its capacity to form a depot at the injection site *in vivo* (30) and also to attract immunocompetent cells to the area (31). On the other hand, some studies have raised the issue of a possible direct immunostimulation mechanism of CS through the Toll-

like receptor 4 (TLR4) (32, 33). Unfortunately the results published are inconclusive due to the different nature and purity of the CS used in these studies. Irrespective of the potential inherent immunostimulatory behavior of CS, it is known that the association of antigens to particulate carriers facilitates their uptake by APCs and subsequent activation (5, 34). In particular, nanostructures composed of different cationic biomaterials, such as cationized gelatin (35), poly-L-lysine or protamine (36), have been shown to positively promote recognition and uptake by APCs. Likewise, CS-based nanoparticles increased antigen internalization due to their strong association to the outer membrane of the dendritic cells (37). Therefore, the association of HB to CSNC+, characterized by a cationic surface charge and predominant presence of CS on their surface, could have importantly contributed to its adequate presentation to the immune system and moreover, to an enhanced activation of APCs and further development of a strong adaptive immune response.

One of the main goals in vaccination has been to reduce the number of injections but achieving an efficient immune protection. Indeed, a vaccine able to generate long-term immune responses after a single immunization offers many advantages, such as reducing the risk of patients' under-protection due to a deficient compliance to the immunization schedule, minimizing waste disposal, and decreasing the costs related to vaccination (5, 38). The sustained effect observed for CSNC+ after a single administration (**Figure 3B**) could be attributed to a prolonged antigen delivery to peripheral APCs possibly due to an accumulation of the nanostructures at the injection site (depot effect) and subsequent drainage to the lymph nodes. Additionally, the strong interaction between HB and the polysaccharidic shell of CSNC may have also contributed to this effect, enhancing the retention of the associated antigen and enabling its cellular uptake for long periods of time (39). These results provide the first evidence of the ability of CSNC to elicit high specific, long-lasting and protective IgG levels against HB after a single-dose vaccination regimen.

To study the effect of CSNC+ prototype on modulating the elicited immune response, IgG1 and IgG2a levels were analyzed in sera collected from vaccinated mice. The ratio IgG1/IgG2a is used as indicator of the predominant immune response and cells involved (predominant Th1 or Th2 immune response).The type of immune response elicited by CSNC+ was strongly dependent on the immunization regimen. A single dose with CSNC+ resulted predominantly in a Th2-mediated response (humoral), whereas both Th1- and Th2-type responses were induced after booster immunization (**Figure 4**). This type of response was also reported for CS aqueous solutions mixed with model antigen (β-galactosidase) (30) and for ovalbumin-loaded CS nanoparticles administered subcutaneously (40). Overall, these findings suggest the potential of CS and CS nanocarriers to promote a mixed Th1/Th2 immune response.

A critical feature of an antigen delivery carrier is its ability to preserve the stability of the associated antigen during storage. Initially in this study, we observed CSNC+ maintained its physicochemical properties for one month during storage under refrigerated conditions (**Figure 5**). In a second instance, we explored the freeze-drying method as a way to improve long-term stability of colloidal formulations and avoid cold chain restrictions. In a dry environment, nanostructures and the associated bioactive molecule can be protected from degradation, while their original physicochemical properties can be recovered upon rehydration (41).

The results evidenced the feasibility to transform the aqueous suspension of CSNC+ into a dry powder that can be rehydrated, while maintaining the original physicochemical properties (**Figure 6**). Furthermore, upon reconstitution, the dried formulation maintained the adjuvant properties following *in vivo* administration (**Figure 7**). As the dry form may be a suitable presentation for long-term storage, the preservation of the immune behavior of the nanovaccine upon freeze-drying is critical (42). This is indeed an advantage over common aluminum salts that cannot be frozen and consequently freeze-dried. The particulate structure of alum

can be destroyed after freezing, leading to a loss of potency of the vaccine (43), which is an important drawback leading to the necessity of strictly maintaining the cold chain during transportation and storage, a particularly difficult requirement for developing countries with deficient logistic infrastructures (5, 44).

The results of this work represent the first proof-of-principle of the potential of chitosan nanocapsules (CSNC) as antigen delivery adjuvants, in particular for a vaccine using the recombinant hepatitis B surface antigen (HB) as model antigen. Furthermore, these results provide preliminary evidence of the value of this technology as a single-dose immunization strategy against the disease. With this first study, we were able to establish the optimal organization of the antigen molecules on the nanocarrier's surface to enhance the specific immune response using the CSNC platform. However, from the multifunctional structure of the CSNC it could also be deduced that further improvements could be achieved by incorporating additional immunostimulants in the CSNC's core. In addition, this new technology may also represent a way to preserve the stability of the antigen in a freeze-dried form. Finally, from the conceptual point of view, the results of this work further assess the value of positively charged nanocarriers as a way to facilitate antigen presentation to the immune cells.

ACKNOWLEDGEMENTS

We would like to thank Shantha Biotechnics Limited (Hyderabad, India) for providing us the antigen (rHBsAg) and the advice provided by Martin Friede from the World Health Organization. The technical assistance on animal experimentation of Rafael Romero, Andrea Hernández and Christian Sánchez Espinel is highly appreciated.

REFERENCES

1. Baylor N, Egan W & Richman P (2002) Aluminum salts in vaccines - US perspective. *Vaccine* 20: S18-S23.

2. Wilson-Welder JH, *et al* (2009) Vaccine adjuvants: Current challenges and future approaches. *J Pharm Sci* 98: 1278-1316.

3. Perrie Y, Mohamed AR, Kirby D, McNeill SE & Bramwell VW (2008) Vaccine adjuvant systems: Enhancing the efficacy of sub-unit protein antigens. *Int J Pharm* 364: 272-280.

4. De Temmerman M, *et al* (2011) Particulate vaccines: On the quest for optimal delivery and immune response. *Drug Discov Today* 16: 569-582.

5. Vicente S, Prego C, Csaba N & Alonso MJ (2010) From single-dose vaccine delivery systems to nanovaccines. *J Drug Deliv Sci Technol* 20: 267-276.

6. Xiang SD, *et al* (2006) Pathogen recognition and development of particulate vaccines: Does size matter?. *Methods* 40: 1-9.

7. Dobrovolskaia MA & Mcneil SE (2007) Immunological properties of engineered nanomaterials. *Nat Nanotechnol* 2: 469-478.

8. Zolnik BS, Gonzalez-Fernandez A, Sadrieh N & Dobrovolskaia MA (2010) Minireview: Nanoparticles and the immune system. *Endocrinology* 151: 458-465.

9. Van der Lubben IN, Verhoef JC, Borchard G & Junginger HE (2001) Chitosan and its derivatives in mucosal drug and vaccine delivery. *Eur J Pharm Sci* 14: 201-207.

10. Atmar RL, *et al* (2011) Norovirus vaccine against experimental human norwalk virus illness. *N Engl J Med* 365: 2178-2187.

11. El-Kamary SS, *et al* (2010) Adjuvanted intranasal norwalk virus-like particle vaccine elicits antibodies and antibody-secreting cells that express homing receptors for mucosal and peripheral lymphoid tissues. *J Infect Dis* 202: 1649-1658.

12. Garcia-Fuentes M & Alonso MJ (2012) Chitosan-based drug nanocarriers: Where do we stand?. *J Control Release* 161: 496-504.

13. Csaba N, Garcia-Fuentes M & Alonso MJ (2009) Nanoparticles for nasal vaccination. *Adv Drug Deliv Rev* 61: 140-157.

14. Prego C, *et al* (2010) Chitosan-based nanoparticles for improving immunization against hepatitis B infection. *Vaccine* 28: 2607-2614.

15. Vila A, Sánchez A, Tobío M, Calvo P & Alonso MJ (2002) Design of biodegradable particles for protein delivery. *J Control Release* 78: 15-24.

16. Vila A, *et al* (2004) Low molecular weight chitosan nanoparticles as new carriers for nasal vaccine delivery in mice. *Eur J Pharm Biopharm* 57: 123-131.

17. Amidi M, *et al* (2007) N-trimethyl chitosan (TMC) nanoparticles loaded with influenza subunit antigen for intranasal vaccination: Biological properties and immunogenicity in mouse model. *Vaccine* 25: 144-153.

18. Slutter B, *et al* (2010) Conjugation of ovalbumin to trimethyl chitosan improves immunogenicity of the antigen. *J Control Release* 143: 207-214.

19. Borges O, *et al* (2008) Alginate coated chitosan nanoparticles are an effective subcutaneous adjuvant for hepatitis B surface antigen. *Int Immunopharmacol* 8: 1773-1780.

20. Zhao K, *et al* (2011) Preparation and immunological effectiveness of a swine influenza DNA vaccine encapsulated in chitosan nanoparticles. *Vaccine* 29: 8549-8556.

21. Jiang L, *et al* (2007) Novel chitosan derivative nanopartictes enhance the immunogenicity of a DNA vaccine encoding hepatitis B virus core antigen in mice. *J Gene Med* 9: 253-264.

22. Prego C, Torres D & Alonso MJ (2006) Chitosan nanocapsules as carriers for oral peptide delivery: Effect of chitosan molecular weight and type of salt on the in vitro behaviour and in vivo effectiveness. *J Nanosci Nanotechnol* 6: 2921-2928.

23. Shouval D (2003) Hepatitis B vaccines. *J Hepatol* 39: S70-S76.

24. Brewer JM (2006) (How) do alumiun adjuvants work?. *Immunol Lett* 102: 10-15.

25. Wang W (2000) Lyophilization and development of solid protein pharmaceuticals. *Int J Pharm* 203: 1-60.

26. Oyarzun-Ampuero FA, Garcia-Fuentes M, Torres D & Alonso MJ (2010) Chitosan-coated lipid nanocarriers for therapeutic applications. *J Drug Deliv Sci Tec* 20: 259-265.

27. Sloat BR, Sandoval MA, Hau AM, He Y & Cui Z (2010) Strong antibody responses induced by protein antigens conjugated onto the surface of lecithin-based nanoparticles. *J Control Release* 141: 93-100.

28. Schroeder U, *et al* (2009) Peptide nanoparticles serve as a powerful platform for the immunogenic display of poorly antigenic actin determinants. *J Mol Biol* 386: 1368-1381.

29. Ma Y, *et al* (2011) The role of surface charge density in cationic liposome-promoted dendritic cell maturation and vaccine-induced immune responses. *Nanoscale* 3: 2307-2314.

30. Zaharoff DA, Rogers CJ, Hance KW, Schlom J & Greiner JW (2007) Chitosan solution enhances both humoral and cell-mediated immune responses to subcutaneous vaccination. *Vaccine* 25: 2085-2094.

31. Peluso G, *et al* (1994) Chitosan-mediated stimulation of macrophage function. *Biomaterials* 15: 1215-1220.

32. Dang Y, *et al* (2011) The effects of chitosan oligosaccharide on the activation of murine spleen CD11c(+) dendritic cells via toll-like receptor 4. *Carbohydr Polym* 83: 1075-1081.

33. Villiers C, *et al* (2009) From secretome analysis to immunology. Chitosan induces major alterations in the activation of dendritic cells via a TLR4-dependent mechanism. *Mol Cell Proteomics* 8: 1252-1264.

34. Storni T, Kündig TM, Senti G & Johansen P (2005) Immunity in response to particulate antigen-delivery systems. *Adv Drug Deliver Rev* 57: 333-355.

35. Zwiorek K, *et al* (2008) Delivery of cationic gelatin nanoparticles strongly increases the immunostimulatory effects of CpG oligonucleotides. *Pharm Research* 25: 551-562.

36. Foged C, Brodin B, Frokjaer S & Sundblad A (2005) Particle size and surface charge affect particle uptake by human dendritic cells in an in vitro model. *Int J Pharm* 298: 315-322.

37. Bal SM, *et al* (2010) Efficient induction of immune responses through intradermal vaccination with N-trimethyl chitosan containing antigen formulations. *J Control Release* 142: 374-383.

38. Aguado MT (1993) Future approaches for vaccine development - single-dose vaccines using controlled-release delivery systems. *Vaccine* 11: 596-597.

39. Henriksen-Lacey M, *et al* (2010) Liposomal cationic charge and antigen adsorption are important properties for the efficient deposition of antigen at the injection site and ability of the vaccine to induce a CMI response. *J Control Release* 145: 102-108.

40. Wen Z, Xu Y, Zou X & Xu Z (2011) Chitosan nanoparticles act as an adjuvant to promote both Th1 and Th2 immune responses induced by ovalbumin in mice. *Marine Drugs* 9: 1038-1055.

41. Chen G & Wang W (2007) Role of freeze-drying in nanotechnology. *Dry Technol* 25: 29-35.

42. Sloat BR, Sandoval MA & Cui Z (2010) Towards preserving the immunogenicity of protein antigens carried by nanoparticles while avoiding the cold chain. *Int J Pharm* 393: 197-202.

43. Zapata MI, Peck GE, Hem SL, White JL & Feldkamp JR (1984) Mechanism of freeze-thaw instability of aluminum hydroxycarbonate and magnesium hydroxide gels. *J Pharm Sci* 73: 3-9.

44. Friede M & Aguado MT (2005) Need for new vaccine formulations and potential of particulate antigen and DNA delivery systems. *Adv Drug Deliver Rev* 57: 325.

CAPÍTULO 3

CAPÍTULO 3

Co-delivery of viral proteins and TLR7 agonist from polysaccharide nanocapsules: a needle-free vaccination strategy

Este trabajo ha sido realizado en colaboración con: Mercedes Peleteiro, Belén Díaz-Freitas y África González-Fernández.

Immunology. Biomedical Research Center (CINBIO). University of Vigo, 36310 Campus Lagoas de Marcosende, Vigo; Spain.

ABSTRACT

Here we report a new nasal vaccination strategy intended to elicit both, humoral and cellular immune responses. The strategy relies on the use of a multifunctional antigen nanocarrier consisting of a hydrophobic nanocore, which can allocate lipophilic immunostimulants, and a polymeric corona made of chitosan (CS) intended to associate antigens and facilitate their transport across the nasal mucosa. The TLR7 agonist imiquimod and the recombinant hepatitis B surface antigen (rHBsAg), were selected for the validation of the nanocarrier. The resulting multifunctional nanocapsules had a nanometric size (218 nm), a high positive zeta potential (+45 mV) and great antigen association efficiency (70 %). They also exhibited the ability to enter macrophages *in vitro* and to effectively deliver the associated imiquimod intracellularly, as determined by the intense secretion of pro-inflammatory cytokines (i.e. IL-1α, IL-6 and TNF- α). Finally, the effect of the co-delivery of rHBsAg and imiquimod from the nanocapsules was evidenced upon intranasal administration to mice. The nanocapsules containing imiquimod elicited a protective immune response characterized by increasing IgG levels over the time and developed specific immunological memory. Additionally, the levels of serum IgG subclasses (IgG1 and IgG2a) indicated a balanced cellular/humoral response, thus suggesting the capacity of the nanocapsules to modulate the systemic immune response upon nasal vaccination.

INTRODUCTION

Hepatitis B is an inflammatory disease of the liver caused by the hepatitis B virus (HBV). The virus is transmitted through biological fluids by direct contact (perinatal, sexual contact, misuse of needles, etc.) and it is globally distributed, although the main endemic areas are developing countries in the Subsaharian Africa and the South-West of Asia. The most dramatic consequences of the disease are related to the chronic infection, which may lead to cirrhosis or hepatocarcinoma. Preventing the infection is the most effective way to control the disease. The currently available vaccine against hepatitis B has the recombinant hepatitis B surface antigen (rHBsAg) formulated with the adjuvant alum (1). Despite its demonstrated efficacy, a limitation of this vaccine relies on the requirement of being injected. This fact greatly contributes to HBV spreading as a high proportion of new infections occur by the mis-use and re-use of contaminated needles. This problem is especially severe in developing countries (with high prevalence rates), where re-use of needles and improper waste disposal is very common. Being conscious of this dramatic situation, different philanthropic institutions, such as the Bill & Melinda Gates Foundation through the Grand Challenges in Global Health Initiative, aimed to solve this vaccination failure and enhance immunization coverage to protect the population against infectious diseases (2). Within this frame, the nasal route might represent an interesting option for the development of needle-free vaccination strategies. The key for the success of these strategies will very much depend on their ability to deliver the antigen to the appropriate immunocompetent cells (3). The use of antigen nanocarriers has significantly contributed to achieve this goal, mainly because of their capacity to facilitate the transport of antigens across the nasal mucosa (4). Among the nanocarriers investigated so far, those based on chitosan have shown a promising potential because of their ability to elicit systemic and mucosal immune responses upon nasal immunization against a wide variety of antigens and DNA-based vaccines (5-10).

Recently, further improvements on the efficacy of nanovaccines have been identified in the combination of antigens and immunostimulants within the same nanocarrier (11). For example, the co-association of immunostimulants, such as CpG, LPS and non-toxic subunit of cholera toxin, and model antigens to nanocarriers (8, 12-14), has been found to potentiate systemic immune responses upon nasal immunization.

In the present work, we have attempted to combine the ability of chitosan-based nanostructures to overcome mucosal barriers with the interesting immunological features of the TLR7 agonist imiquimod in a multifunctional nanocarrier, such as the chitosan nanocapsules (15). The core-corona architecture of these nanocarriers enables the surface presentation of subunit antigens and the co-delivery of additional immunoactive molecules, such as imiquimod, included in the oily core. Imiquimod is known to work as a modulator of the innate immunity by activating antigen presenting cells (i.e. dendritic cells and macrophages) via the intracellular Toll-like receptor 7 (TLR 7) (16). This effect has been observed following topical and intradermal administration (17-19). However, its application for mucosal immunization has not been reported so far. Briefly, the goal of this work was to develop a nanocapsular system adapted for the co-delivery of rHBsAg and imiquimod following nasal administration and to assess the efficacy of the resulting nanovaccine in terms of inducing a protective immune response against hepatitis B.

MATERIALS AND METHODS

Materials

Ultrapure chitosan hydrochloride salt (Protasan UP CL 113, MW 125 kDa, acetylation degree 14%) was purchased from Novamatrix (Sandvika, Norway). Miglyol® 812 is a neutral oil composed of triglycerides of medium chain fatty acids and was donated by Sasol Germany GmbH (Witten, Germany). The emulsifier soybean L-α-lecithin Epikuron 145V was a gift from Cargill (Barcelona, Spain). The recombinant hepatitis B surface antigen (rHBsAg; HB from now in the text) was kindly donated

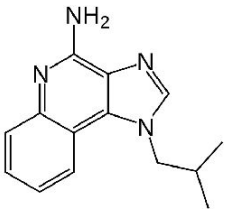

by Shantha Biotechnics Ltd (Hyderabad, India) as an aqueous suspension in phosphate buffer saline (PBS) with a protein concentration of 0.16mg/ml. Imiquimod (imidazoquinoline analogue – figure on the left) (Mw 276.11) was purchased by InvivoGen (San Diego, CA). Rhodamine-6G (λ_{max}=543), BCIP (5-Bromo-4-Chloro-3-Indolyl Phosphate), ABTS (2,2′-Azino-bis(3-ethylbenzthiazoline-6-sulfonic acid)) and other analytical grade reagents were acquired from Sigma-Aldrich (St Louis, MO).

Antibodies

Western-Blot: Mouse monoclonal antibody (mAb) against human C3 was obtained from Abcam (Cambridge, UK). Secondary polyclonal goat anti-mouse IgG conjugated to alkaline phosphatase were from Dako (Glostrup, Denmark).

ELISA: Mouse and rabbit mAbs against HB were purchased from Biokit (Barcelona, Spain) and Acris Antibodies GmbH (Hiddenhausen, Germany), respectively. Secondary Abs (both goat anti-rabbit and anti-mouse IgG, IgG1, IgG2a conjugated to horseradish peroxidase) were from Southern Biotech (Birmingham, AL).

Preparation of chitosan nanocapsules.

Chitosan nanocapsules were prepared by the solvent displacement technique as described in a previous report (20). Briefly, the preparation of blank nanocapsules consisted of dissolving 40 mg and 0.25 ml of Miglyol® 812 in a mixture of ethanol and acetone. This organic phase was poured under magnetic stirring upon an aqueous solution composed of 20 mL of water containing chitosan (0.05%), resulting in the immediate formation of the nanocapsules.

Imiquimod-containing CS nanocapsules and fluorescent CS nanocapsules were obtained by encapsulating either imiquimod or rhodamine-6G within the inner oily core of the nanocapsules. The preparation consisted in dissolving the lipophilic compound in the organic phase and then, the

procedure was followed as described above for blank nanocapsules. These compounds were included in a theoretical loading of 0.6 and 0.02%, respectively.

A nanoemulsion consisting of the stabilized lecithin/Miglyol® 812 nanodroplets without chitosan coating was also prepared. To obtain a homogeneous dispersion of lecithin/Miglyol® 812 nanodroplets, the procedure was performed as described for blank nanocapsules, but chitosan was not incorporated in the aqueous phase.

For all the preparations, the organic solvents were removed by evaporation under vacuum immediately after the formation of nanocapsules (Büchi Labortechnik AG; Flawil, Switzerland).

Finally, the nanostructures were isolated by ultracentrifugation (Optima™ L-90K Ultracentrifuge, Beckman Coulter; Fullerton, CA) at 42000xg for 1 hour at 15ºC and then completed until a constant volume of 10 mL.

Preparation of HB-surface assembled chitosan nanocapsules.

The association of the antigen onto the polymeric surface of nanocapsules was accomplished by ionic interaction. For this purpose, the stock solution of HB was desalted and concentrated to 0.5 mg/mL by ultrafiltration (Amicon Ultra4, Millipore; Cork, Ireland). The resulting HB aqueous solution was immediately mixed with the nanocapsules suspension (containing imiquimod or not) in a ratio CS:HB of 1:0.25 (w/w). Then, both components were incubated for 1 hour at room temperature (RT). The control nanoemulsion was also incubated with the HB aqueous solution in a ratio of 1:0.025 (w/w) and further concentrated by ultrafiltration in order to achieve the same antigen concentration than the formulations of HB-surface assembled nanocapsules.

Particle size and ξ potential measurements.

Particle size and polydispersity index were measured by photon correlation spectroscopy (PCS) using a Zetasizer Nano-S (Malvern Instruments; Malvern, UK). Nanocapsules were adequately diluted in

filtered water. Each analysis was performed at 25ºC with a detection angle of 90^0.

ζ potential measurements were performed by laser doppler anemometry (LDA) (Zetasizer Nano-S, Malvern Instruments; Malvern, UK). Nanocapsules were properly diluted in an aqueous solution of KCl 10^{-3} M and placed in a folded capillary cell especially designed to use in this equipment.

Quantification of HB association to chitosan nanocapsules.

The HB adsorbed onto the surface of blank or imiquimod-loaded CS nanocapsules was indirectly quantified by measuring the concentration of free antigen remained in supernatant after separation of the nanostructures by ultracentrifugation (42000xg, 1h, 15ºC). The HB association efficiency (**A.E.%**) was then calculated by the difference between the total concentration in the suspension (**Ct**) and the concentration of free antigen detected in the supernatant (**Cs**), as indicated below:

$$A.E.\% = \frac{[Ct - Cs]}{[Ci]} \times 100$$

A microtiter plate-based sandwich ELISA was used to measure the concentration of free HB (Murex HBsAg Version 3, Murex Biotech Ltd; Dartford, UK). This ELISA kit uses a mixture of mAbs to specifically detect the "a" epitopes of HB. For quantification, a calibration curve was made using a solution of HB mixed with the supernatants of either blank or imiquimod-loaded CS nanocapsules, at decreasing concentrations. The blank sample consisted of the supernatants without HB. All measurements were performed in triplicate.

Determination of encapsulation efficiency of imiquimod.

The amount of imiquimod encapsulated within the oily core of CS nanocapsules was indirectly quantified. Briefly, nanocapsules encapsulating imiquimod were ultrafiltrated using Amicon Ultra4 filter tubes (Millipore; Cork, Ireland). The filtered aqueous solution containing

the free drug was subsequently submitted to HPLC analysis. The concentration was determined using a calibration curve made up with standard solutions of imiquimod. The encapsulation efficiency was then calculated using the formula for A.E.% shown in the previous section.

Analysis of complement activation.

The activation of the complement cascade induced by blank or imiquimod-loaded CS nanocapsules was studied by Western-blot, analyzing the degradation of C3 factor. A pool of human plasma from healthy donors was incubated with two different concentrations of the two prototypes (100 and 1000µg/ml) in the presence of veronal buffer (pH 7.4). Equal volumes of plasma, buffer and nanocapsules (50 µL each) were mixed together and incubated at 37°C for 1 hour. Cobra venom factor (CVF) (Quidel Corporation; San Diego, CA) and PBS were used as positive and negative controls, respectively. The mixture was centrifuged at 16000xg for 30 minutes in order to separate the nanocapsules. Supernatants containing complement proteins were loaded (2 µL) onto a 10% SDS-PAGE gel and then transferred to a PVDF membrane (Immun-Blot, Biorad; Hercules, CA) using the Transblot Semidry Transfer Equipment (Biorad; Hercules, CA). PVDF membranes were blocked overnight at 4ºC with 5% non-fat dry milk in TBST. Then the membrane was washed and incubated for 90 minutes at RT with a mouse mAb against human C3 diluted 1:1000. After intensive washes, membranes were incubated with secondary polyclonal goat anti-mouse IgG Abs conjugated with alkaline phosphatase diluted 1:2000 at RT for 1 hour. The membrane was finally revealed with BCIP.

***In vitro* cell studies**

Cells and culture

The adherent RAW 264.7 murine macrophages cell line was purchased from ATCC (Manassas, VA). The cells were cultured in RPMI supplemented with 10% (v/v) heated-inactivated fetal bovine serum (FBS) (PAA; Pasching, Austria), 2 mM glutamine and 100 U/mL of

penicillin/streptomycin (further called complete medium along the text), at 37ºC in 5% CO_2 atmosphere. Cells were split every day to maintain 70-80% confluent cultures.

Murine peritoneal macrophages were obtained from female BALB/c mice (6-8 weeks old). 5 mL of DMEM medium (Gibco; Grand Island, NY), containing 10% FBS were injected into the mouse peritoneal cavity and cells were then collected with a Pasteur pipette. After centrifugation at 100xg for 5 min at 4°C, the cell pellet was resuspended in complete medium.

Cell viability assay: *xCELLigence® system*

To measure the effect of blank and imiquimod-loaded CS nanocapsules on cellular viability, the xCELLingence® RTCA DP Instrument (Roche Diagnostics; Penzberg, Germany) was used following manufacturer's instructions. This system measures the variations of impedance caused by cell growth when cells are incubated on special plates containing gold electrodes.

The xCELLigence® device was placed inside the incubator (37ºC and 5% CO_2) and 1.5 x 10^4 RAW 264.7 cells per well (with gold electrodes) were incubated with 200 μL RPMI 10% FBS during 18 hours until reaching the exponential phase. At that point, nanocapsules were added at three different concentrations (25, 50 and 100 μg/mL) and incubated for 48 hours. As negative controls, only medium or nanocapsules alone were added to individual wells. Continuous monitoring of impedance (correlated with the amount of cells) was performed during the whole procedure with intervals of 15 minutes between each impedance measurement.

Cellular uptake by macrophages.

Adherent RAW 264.7 cells were plated (5×10^6 cells) in a 24-wells plate with 1 mL of complete medium in the presence or not of 50 μg/mL of nanocapsules labeled with rhodamine-6G for 30 minutes. After three washes with PBS to remove non internalized nanocapsules, cells were

observed under an inverted fluorescent microscope (IX50, Olympus Optical Co GmbH; Hamburg, Germany).

For flow cytometry analysis, adherent cells were incubated with 50 µg/mL of fluorescent nanocapsules for 30 minutes. Cells were then washed once with PBS and detached with 200µL of Accutase® (PAA; Pasching, Austria) for 10 minutes at 37ºC and 5% CO_2. Finally, cells were washed with complete medium and centrifuged. The resulting suspension of cells was analyzed using a flow cytometer (FC500, Beckman-Coulter; Miami, FL).

The final confirmation of internalization of nanocapsules was performed using a confocal microscope (Leica SP5; Mannheim, Germany). Cells were seeded on a glass cover-slip (Menzel-Gläser; Braunschweig, Germany) in a 24-wells plate and incubated with the fluorescent nanocapsules as described above. After several washes, cells were incubated with Alexa Fluor 488-phalloidin (Invitrogen; Eugene, OR) for 20 minutes in order to stain the cellular cytoskeleton. Finally, the cover-slips containing the attached cells were mounted over slides in the presence of ProLong® Gold Antifade mounting medium (Invitrogen; Eugene, OR) containing DAPI to stain the nucleus.

Cytokine profile evaluation

For the assessment of cytokine production, 1×10^5 mouse peritoneal macrophages were incubated for 24 hours in the presence of both nanocapsules prototypes at two different concentrations: 10 and 100 µg/mL. Nanocapsules encapsulating imiquimod contained 3.5 and 35 µg of imiquimod, respectively. As positive and negative controls, cells were incubated with either 1 µg/mL of lipopolysaccharide (LPS) (InvivoGen; San Diego, CA) or medium, respectively. After 24 hours, supernatants were collected, centrifuged at 100xg for 5 min at 4ºC, and stored at -20ºC before analysis. Levels of IL-1α, IL-6, IL-10 and TNF-α cytokines were determined using the FlowCytomix™ assay (eBioscience; Vienna, Austria) following manufacturer´s protocol. Briefly, using a 96-wells plate, 25 µL of Ab-coated microspheres were incubated with 25 µL of

culture supernatants and 50 µL of biotin-conjugated secondary Abs for 2 hours at RT on a microplate shaker. After several washes, 50 µL of streptavidin conjugated to phycoeythrin and 100 µL of PBS-T were added to the preparation and incubated for 1 hour at RT on a microplate shaker. Finally, phycoeythrin-binded beads were studied by flow cytometry.

In vivo studies

Animals

Female BALB/c mice (4-5 weeks) were housed in filter-top cages in a 12h light/12h dark cycle at constant temperature (22ºC) without any diet restrictions. All protocols were adapted to the guidelines of the Spanish regulations (Royal Decree 1201/2005) regarding the use of animals in scientific research and under the approval of the Ethical Committee of the University of Vigo.

Immunization schedule and collection of serum samples

Mice were randomly distributed in groups of 10 animals which were intranasally immunized with the two prototypes of nanocapsules (with and without imiquimod) and the control nanoemulsion at weeks 0 and 4 (**Table 1**). The group immunized with imiquimod-loaded nanocapsules received a late third dose at week 28. For all immunizations, 10 µg of HB associated to the nanostructures were administered. As well, nanocapsules encapsulating imiquimod contained 10 µg of imiquimod per mouse.

Table 1: Immunization schedule and sampling

Formulation	HB/Imiquimod dose (µg)	Schedule (weeks)	Bleeding (weeks)
CS nanocapsules	10 / --	0, 4	6, 10, 15, 19
Imiquimod-CS nanocapsules	10 / 10	0, 4, 28	6, 10, 15, 19, 37
Nanoemulsion	10 / --	0, 4	6, 10, 15, 19

Blood samples were collected from the mouse maxillary vein starting the second week post-primary immunization until week 20, as detailed in **Table 1**. An additional bleeding at week 37 was performed to the group immunized with imiquimod-loaded nanocapsules.

Quantification of HB-specific IgG and IgG subtypes by ELISA

A solution of HB (5 μg/ml in carbonate buffer - pH 9.6) was incubated in maxisorp 96-wells plates overnight at 4ºC. HB-coated wells were then blocked with a PBS-BSA 1% solution for 1h at 37ºC in order to minimize non-specific interactions. Serum samples and control mouse anti-HB IgG mAb solution were serially diluted and incubated for 2h at 37ºC. In parallel, control rabbit antiserum of known concentration (mIU/mL) was used in order to further transform serum titers into international units. Then, the secondary Abs (goat anti-mouse IgG or anti-rabbit IgG conjugated to horseradish peroxidase) were added to each well and incubated for 1h at 37ºC. Finally, bound Abs were revealed with ABTS and optical density was measured by spectrophotometry (λ=405 nm) using EnVision 2104 Multilabel Reader (Perkin Elmer; Walthman, MA). The IgG titers were expressed in μg/mL and mIU/mL.

Specific IgG subtypes (IgG1 and IgG2a) against HB were also quantified in a pool of sera collected from mice immunized with nanocapsules containing imiquimod. ELISA protocol was performed as described above, but polyclonal goat anti-mouse IgG1 and IgG2a Abs (conjugated to horseradish peroxidase) were used as secondary Abs. Furthermore, the ratio between both IgG subtypes (IgG1/IgG2a) was calculated. All serum samples were tested at least twice and in duplicate.

Statistical analysis

The analysis of variance (ANOVA) was performed using Statgraphics Plus 5.1. Neuman-Keuls post-hoc analysis was employed to establish significant differences between groups. Differences were considered significant at a level of $p < 0.05$.

RESULTS AND DISCUSSION

Chitosan nanocapsules are a core-corona type of nanostructures formed by a liquid hydrophobic core (liquid oil) and a chitosan (CS) shell (15). In the present work these nanostructures have been adapted to accommodate the lipophilic immunostimulant imiquimod in the lipid core and the rHBsAg (HB) on the polymer corona, with the final goal of co-delivering both of them to antigen presenting cells (APCs) upon nasal immunization.

The surface association of HB to CS nanocapsules has been previously studied (20) in order to establish the optimal surface properties to achieve immunopotentiation after intramuscular injection. In the present work, the incorporation of imiquimod in oily core to be co-delivered with HB was explored as an interesting strategy to enhance the immune response upon nasal vaccination.

Development and characterization of fluorescent and imiquimod/HB-loaded chitosan nanocapsules

Encapsulation of the immunostimulant imiquimod and rhodamine-6G into chitosan nanocapsules.

CS nanocapsules with a mean particle size around 200 nm and positive surface charge (+45 mV) were prepared by the solvent displacement technique, as described elsewhere (20) (**Table 2**). A nanoemulsion was also prepared using the same conditions but omitting the polysaccharidic coating. The nanoemulsion droplets had a mean diameter of 130 nm and negative ξ potential (-39 mV).

Imiquimod was efficiently entrapped (70%) within the oily core of CS nanocapsules without major alterations of the physicochemical characteristics found for blank nanocapsules (particle size: 200 nm; ξ potential: +47 mV). This was possible because of the high solubility of the molecule in the lipid nanocore. This strategy was also followed for labeling the nanocapsules with a fluorescent probe in order to visualize them in *in vitro* cell cultures. Hence, rhodamine-6G, due to its lipophilic

character, was also efficiently encapsulated (around 80%) without altering the physicochemical characteristics of blank nanocapsules (**Table 2**).

Table 2: Physicochemical characterization of the different prototypes of chitosan nanocapsules and the nanoemulsion, associating or not the HB.

CS nanocapsules composition	Size (nm)	PdI	ξ potential (mV)	% A.E. HB	% A.E. Im. / Rh.
Blank	196 ± 12	<0.2	+45 ± 1	---	---
Blank:HB	245 ± 53	<0.2	+41 ± 6	77 ± 3	---
Im.	199 ± 7	<0.2	+47 ± 1	---	70
Im.:HB	218 ± 9	<0.2	+45 ± 6	70 ± 2	70
Rh	220 ± 1	<0.2	+40 ± 1	---	80 ± 6
Nanoemulsion	129 ± 2	<0.2	-39 ± 3	---	---
Nanoemulsion:HB	125 ± 1	<0.2	-52 ± 7	70 ± 3	---

CS: chitosan; HB: recombinant hepatitis B surface antigen; Pdl: polydispersity index; A.E.: association efficiency; Im.: imiquimod; Rh. rhodamine-6G.

Surface assembly of HB onto chitosan nanocapsules and imiquimod-loaded chitosan nanocapsules.

The association of HB to the cationic surface of CS nanocapsules was achieved by electrostatic interaction (HB ζ potential: -20 mV). In a previous work (20), we observed that the ratio of CS associated to the nanocapsules vs. the amount of antigen (CS/HB, w/w) was crucial in order to induce an intense and prolonged immune response against HB when administered intramuscularly. The presence of CS on the surface composition of the resulting HB-surface assembled nanocapsules was postulated to be a relevant characteristic for the immunopotentiating properties and also for enhancing the interaction of the nanostructures

with the epithelial cells of the mucosa (21). Based on this information, CS nanocapsules containing imiquimod or not, were incubated with HB in a ratio CS/HB 1/0.25 (w/w). As expected, the resulting HB-surface assembled nanocapsules exhibited a particle size slightly larger than that of blank nanocapsules (220-250 nm). The antigen was very efficiently associated (~ 75%) regardless the composition of the oily core, however, the surface charge was still highly positive, around +43 mV.

The incorporation of HB to the nanoemulsion was also very high (70%) and resulted in an increment of ξ potential to more negative values (from –39 mV to –52 mV) without any variation of the droplet size. This was attributed to hydrophobic interactions between the oil nanodroplets with the lipid components and protein hydrophobic domains of the HB (22).

In summary, CS nanocapsules were able to associate the model antigen (HB) onto their surface, as well as lipophilic molecules (imiquimod and rhodamine-6G) within their hydrophobic core while maintaining nanometric particle size, homogeneous population of particles, and positive surface charge. To our knowledge, this is the first report of a nanosystem combining both an antigen and a TLR7 agonist drug. Imiquimod has already been co-administered with the antigen, for instance mixed in a suspension of nanoparticles (18). However, the co-delivery of antigen and this immunomodulator from the same nanocarrier has not been attempted. Besides, the application of imiquimod as vaccine adjuvant has been limited to topical and intradermal administrations (17, 19). Therefore, we have postulated that simultaneous co-delivery of imiquimod and the antigen from the same nanocarrier could be an effective approach for achieving a robust response following nasal immunization.

Activation of the complement cascade by chitosan nanocapsules.

To examine whether CS nanocapsules have potential effects on the activation of the complement cascade, the C3 complement factor and its split products were analyzed by Western-Blot. The complement cascade is one of the most important components of the humoral innate immune

system. It is involved in the recognition and clearance of invading agents and it also mediates inflammation and promotes phagocytosis. It is composed of a complex group of serum proteins which are activated in cascade through three possible routes: classical, alternative or lectin-mediated. The common step in all of them is the cleavage of the C3 factor (23).

The results indicated that neither blank CS nanocapsules nor imiquimod-loaded CS nanocapsules induced C3 cleavage at the concentrations tested (100 and 1000 μg/mL). As shown in **Figure 1**, the band intensity corresponding to C3 split products was similar to the negative control (MW ~42), which corresponds to the basal degradation of C3.

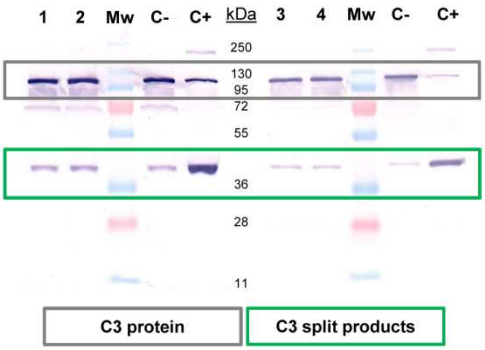

Figure 1: Analysis of C3 complement factor by Western-Blot. Blank and imiquimod-loaded CS nanocapsules at 1000 μg/mL, (1 and 2, respectively) or 100 μg/mL, (3 and 4, respectively). C-: human plasma serum incubated with PBS; C+: cobra venom factor. MW corresponds to the molecular weight of the protein marker (kDa).

Taking into account the core-corona structure of the nanocapsules, theoretically their interaction with complement proteins would be mainly governed by CS. The results reported so far on the complement activation properties of CS have been quite variable (24, 25), probably due to the various types and sources of not always well-characterized CS. In general, CS has been found to cause depletion of complement proteins in serum (26, 27). However, this depletion has been attributed to a simple electrostatic interaction between CS and the complement proteins

without entailing the production of split products (25). Indeed, recent studies have agreed on the fact that highly deacetylated CS (around 80%), either in solution (25, 27) or in the form of nanoparticles (28), does not induce the activation of the complement cascade. The results presented herein basically agree with these previous findings. Due to the high density of glucosamine subunits in the chitosan backbone (85.5% free amino groups), complement proteins can interact electrostatically with the polysaccharidic coating without further activation of the complement cascade. Consequently, these nanostructures are not expected to induce major inflammatory responses mediated by complement activation.

In vitro cell assays

Cell internalization of chitosan nanocapsules and potential cytotoxic effects.

For a vaccine formulation, recognition and uptake by antigen presenting cells (APCs) is crucial for the initiation of the immune response. The antigen has to be taken up and processed by APCs in order to be further presented to T cells and trigger the adaptive immune response. Therefore, recognition and capture of fluorescent nanocapsules by macrophages was assessed. Three different concentrations of nanocapsules (10, 25 and 50 μg/mL) were incubated with RAW 264.7 cells and analyzed by optical microscopy, flow cytometry and confocal microscopy. Internalization was found to occur in a dose dependent manner, reaching a maximum for a nanocapsules concentration of 50 μg/mL. The results obtained for this concentration are illustrated in **Figure 2**. The image obtained by optical microscopy (**Figure 2A**) shows a high density of fluorescent cells due to internalization of fluorescent nanocapsules. In addition, the analysis of the cells by flow cytometry revealed that 90% of cells have internalized nanocapsules during the incubation time (**Figure 2B**) and confocal microscopy images evidenced their localization within the macrophages (**Figure 2C**).

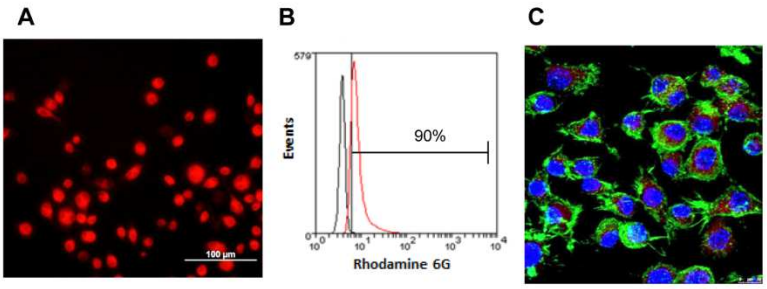

Figure 2: Internalization of fluorescent CS nanocapsules labeled with rhodamine 6G (50 µg/mL) in macrophages measured using three different techniques: A) optical fluorescence microscopy; B) flow cytometry and C) confocal microscopy (red channel: nanocapsules; green channel: Alexa Fluor 488-phalloidin; blue channel: DAPI).

In general, particulate delivery systems are known to be taken up by phagocytic cells, however, their uptake is highly influenced by their particle size, composition and surface charge (29, 30). As reported for other cationic nanostructures (29, 31, 32), the positive surface charge is very relevant in promoting internalization by phagocytic cells. In addition, the internalization was observed to occur at very short time points (30 minutes) as occurs for other chitosan-based nanocarriers (29). However, longer incubation times (until 48 hours) had adverse consequences in cell viability. The xCELLigence® system was used to monitor cell growth during 48 hours in contact with CS nanocapsules with and without imiquimod at 25, 50 and 100 µg/mL. In this study it was found that blank nanocapsules reduced cell viability over time, this effect being markedly dose dependent (**Figure 3**). On the other hand, nanocapsules containing imiquimod showed less toxicity and even induced cell proliferation at low concentration (25 µg/mL) after 24 hours of incubation. These results were further confirmed by a colorimetric viability assay (Quick Cell Proliferation Assay, GenScript) (data not shown).

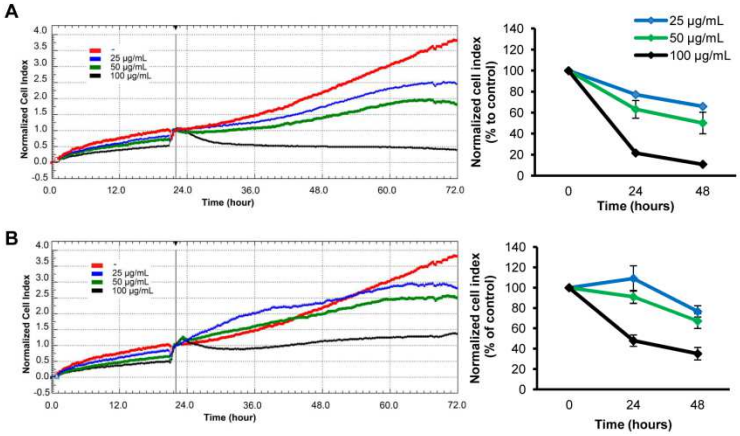

Figure 3: Real-time monitoring of cell growth by xCELLingence system. Different concentrations of blank (**A**) and imiquimod-loaded CS nanocapsules (**B**) were incubated during 48 hours with Raw 264.7 cells at 3 different concentrations (25, 50 and 100 µg/mL – blue, green and black lines, repectively). Red line: cells incubated with culture medium (control). Vertical black line indicates the addition of the nanocapsules to the cells after 24 hours growing.

As previously shown, CS nanocapsules are internalized by macrophages within a short period of time (30 minutes) in a dose-dependent manner. The effect of the concentration was also evidenced on cell viability and at longer times. These results suggest a close relation between the internalization extent and cell viability. The intracellular accumulation of high amounts of nanocapsules over 48 hours may have importantly impaired macrophage function and cause cell death. Curiously, cell viability increased when CS nanocapsules were loaded with imiquimod. This could be attributed to the effect of imiquimod on cell activation as later discussed. Because of this activation, cells might have reduced their phagocytic activity (33), and thus, the accumulation of nanocapsules within the cells.

In summary, cell internalization of CS nanocapsules leads to a reduction on cell viability at long time points (48 hours). However, the intracellular release of encapsulated immunostimulant (imiquimod) promoted cell activation and decreased the cytotoxic effect of the vehicles.

In vitro secretion of cytokines by macrophages upon exposure to chitosan nanocapsules and imiquimod-loaded chitosan nanocapsules

The cytokines induced by CS nanocapsules and imiquimod-loaded CS nanocapsules in murine peritoneal macrophages were studied using the FlowCytomix™ assay, which allows a simultaneous quantification of several cytokines secreted by cultured cells. In this experiment, we have determined the main cytokines produced by murine macrophages (IL-10, IL-1α, IL-6 and TNF-α) after 24 hours of incubation with two different doses of nanocapsules (10 and 100 μg/mL). The results obtained (**Figure 4**) indicate that only those containing imiquimod were able to stimulate the production of all the cytokines studied, except IL-1α, and this response was evidently dose-dependent. In particular, an intense production of IL-10 was observed, achieving higher levels than the positive control (LPS). On the other hand, blank CS nanocapsules did not have any effect on cytokine release by peritoneal macrophages and only a slight increment in IL-10 levels was found for this prototype. In fact, concentrations of IL-1α, IL-6 and TNFα were similar to negative control (medium). These findings evidenced that, although the nanocapsules can be recognized and internalized by macrophages, the encapsulated immunostimulant is crucial to induce a cytokine response.

Imiquimod is an imidazolquinolamine compound with antiviral and antitumor activities, whose effect is a consequence of a potent activation of the innate immune system (16). Hence, imiquimod acts mainly on APCs (macrophages, monocytes and dendritic cells (34)) by activating Toll-like receptor 7 (TLR7), which is intracellularly present in the membrane of endosomes of APCs and this activation leads to the production of pro-inflammatory cytokines. Indeed, in agreement with previous reports (35, 36), we have observed an important induction of pro-inflammatory cytokines (IL-6 and TNF-α) by imiquimod-loaded nanocapsules in a marked dose-dependent manner, while the levels of IL-1α were negligible. On the other hand, this intense stimulation may have triggered a self-regulatory response by inducing the production of IL-10,

a non-inflammatory cytokine able to attenuate the effect of the pro-inflammatory cytokines (37).

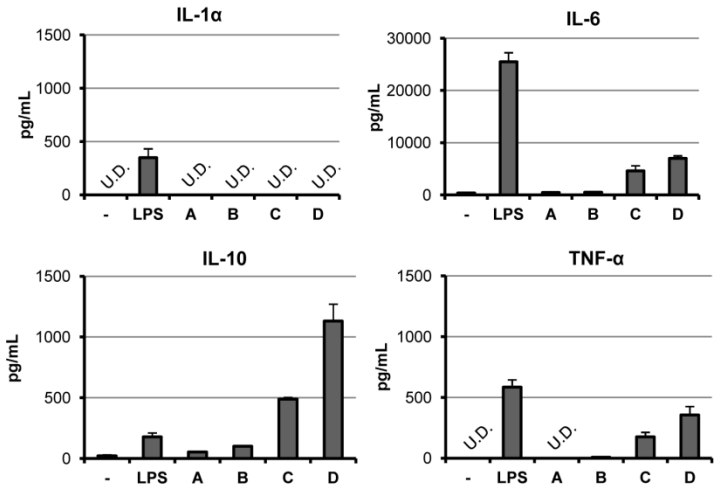

Figure 4: Cytokine production of mouse peritoneal macrophages incubated with blank and imiquimod-loaded CS nanocapsules at two different doses (10 and 100 μg/mL) during 24 hours. Negative control was culture medium, and positive control was LPS (1 μg/mL). Average concentration (pg/mL) of IL-1α, IL-6, IL-10 and TNF-α in culture supernatants. Data from one representative experiment (performed twice in duplicates). UD: undetectable levels (IL-1α < 15.7 pg/mL; TNF-α < 2.1 pg/mL). A & B: blank CS nanocapsules incubated at 10 and 100 μg/mL, respectively; C & D: imiquimod-loaded CS nanocapsules incubated at 10 and 100 μg/mL, respectively.

Immunization studies

Enhancement and prolongation of the systemic immune response against HB after intranasal immunization with imiquimod-loaded chitosan nanocapsules.

The systemic humoral immune response was assessed in BALB/c mice after intranasal immunization with both prototypes of HB-surface assembled CS nanocapsules (blank and loaded with imiquimod) and nanoemulsion control. Animals were immunized following a boost-dose schedule and total IgG levels were monitored during 19 weeks (**Table 1**) in order to study the kinetics profile of the elicited immune response

(**Figure 5A**). Serum protection levels were achieved by both prototypes after the boost dose, when anti-HB IgG concentration exceeded 10 mIU/mL (IgG concentration considered protective for humans (1)). On the other hand, the IgG response elicited by control nanoemulsion was negligible during the entire study. These data evidenced the relevance of the polysaccharidic shell to promote the interaction of the nanocarriers with the mucosa and subsequently, enhance antigen transport across the mucosal barrier. This observation is in agreement with the capacity of internalization of chitosan nanocapsules across the nasal mucosa previously reported by Prego et al. (38). In general, chitosan-based nanocarriers have demonstrated their capacity to overcome mucosal barriers and effectively transport the associated bioactive molecule in order to induce a systemic effect. Due to these interesting properties, their application for mucosal vaccine delivery has been already studied, particularly by the nasal route. For example, chitosan in the form of cross-linked nanoparticles has demonstrated its ability to entrap different types of antigens (i.e. hepatitis B (6), tetanus toxoid (5), influenza (7), etc.) and elicit high and prolonged systemic immune responses when administered intranasally. As reported by the number of studies (39), certainly, nanostructured chitosan importantly contributes to enhance the passage of antigens through the nasal mucosa and deliver them to the underlying immunocompetent cells.

The encapsulation of imiquimod into the nanocapsules and its co-delivery with the antigen was found to be critical in order to achieve a continuous increase of the antibody levels over time. These findings correlate with the results of *in vitro* studies, previously discussed. In cell culture, nanocapsules containing imiquimod were able to stimulate macrophages and produce higher levels of pro-inflammatory cytokines than those without imiquimod. This positive effect on APCs could have also occurred *in vivo*, thus promoting cell activation and the initiation of the adaptive immune response. In agreement with our hypothesis, the co-delivery of the antigen and the immunostimulant drug (both within the

same vehicle) resulted in a positive effect on the induction and progression of the specific immune response. Therefore, both the improved antigen delivery through the mucosa together with the immunoestimulant effect of imiquimod, may be responsible for the observed increased immune response.

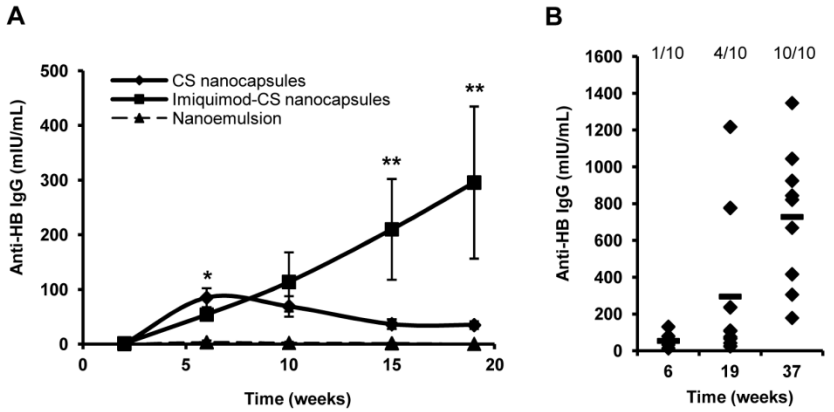

Figure 5: Systemic immune response after two intranasal immunizations (0, 4 weeks) to BALB/c mice with blank and imiquimod-loaded CS nanocapsules and nanoemulsion (NE) associating HB. **(A)** The plot represents total anti-HB IgG quantified at different time points post primary immunization (mean +/- SEM). Statistically significant differences are indicated for * Blank & imiquimod-loaded CS nanocapsules vs NE ($p<0.05$). ** Imiquimod-loaded CS nanocapsules vs blank CS nanocapsules & NE ($p<0.05$). **(B)** Effect of late third nasal dose with imiquimod-loaded CS nanocapsules. Individual IgG concentration in each mouse (diamonds) and mean of ten mice (dash) at early, intermediate and late time points. Fractions represent the number of mice with higher anti-HB IgG than 100 mIU/mL, versus the total number of mice in each group.

The progressive increment of IgG levels in mice immunized with imiquimod-loaded nanocapsules and their interesting *in vitro* profile, encouraged us the administration of a third dose at week 28 in order to study the effect of a late mucosal immunization. **Figure 5B** represents the individual values of anti-HB IgG of each mouse of the group and the average at early, intermediate and late time points. After first boost dose, the antibody levels importantly increased (from week 6 to 19). Nevertheless, this response was much more intense in some animals than

in others. After the late third dose, every single animal of the group became totally seroprotected raising the average levels up to 720 mIU/mL (>100 mIU/mL for humans has been considered full protection (40)). This intense response has been associated to the presence of immunologic memory. The immune system may have interpreted this last immunization as a viral challenge, and respond rapidly by raising the antibodies production. This effect is considered a sign of a proper early immunization, suggesting that the boost dose was not needed to sustain protection due to the strong immunologic memory developed (41).

In summary, these results elucidated the relevance of a) an adequate vehicle to transport the antigen across biological barriers, b) a proper priming of the immune system with an immunostimulant, such as the imiquimod, associated to the same vehicle with the antigen and c) a late third immunization to achieve high and protective immunoglobulin levels against hepatitis B using a mucosal immunization approach. Overall, the relevance of these data rely on the possibility of immunization against hepatitis B through a mucosal route using a nanovaccine and hence, avoiding the use of needles. In addition, we have determined the quality of the elicited immune response by the generation of seroprotection and immunologic memory even after a reduced number of doses.

Modulation of the immune response with imiquimod-loaded CS nanocapsules upon intranasal immunization.

The ratio IgG1/IgG2a (serum IgG subtypes) helps to analyze the main type of the adaptive immune response activated by the CS nanocapsules containing imiquimod, that is, mediated by Th1 or Th2 lymphocytes. While a predominant Th2 activation induces a humoral response characterized by the main production of IgG1, the presence of IgG2a subtype is related to cellular immune responses mediated by Th1 lymphocytes. To evaluate how this nanocarrier modulates the type of immune response, the specific anti-HB IgG1 and IgG2a subtypes in mouse sera were measured (**Figure 6**). Data regarding the IgG1/IgG2a ratios

show that imiquimod-loaded nanocapsules induced a combined Th cell response, eliciting high levels of both IgG1 and IgG2a (IgG1/IgG2a ratios from 0.96 to 2). It is especially relevant the IgG1/IgG2a ratio of 0.96 at week 37. This means that after a late nasal immunization, the nanocarriers can bias the immune response towards the cellular type, which is the preferable in the control of viral infections, such as the HBV. Imiquimod has been described to stimulate and modulate the acquired immunity, in particular the cellular response (Th1) (42). In fact, the clinical application of this drug is the treatment of viral infections, mainly due to the effects exerted on the immune system, crucial to clear the virus from the infected cells.

In summary, both cellular and humoral immune responses are activated by the imiquimod-loaded CS nanocapsules. However, a late third immunization is able to further increase the Th1 response, which is the expected one for a viral vaccine.

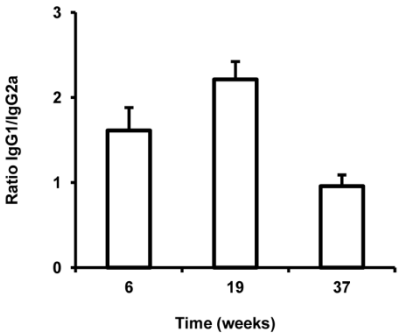

Figure 7: Representation of the type of immune response against HB elicited by imiquimod-loaded CS nanocapsules using the ratio of anti-HB IgG1/IgG2a. The ratios were calculated from IgG subtypes levels determined in sera collected from immunized mice at early, intermediate and late time points (6, 19 and 37 weeks).

CONCLUSIONS

Overall, the optimization of CS nanocapsules was oriented to enhance systemic immune responses against HB when administered through a mucosal route. This was achieved due to the versatility of the structure of

the nanocapsules which enabled the association of the HB and the imiquimod within the same vehicle while maintaining adequate physicochemical properties: nanometric particle size, positive surface charge and high antigen and imiquimod association efficiency. The combination of both the immunostimulant and the antigen within the same nanocarrier enabled to improve the specific immune response upon nasal immunization, but also to modulate it in order to elicit Th1-mediated immune responses. Therefore, imiquimod-loaded CS nanocapsules have demonstrated interesting features as a needle-free vaccination alternative.

ACKNOWLEDGEMENTS

This work was supported by a grant from the Bill & Melinda Gates Foundation and Consolider Ingenio 2010, CSD2006-00012 (Ministry of Science and Innovation, Spain) and the Competitive Reference Groups (SUDOE-FEDER: SOE1/P1/E014). We would like to thank Shantha Biotechnics Limited (Hyderabad, India) for providing us rHBsAg and the advice provided by Martin Friede from the World Health Organization. SV and MP acknowledge a fellowship from Spanish Ministry of Education (FPU predoctoral grants program). The technical assistance of Rafael Romero, Andrea Hernández and Christian Sánchez Espinel is highly appreciated.

REFERENCES

1. Yu A, Cheung R & Keeffe E (2006) Hepatitis B vaccines. *Infect Dis Clin North Am* 20: 27-+.

2. Cohen J (2006) Global health: The new world of global health. *Science* 311: 162-167.

3. Neutra MR & Kozlowski PA (2006) Mucosal vaccines: The promise and the challenge. *Nat Rev Immunol* 6: 148-158.

4. Csaba N, Garcia-Fuentes M & Alonso MJ (2009) Nanoparticles for nasal vaccination. *Adv Drug Deliv Rev* 61: 140-157.

5. Vila A, *et al* (2004) Low molecular weight chitosan nanoparticles as new carriers for nasal vaccine delivery in mice. *Eur J Pharm Biopharm* 57: 123-131.

6. Prego C, *et al* (2010) Chitosan-based nanoparticles for improving immunization against hepatitis B infection. *Vaccine* 28: 2607-2614.

7. Amidi M, *et al* (2007) N-trimethyl chitosan (TMC) nanoparticles loaded with influenza subunit antigen for intranasal vaccination: Biological properties and immunogenicity in mouse model. *Vaccine* 25: 144-153.

8. Borges O, *et al* (2008) Immune response by nasal delivery of hepatitis B surface antigen and codelivery of a CpG ODN in alginate coated chitosan nanoparticles. *Eur J Pharm Biopharm* 69: 405-416.

9. Xu W, *et al* (2004) Intranasal delivery of chitosan-DNA vaccine generates mucosal SIgA and anti-CVB3 protection. *Vaccine* 22: 3603-3612.

10. Zhao K, *et al* (2011) Preparation and immunological effectiveness of a swine influenza DNA vaccine encapsulated in chitosan nanoparticles. *Vaccine* 29: 8549-8556.

11. Pashine A, Valiante N & Ulmer J (2005) Targeting the innate immune response with improved vaccine adjuvants. *Nat Med* 11: S63-S68.

12. Slutter B & Jiskoot W (2010) Dual role of CpG as immune modulator and physical crosslinker in ovalbumin loaded N-trimethyl chitosan

(TMC) nanoparticles for nasal vaccination. *J Control Release* 148: 117-121.

13. Alcon V, *et al* (2005) Mucosal delivery of bacterial antigens and CpG oligonucleotides formulated in biphasic lipid vesicles in pigs. *AAPS J* 7: E566-E571.

14. Stano A, *et al* (2011) PPS nanoparticles as versatile delivery system to induce systemic and broad mucosal immunity after intranasal administration. *Vaccine* 29: 804-812.

15. Oyarzun-Ampuero FA, Garcia-Fuentes M, Torres D & Alonso MJ (2010) Chitosan-coated lipid nanocarriers for therapeutic applications. *J Drug Deliv Sci Tec* 20: 259-265.

16. Stanley MA (2002) Imiquimod and the imidazoquinolones: Mechanism of action and therapeutic potential. *Clin Exp Dermatol* 27: 571.

17. Weldon WC, *et al* (2012) Effect of adjuvants on responses to skin immunization by microneedles coated with influenza subunit vaccine. *PLoS One* 7: e41501.

18. Goldinger SM, *et al* (2012) Nano-particle vaccination combined with TLR-7 and -9 ligands triggers memory and effector CD8(+) T-cell responses in melanoma patients. *Eur J Immunol* 42: 3049-3061.

19. Li N, Peng L, Chen X, Nakagawa S & Gao J (2011) Effective transcutaneous immunization by antigen-loaded flexible liposome in vivo. *Int J Nanomed* 6: 3241-3250.

20. Vicente S, *et al* (In press) A polymer/oil based nanovaccine as a single-dose immunization approach

21. Amidi M, Mastrobattista E, Jiskoot W & Hennink WE (2010) Chitosan-based delivery systems for protein therapeutics and antigens. *Adv Drug Deliv Rev* 62: 59-82.

22. Gavilanes F, *et al* (1990) Hepatitis B surface antigen. Role of lipids in maintaining the structural and antigenic properties of protein components. *Biochem J* 265: 857-864.

23. Wilson M, Gaumer H & Salvaggio J (1977) Activation of alternative complement pathway and generation of chemotactic factors by asbestos. *J Allergy Clin Immunol* 60: 218-222.

24. Minami S, Suzuki H, Okamoto Y, Fujinaga T & Shigemasa Y (1998) Chitin and chitosan activate complement via the alternative pathway. *Carbohydr Polym* 36: 151-155.

25. Marchand C*, et al* (2010) C3, C5, and factor B bind to chitosan without complement activation. *J Biomed Mater Res Part A* 93A: 1429-1441.

26. Suzuki Y, Miyatake K, Okamoto Y, Muraki E & Minami S (2003) Influence of the chain length of chitosan on complement activation. *Carbohydr Polym* 54: 465-469.

27. Benesch J & Tengvall P (2002) Blood protein adsorption onto chitosan. *Biomaterials* 23: 2561-2568.

28. Bertholon I, Vauthier C & Labarre D (2006) Complement activation by core-shell poly(isobutylcyanoacrylate)-polysaccharide nanoparticles: Influences of surface morphology, length, and type of polysaccharide. *Pharm Res* 23: 1313-1323.

29. Zaki NM, Nasti A & Tirelli N (2011) Nanocarriers for cytoplasmic delivery: Cellular uptake and intracellular fate of chitosan and hyaluronic acid-coated chitosan nanoparticles in a phagocytic cell model. *Macromol Biosci* 11: 1747-1760.

30. He C, Hu Y, Yin L, Tang C & Yin C (2010) Effects of particle size and surface charge on cellular uptake and biodistribution of polymeric nanoparticles. *Biomaterials* 31: 3657-3666.

31. Foged C, Brodin B, Frokjaer S & Sundblad A (2005) Particle size and surface charge affect particle uptake by human dendritic cells in an in vitro model. *Int J Pharm* 298: 315-322.

32. Zwiorek K*, et al* (2008) Delivery of cationic gelatin nanoparticles strongly increases the immunostimulatory effects of CpG oligonucleotides. *Pharm Research* 25: 551-562.

33. Zhu K, *et al* (2009) Imiquimod inhibits the differentiation but enhances the maturation of human monocyte-derived dendritic cells. *Int Immunopharmacol* 9: 412-417.

34. Gibson S, *et al* (1995) Cellular-requirements for cytokine production in response to the immunomodulators imiquimod and S-27609. *J Interferon Cytokine Res* 15: 537-545.

35. Weeks C & Gibson S (1994) Induction of interferon and other cytokines by imiquimod and its hydroxylated metabolite R-842 in human blood-cells in-vitro. *J Interferon Res* 14: 81-85.

36. Testerman T, *et al* (1995) Cytokine induction by the immunomodulators imiquimod and S-27609. *J Leukoc Biol* 58: 365-372.

37. Moore K, Ogarra A, Malefyt R, Vieira P & Mosmann T (1993) Interleukin-10. *Annu Rev Immunol* 11: 165-190.

38. Prego C, Torres D & Alonso MJ (2006) Chitosan nanocapsules: A new carrier for nasal peptide delivery. *J Drug Deliv Sci Tec* 16: 331-337.

39. Jabbal-Gill I, Watts P & Smith A (2012) Chitosan-based delivery systems for mucosal vaccines. *Expert Opin Drug Deliv* 9: 1051-1067.

40. Shouval D (2003) Hepatitis B vaccines. *J Hepatol* 39: S70-S76.

41. Banatvala J, *et al* (2000) Are booster immunisations needed for lifelong hepatitis B immunity?. *Lancet* 355: 561-565.

42. Wagner T, *et al* (1999) Modulation of Th1 and Th2 cytokine production with the immune response modifiers, R-848 and imiquimod. *Cell Immunol* 191: 10-19.

CAPÍTULO 4

CAPÍTULO 4

Highly versatile immunostimulating nanocapsules for specific immune potentiation

Este trabajo ha sido realizado en colaboración con: Mercedes Peleteiro[1], Belén Díaz-Freitas[1], Susana Martínez-Pulgarín[2], José Ángel Escribano[3], J.I. Neissa[4] y África González-Fernández[1]

[1] Immunology. Biomedical Research Center (CINBIO).University of Vigo, 36310 Campus Lagoas de Marcosende, Vigo; Spain.

[2]Alternative Gene Expression S.L. (ALGENEX), Centro Empresarial, Parque Científico y Tecnológico de la Universidad Politécnica de Madrid, Campus de Montegancedo, 28223 Pozuelo de Alarcón, Madrid, Spain.

[3] Department of Biotechnology, INIA. Autovía A6 Km. 7.5, 28040 Madrid, Spain.

[4] Department of Physiology, Center for Research in Molecular Medicine and Chronic Diseases (CIMUS). University of Santiago de Compostela. 15705 Campus Vida, Santiago de Compostela; Spain.

ABSTRACT

As a contribution to the important role of nanotechnology in the development of new adjuvants, herein, we propose a rational design of squalene-based nanocapsules enabling the accommodation of different types of antigens in association with immunomodulatory molecules. These nanocapsules consist of squalene oil nanodroplets, alone or in association with the immunostimulant imiquimod, surrounded by a polyglucosamine (PG) shell, which enables the association of antigens and promotes their uptake by the antigen presenting cells (APCs). The recombinant hepatitis B surface antigen (rHBsAg) (a virus-like particle) and the hemagglutinin of influenza virus (HA) (a soluble protein) were selected as two different model antigens,which could benefit from the immunoacting nanostructure. The resulting nanovaccines showed a particle size in the range of 200-250 nm, a positive ζ potential (around +60 mV) and a high association efficiency of the two selected antigens (around 75%). Following intramuscular administration to mice, PG nanocapsules were able to elicit long-term immune responses (IgG levels) against both antigens, these responses being higher than those observed for alum (conventional adjuvant) at the same dose. In the case of rHBsAg, a single dose of nanocapsules was able to induce a protective and long-lasting immune response, which was attributed to their prolonged residence time at the injection site and potential interaction with APCs. In addition, the results showed that the co-delivery of imiquimod with the antigen induced a quick and boosted response and biased the immune response towards a Th1 type. In conclusion, this nanocapsular system might be a suitable platform for the co-delivery of different antigens and immunostimulators, offering the possibility of enhancing and modulating the immune response according to the requirements of specific vaccines.

INTRODUCTION

Since the first vaccine against smallpox in the 18th century, routine vaccination prevents a large number of infectious diseases globally. However, the development of new vaccines and vaccination technologies remains to be a critical step towards improving the protection of population. For instance, the development of subunit antigens has improved the safety profile of vaccines by avoiding the inoculation of the whole microbe (1). However, the poor immunogenic character of these new antigens has raised the necessity of new adjuvants in order to boost the specific immune response (2).

The only adjuvant universally accepted for human administration is the alum (aluminium hydroxide or aluminium phosphate), although novel adjuvant systems have been recently introduced in the clinic. For example, AS04™, a combination of alum and MPLA (monophosphoryl lipid A) has been incorporated in the human papilloma vaccine (Cervarix®). Other new adjuvants based on squalene emulsions were authorized in Europe in different seasonal and prepandemic influenza vaccines, such as MF59™ (Aflunov®, Flocivia®, and Focetricia®) and AS03™, which additionally contains α-tocopherol (Prepandrix®, Pandemrix®, Pumarix®).

The current trend in the development of new adjuvants involves their rational design based on the knowledge about the immunity mechanisms (3). Within this frame, antigen delivery systems are gaining increasing recognition because of their ability to interact with antigen presenting cells (APCs) and potentiate immune responses. In fact, currently, a large number of micro- and nano-vaccine delivery systems, differing in their structure and composition, are under extensive preclinical and clinical investigation, some of them being marketed (4).

The capacity of nanocarriers to protect antigens from degradation and to deliver them in a controlled manner concomitantly with immunostimulant molecules to APCs represents key advantages over other adjuvants (5). In fact, recent studies have revealed the possibility of

antigen-loaded nanocarriers to modulate the adaptive immune response by regulating their uptake by APCs and further inducing cellular activation. APCs have the ability to trigger both humoral (specific antibodies production) and cellular (mediated by cytotoxic T cells) immune responses upon antigen capture and subsequent intracellular processing and presentation to $CD4^+$ or $CD8^+$ T cells. Therefore, adequate antigen delivery and activation of APCs can determine the type of immune response elicited against the antigen. This could be an important feature in terms of vaccine design. For instance, achieving cellular responses represents a fundamental step towards combating intracellular pathogens and in cancer immunotherapy (6).

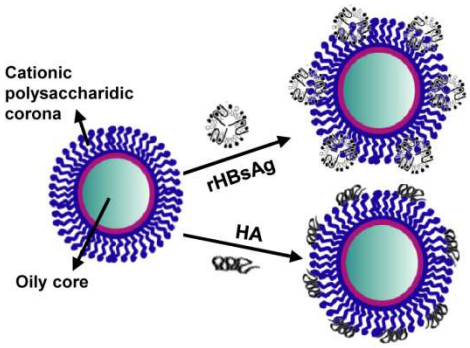

Figure 1: Representation of immunostimulating nanocapsules associating HB and HA on their surface. The cationic polysaccharidic is polyglucosamine (PG); the oily core corresponds to squalene nanodroplets stabilized with lecithin, and eventually, lipophilic immunostimulat drugs such as imiquimod, might be dispersed in this nanocore. Either HB or HA (antigen models of VLP and soluble protein) were associated to the polymeric surface by electrostatic interactions.

Taking this information into account, we have attempted to create a polymer-based nanocarrier which combines the above indicated advantages of nanostructures with the adjuvant properties described for squalene-based emulsions (7). Namely, we present here a core-corona structure containing a lipidic nanocore of squalene surrounded by a polysaccharidic corona (**Figure 1**). A highly deacetylated form of chitosan (CS), further named as polyglucosamine (PG), was the biomaterial

selected for the formation of the outer corona of the system. The selection was based upon our previous positive results using CS-based nanoparticles as antigen delivery systems (8-10) and also on the acceptable safety profile of this biomaterial (11). The more cationic character of this polymer could be an advantage in the interaction of the nanocapsules with APCs. The resulting system is highly versatile as the oily core could be used for the accommodation of lipophilic antigens and adjuvants, whereas the polymeric shell can efficiently associate negatively charged protein/peptide antigens and improve recognition and uptake by APCs.

Therefore, in this work we have developed and evaluated the efficacy of the PG-coated squalene nanoemulsions, or PG nanocapsules, for the delivery of different types of antigens and their capacity of modulation of the immune response. For this purpose, we associated two different antigens: (i) the recombinant hepatitis B surface antigen (HB), representative of a virus-like particle (VLP) (12), and (ii) the hemagglutinin subunit of influenza virus (HA), which is a soluble protein antigen (13). Furthermore, we have also explored the benefit of incorporating the immunomodulatory agent imiquimod within the oily core.

MATERIALS AND METHODS

Materials

Polymers and chemicals

Ultrapure highly deacetylated chitosan in base form (PG) (Ultrasan®, Mw 276 kDa and deacetylation degree 95.5%) was acquired from BioSyntech Canada Inc. (Quebec, Canada). Ultrapure chitosan hydrochloride salt (CS) (Protasan UP CL 113, MW 125 kDa, acetylation degree 14%) was purchased from Novamatrix (Sandvika, Norway). The emulsifier soybean L-α-lecithin Epikuron 145V was a gift from Cargill (Barcelona, Spain). Squalene oil (density 0.855 g/mL) was obtained from Merck (Darmstadt, Germany). Imiquimod is an imidazoquinoline analogue (Mw 276.11) with

potent antiviral activity and immunommodulatory properties and was purchased from InvivoGen (San Diego, USA). Alexa Fluor 750 succinimidyl ester was obtained from Molecular Probes (Eugene, OR). The organic solvents HPLC grade (2-propanol and acetone) and Sudan Red were purchased from Sigma-Aldrich.

Antigens

The recombinant hepatitis B surface antigen (Mw 24 kDa) (rHBsAg, further named as HB) was kindly donated by Shantha Biotechnics Ltd (Hyderabad, India) as an aqueous suspension in PBS with a protein concentration of 0.16mg/ml. It was extracted from *Pichia pastoris* culture and subsequently purified.

Influenza hemagglutinin (HA) was kindly provided by Algenex S.A. (Madrid, Spain). The ectodomain (aa 18–529) of hemagglutinin from the H1N1 A/PR/8/34 influenza virus strain was produced fused with a 6X His tag and the endoplasmic reticulum retention amino-acid sequence KDEL at its 3' end (HAhisKDEL) (Mw 63 kDa). Baculovirus-infected *Trichoplusia ni* larvae were used as living biofactories (IBES® technology). HAhisKDEL (further referred as HA) was purified upon extraction using Co^{2+}-based immobilized metal affinity chromatography (IMAC) resins (TALON®, Clontech; Mountain View, CA) as previously described (13). The antigen was provided as a freeze-dried powder and it was reconstituted with water to get a stock concentration of 0.62 mg/mL and aliquoted.

ELISA reagents and antibodies for HB

HB was quantified using the ELISA kit Murex HBsAg Version 3 (Murex Biotech Limited, Dartford, UK) provided with specific monoclonal antibodies (Abs) to detect epitope "a" of HB.

Abs used for ELISA analysis of serum samples from hepatitis B immunized mice were: a) rabbit and mouse monoclonal Abs against HB, purchased from Biokit (Barcelona, Spain) and Acris Abs GmbH (Hiddenhausen, Germany), respectively; and b) secondary Abs (both goat

anti-rabbit and anti-mouse IgG, IgG1, IgG2a conjugated to horseradish peroxidase) were from Southern Biotech (Birmingham, AL).

ELISA reagents and antibodies for HA

For HA detection by Dot-Blot, mouse monoclonal anti-6X His tag® was used as primary antibody (Ab) and the secondary Ab was a goat polyclonal Ab to mouse IgG conjugated to horseradish peroxidase (IgG-HRP). Both were purchased from abcam pcl (Cambridge, UK).

For specific detection of total IgG Abs in serum of HA-immunized mice, a sheep anti-mouse IgG-HRP purchased from GE Healthcare (Little Chalfont, UK) was used as secondary Ab.

Cells and culture

The adherent RAW 264.7 murine macrophages cell line was purchased from ATCC (Manassas, VA). Cells were cultured in complete medium at 37ºC in 5% CO_2 atmosphere and split every day to maintain 70-80% confluent cultures.

Murine peritoneal macrophages were obtained from female BALB/c mice (6-8 weeks old). 5 mL of DMEM (Gibco; Grand Island, NY), containing 10% FBS were injected into the mouse peritoneal cavity and cells were collected with a Pasteur pipette. After centrifugation at 100xg for 5 min at 4°C, the pellet of cells was resuspended in complete medium.

Complete medium was composed of RPMI supplemented with 10% (v/v) heated-inactivated fetal bovine serum (FBS) (PAA; Pasching, Austria), 2 mM glutamine and 100 U/mL of penicillin/streptomycin.

Animals

In vivo fluorescence imaging studies

FVB mice were housed under controlled conditions with a 12h dark / 12h light cycle. During imaging procedure, animals were maintained under general anesthesia (inhaled isoflurane/oxygen mixture). Isoflurane 4-5% was used for induction and 2% for maintenance of anesthesia. In order to avoid a decrease of body temperature, mice were laid over a warmed

surface (35ºC). After each imaging analysis, mice were left to recover freely until they could normally breathe and walk.

HB and HA immunization studies

Female BALB/c mice (4-5 weeks old) were purchased from Harlan (Barcelona, Spain). Mice were housed in filter-top cages in a 12 h light / 12 h dark cycle with constant temperature environment of 22ºC and provided with food and water *ad libitum*.

All protocols were adapted to the guidelines of the Spanish regulations (Royal Decree 1201/2005) regarding the use of animals in scientific research and under the approval of the ethical committee of the University of Santiago de Compostela, University of Vigo and INIA.

Preparation of polysaccharidic-coated squalene nanoemulsions: immunostimulating nanocapsules.

The preparation of these polysaccharide (PG and CS) and squalene-based nanocapsules was performed by the solvent displacement technique (10).

In a first set of experiments, different amounts of lecithin (40, 50, 60, 70 and 80 mg) and 0.25 ml of squalene were co-dissolved in 2-propanol (500 µl). This organic phase was completed with 9.5 mL of acetone and immediately poured under magnetic stirring upon 20 ml of an aqueous solution of CS (0.05% or 0.025%), resulting in the spontaneous formation of the core-corona nanostructures with different CS:lecithin ratios. For 0.05% of CS in the aqueous phase: 1:4, 1:5, 1:6, 1:7 and 1:8. For 0.025%: 1:8, 1:10 1:12, 1:14 and 1:16. As a common final step for all formulations, the organic solvents were totally removed by evaporation under vacuum (Büchi Labortechnik AG; Flawil, Switzerland), isolated by ultracentrifugation at 42000xg for 1hour at 15ºC (Optima™ L-90K Ultracentrifuge, Beckman Coulter; Fullerton, CA) and then resuspended in water to a final concentration of the polysaccharide of 1 mg/mL.

Based on the best formulation conditions for CS nanocapsules, the coating with PG was then attempted. Thus, the organic phase was composed of squalene (0.125 mL) and lecithin (60 mg) in 2-propanol/acetone, which

was poured upon the aqueous phase (GL 0.025% in 0.05% acetic acid solution) under magnetic stirring. The organic solvents were also removed and nanocapsules isolated by centrifugation.

Imiquimod was eventually encapsulated in PG nanocapsules. For this purpose, this lipophilic drug was dissolved in squalene in a 0.87% (p/p) theoretical loading prior to its incorporation into the organic phase. Then, the preparation procedure described above was followed to finally obtain imiquimod-PG nanocapsules.

The encapsulated imiquimod was indirectly determined by measuring the concentration of the drug in the aqueous phase after separation of the nanocapsules using the Amicon Ultra4 filter tubes (Millipore; Cork, Ireland). The filtered aqueous solution was then submitted to HPLC analysis and the concentration was calculated using a calibration curve made up with standard solutions of imiquimod. The association efficiency of imiquimod (A.E.) was calculated using the following formula, where Ct is the theoretical concentration in the formulation and Ca is the concentration in the aqueous phase.

$$A.E.(\%) = \frac{Ct - Ca}{Ct}$$

Physicochemical characterization

Particle size and polydispersity index were measured by photon correlation spectroscopy (PCS) using a Zetasizer Nano-S (Malvern Instruments; Malvern, UK). Nanostructures were adequately diluted in filtered water. Each analysis was performed at 25ºC with a detection angle of 90º. For ζ potential determinations, the nanostructures were diluted in an aqueous solution of KCl 10^{-3} M and placed in a folded capillary cell especially designed to use in this equipment for measurements by laser doppler anemometry (LDA).

Fluorescent labeling of PG nanocapsules

PG nanocapsules were fluorescently labeled following two different strategies:

1) Encapsulation of Rhodamine-6G within the oily core.

For this purpose, rhodamine-6G was dissolved in the organic phase in a theoretical loading 1.25% (w/w). Then, the preparation protocol was conducted as described in the previous section to finally obtain the fluorescent nanocapsules. The encapsulation efficiency was indirectly calculated after separation of the free fluorescent probe by ultracentrifugation (42000xg, 1hour, 15ºC) and quantified by spectrofluorimetry (Fluorescence Spectrometer LB 50, Perkin-Elmer; Wantan, MA).

2) Conjugation of Alexa Fluor 750 to PG prior to preparation of nanocapsules.

Alexa Fluor 750 carboxylic acid succinimidyl ester was reconstituted with DMSO until a concentration of 10 mg/mL, as indicated by the manufacturer. 5 mg of PG were dissolved in 2.5 ml of water and 80 µl of acetic acid 0.1%. Under constant magnetic stirring, 20 µl of Alexa Fluor 750/DMSO solution were added dropwise. The reaction was maintained during 1 hour. The conjugation occurs when succinimidyl ester groups of the fluorescent probe react with the free amino groups of PG, establishing an amide link between the fluorophore and the polymer. Then, the polymeric solution was dialyzed using Slide-A-Lyzer dialysis cassettes of 20 MWCO (Thermo Scientific; Rockford, IL) in order to remove the free fluorescent probe. The polymer labeled with Alexa Fluor 750 (Alexa Fluor 750-PG) was incorporated in the aqueous phase for the preparation of NIR fluorescent nanocapsules and the preparation was then performed as described for blank nanocapsules.

Association of HB and HA to PG nanocapsules.

The association of the antigens onto the polymeric surface of PG nanocapsules was accomplished by ionic interaction. For this purpose, the stock solution of HB was desalted and concentrated to 0.5 mg/mL by ultrafiltration (Amicon Ultra4, Millipore; Cork, Ireland). The resulting HB aqueous solution was immediately mixed with PG nanocapsules

suspension (PG 1 mg/mL) in a ratio PG:HB 1:0.25 (w/w) (10). Then, both components were incubated for 1 hour at room temperature.

For HA association, the buffer of the stock solution was exchanged by NaOH 10^{-8} M using the Amicon Ultra4 filtration tubes in order to maintain the negative charge of the protein (HA theorical isoelectric point = 6.69). The concentration was adjusted to 0.375 mg/mL and this solution was then incubated with PG nanocapsules in a ratio 1:2.5 under the same conditions of HB.

Antigen association efficiency evaluation.

Association efficiency was indirectly calculated after separation of nanocapsules by centrifugation at 20000xg, 30 minutes and 15ºC (Hettich Zentrifugen; Tuttlingen, Germany). Free antigen was measured in collected supernatants from PG nanocapsules associating HB and HA, by ELISA and Dot-Blot, respectively. To calculate the association efficiency, the formula shown above for imiquimod was used.

Quantification of HB

The commercial kit Murex HBsAg Version 3 was used following the manufacturer's instructions for detecting HB. A calibration curve was made using the stock solution of HB mixed with supernatants of blank PG nanocapsules at the same proportion of the samples in order to quantify the concentration of HB in the samples.

Quantification of HA

Dot-Blot technique was used for quantification of HA concentration. Samples of supernatants and standard solutions (for calibration curve) were directly dropped on a PVDF membrane (2 µl). To detect the antigen, the membrane was firstly incubated with a mouse monoclonal Ab against the terminal His tag domain of the protein (1:1000) and then, with a goat anti-mouse IgG-HRP (1:20000). Antigen-Ab complexes were visualized by chemoluminiscence using the detection kit ECL Plus Western Blotting Detection Reagents (Amersham Biosciences, UK).

Subsequent analysis of dots intensity was performed by digitalizing the image and then using ImageJ© software (NIH; Bethesda, MD).

In vitro cell studies

Internalization of PG nanocapsules by macrophages

Adherent RAW 264.7 cells were plated (5×10^5 cells) in a 24-wells plate with 1 mL of complete medium in the presence or not of 50 μg/mL of PG nanocapsules labeled with rhodamine-6G for 30 minutes. After 3 washes with PBS to remove non-internalized nanostructures, cells were observed under an inverted fluorescence microscope (IX50, Olympus Optical Co GmbH; Hamburg, Germany).

For flow cytometry analysis the adherent cells were detached with Accutase® (PAA; Pasching, Austria) after incubation with the fluorescent PG nanocapsules. Cells were washed once with PBS and then incubated with 200 μL of Accutase® for 10 minutes at 37ºC and 5% CO_2. Finally, cells were washed with complete medium and centrifuged. The resulting suspension of cells was analyzed using a flow cytometer (FC500, Beckman-Coulter; Miami, FL).

Cytokine profile evaluation

For the assessment of cytokine production, 1×10^5 mouse peritoneal macrophages were incubated for 24 hours in the presence of PG and imiquimod-PG nanocapsules, at two different concentrations: 10 and 100 μg/mL. imquimod-PG nanocapsules incubated with macrophages contained 2 and 20 μg of imiquimod, respectively. As positive and negative controls, cells were incubated with either 1 μg/mL of lipopolysaccharide (LPS) (InvivoGen; San Diego, CA) or medium, respectively. After 24 hours, supernatants were collected, centrifuged at 100xg for 5 min at 4ºC, and stored at -20ºC before analysis. Levels of IL-1α, IL-6, IL-10 and TNF-α cytokines were determined using the FlowCytomix™ assay (eBioscience; Vienna, Austria) following manufacturer's protocol. Briefly, using a 96-wells plate, 25 μL of Ab-coated microspheres were incubated with 25 μL of culture supernatants

and 50 µL of biotin-conjugated secondary Abs for 2 hours at room temperature (RT) under horizontal agitation. After several washes, 50 µL of streptavidin-phycoerythrin and 100 µL of BSA 1% in PBS were added to the preparation for 1 hour at RT under agitation. Finally, beads were studied by flow cytometry.

Cell viability assay: *xCELLigence® system*

To measure the effect of PG and imiquimod -PG nanocapsules on cell viability, the xCELLingence® RTCA DP Instrument (Roche Diagnostics; Penzberg, Germany) was used following manufacturer's instructions. This system measures the variations in impedance caused by cell growth when cells are incubated on special plates containing gold electrodes.

Adherent RAW 264.7 cells were cultured until optimal cell number was achieved. The xCELLigence® device was placed inside the incubator (37ºC and 5% CO_2) and 1.5 x 10^4 cells per well (with gold electrodes) were incubated with 200 µL of complete medium during 18 hours until reaching the exponential phase. PG and imiquimod-PG nanocapsules were added at three different concentrations (25, 50 and 100 µg/mL) at 24th hour of culture and incubated with cells for 48 hours. As negative controls, medium and nanocapsules alone were added to individual wells. Continuous measurements of impedance (correlated with the amount of cells) were performed during the whole procedure in intervals of 15 minutes.

Non-invasive fluorescence *in vivo* imaging

PG nanocapsules labeled with Alexa Fluor 750 (50 µl) were injected intramuscularly in the hind leg of female FVC mice (4-5 weeks). An aqueous solution of Alexa Fluor 750-labeled PG (1 mg/ml) and PBS were used as controls by injecting the same volume at the same site. The injected fluorescent intensity was normalized for both the fluorescent nanocapsules and the soluble labeled PG solution in order to administer the same intensity in each animal.

Planar images were acquired using excitation and emission filters 710 and 780 nm, respectively, with exposure time of 10 seconds. The emitted fluorescent signal was monitored during 2 weeks using IVIS Imaging System 200 Series (Xenogen Corp.; Alameda, CA) at different time points post-injection (hours: 0.5, 2, 4, 8; and days: 1, 2, 7, 14). The acquired images were further analyzed using the Living Image® software (Caliper Life Sciences; Hopkinton, MA).

Immunization regimens

HB immunization

PG and imiquimod-PG nanocapsules were evaluated in female BALB/c mice. Animals were randomly distributed in groups of 10 mice. 10 μg of HB associated to the nanostructures were administered in a single-dose or in two doses separated 4 weeks (**Table 1**). The injection (50 μl) was performed intramuscularly in the hind leg of the mouse. Blood samples were collected from the maxillary vein at weeks 6, 9, 13, 17, 22, 26.

Table 1: Immunization schedule for hepatitis B.

Formulation	HB dose (μg)	Schedule (weeks)	Bleedings (weeks)
PG nanocapsules	10	0	9, 13, 17, 22, 26
	10	0,4	6, 9, 13, 17, 22, 26
Imiquimod-PG nanocapsules	10	0	6, 9, 13, 17, 22, 26
	10	0,4	9, 13, 17, 22, 26
HB-alum	10	0,4	6, 9, 13, 17, 22, 26

Influenza immunization

Two groups of 5 female BALB/c mice were immunized with two different doses of HA associated to PG nanocapsules (2 and 7.5 μg) following a 3-dose schedule (weeks 0, 3 and 5) (**Table 2**). Two control groups of mice

were immunized with 7.5 µg of alum-HA or 7.5 µg of fluid HA, respectively, following the same regimen. 50 µl of the formulations (PG:HA nanocapsules or controls) were injected in the subcutaneous cavity over the neck. Blood samples were collected from the maxillary vein at weeks 3, 5, 7 and 28.

Table 2: Immunization schedule for influenza

Formulation	HA dose (µg)	Schedule (weeks)	Bleedings (weeks)
PG nanocapsules	7.5 2	0, 3, 7	3, 5, 7, 28
HA-alum	7.5	0, 3, 7	3, 5, 7, 28
Plain HA	7.5	0, 3, 7	3, 5, 7, 28

Determination of serum specific antibodies

HB immunized mice

Serum anti-HB IgG endpoint titers were measured by ELISA. For this purpose, maxisorp microtiter wells (Nunc; Denmark) were coated with 5 µg/mL of HB in carbonate buffer (pH 9.6) overnight at 4ºC. Plates were then blocked with BSA 1% in PBS for 1 hour at 37ºC in order to minimize non-specific interactions. Serum samples and a mouse IgG monoclonal Ab directed against HB (used as control in the calibration curve) were serially diluted and incubated for 2 hours at 37ºC. All serum samples were tested at least twice and in duplicate. Control rabbit antiserum of known concentration was used in order to transform serum titers into international units (mIU/mL). Secondary Abs (goat anti-mouse IgG-HRP) were added to each well and incubated for 1 hour at 37ºC. Bound Abs were revealed with ABTS and the titers were expressed in mIU/mL.

To calculate the ratio IgG1/IgG2a, both IgG subtypes were analyzed in a pool of sera from all mice of each group following the same ELISA protocol. In this case, polyclonal goat anti-mouse IgG1 and IgG2a Abs, both conjugated with HRP, were used as secondary Abs. Then the ratio between IgG1/IgG2a levels was calculated in relation to the optical density levels.

Influenza immunized mice

The HA-specific IgG response was evaluated by ELISA. Purified HAhisKDEL in carbonate/bicarbonate buffer (pH 9.6) was used to coat ELISA maxisorp microplates (Nunc; Denmark) by incubating 500 ng/well of the protein overnight at 4 ºC and then blocked using the blocking buffer (PBST-2% BSA) for 1 hour at 37ºC. Two-fold dilutions of serum samples in blocking buffer (from 1:100 to 1:12800) were incubated for 1 hour at 37ºC with agitation. Then anti-mouse IgG-HRP secondary Ab was added (1:2000 in blocking buffer). For substrate reactions, ABTS was added and the peroxidase reaction was allowed to react for 15 min at RT in order to develop immunocomplexes. Plates were read at 405 nm in an ELISA microplate reader (Multiskan EX, Thermo Electron Corp.; Vantaa, Finland). Intense washings between incubations were performed with PBST (PBS-0.1% Tween 20) in order to remove non-bound Abs.

Statistical analysis

The analysis of variance (ANOVA) was performed using Statgraphics Plus 5.1. Tukey post-hoc analysis was employed to establish significant differences between groups. Differences were considered significant at a level of $p < 0.05$.

RESULTS

Development and characterization of immunostimulating nanocapsules

Preparation of immunostimulating nanocapsules

The development of immunostimulating nanocapsules was based on our previous experience on the use of chitosan (CS) nanocapsules for vaccine

delivery (10). Hence, polyglucosamine (PG) nanocapsules were spontaneously formed upon mixing an organic phase containing lecithin and squalene, and an aqueous phase containing PG dissolved in water. The specificity of this new nanocarrier as compared to the previous CS nanocapsules relies on the use of squalene and a highly deacetylated form of CS (PG), components of the core and the polymeric corona respectively, as well as the encapsulation of a lipophilic immunostimulant drug.

First, the most adequate conditions for preparation of nanocapsules with squalene nanocore were established taking the previously developed CS nanocapsules (10) as a reference (oily core composed of Miglyol® 812). Hence, CS nanocapsules containing squalene were prepared with increasing CS:lecithin ratios (from 1:4 to 1:16) by incorporating different proportions of lecithin (final concentrations in the formulation 0.4, 0.5, 0.6, 0.7%, respectively), as well as two different concentrations of CS (0.05 and 0.025%) in the aqueous phase. The volume of squalene (0.25 mL) was maintained for each formulation. The colloidal stability and physicochemical properties of the resulting nanocapsules were taken as the main criteria in the optimization process.

Colloidal stability of CS nanocapsules was assessed by identifying any leakage of squalene after applying high speed centrifugation. For this purpose, squalene was stained with a fat dye (Sudan III Red) prior to preparation. Because of the low density of squalene (0.85 mg/mL), the non-incorporated oil was clearly appreciable as a red layer of oil floating over the aqueous suspension after ultracentrifugation. We observed that lecithin concentrations of around 0.6% were able to retain the total oil volume and form a stabilizing corona around the oily nanodroplets. However, higher lecithin concentrations (0.7 and 0.8%) led to the formation of solid particles which were visualized in the form of a sediment upon ultracentrifugation (14).

Along with these macroscopic observations, particle size and ξ potential measurements of the nanostructures were performed. As shown in **Figure**

2A, the mean particle size was slightly influenced by both, lecithin and chitosan concentration (ranging from 200 to 230 nm) whereas the ζ potential values increased from +35mV to +45 mV (**Figure 2B**) depending on the proportion of CS in the formulation.

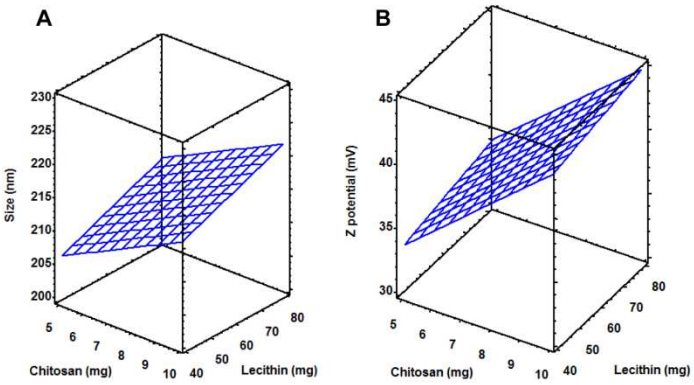

Figure 2: Influence of amount of lecithin and chitosan on the mean particle size and zeta potential of chitosan nanocapsules containing a squalene core. A) Size and B) ξ potential variations according to the mass ratio CS:lecithin (1:4 to 1:16).

Based on these results, we selected the appropiate amounts of lecithin and squalene and substituted CS with a deacetylation degree of 85% by that of deacetylation degree 95.5%, herein named as PG. Under such conditions, PG nanocapsules were obtained with a mean particle size of 172 nm, low polydispersity index (PdI 0.16) and very high positive surface charge (+66 mV) (**Table 3**). In addition, the lipophilic immunostimulant drug, imiquimod, was moderately incorporated within the oily core of PG nanocapsules (40%) without substantially modifying those original physicochemical properties, as shown in **Table 3**: particle size 198 nm, PdI 0.07 and ζ potential +63 mV.

Fluorescent labeling of PG nanocapsules.

PG nanocapsules were fluorescently labeled using two different strategies and dyes. Labeling with rhodamine-6G was used for assessing the uptake of PG nanocapsules by macrophages, whereas Alexa Fluor 750 was used

for *in vivo* NIR (near-infrarred) imaging purposes due to excitation and emission wavelength peaks required for this technique.

Rhodamine-6G is a fluorescent probe with lipophilic character, and therefore it was included within the oily compartment of PG nanocapsules. The encapsulation of rhodamine-6G was accomplished by incorporating the molecule in the organic phase during preparation. The resulting PG nanocapsules labeled with rhodamine-6G had a particle size of 190 ± 2 nm, homogenous distribution (PdI 0.14 ± 0.02) and positive ζ potential (+60 ± 2 mV), which were very similar to those exhibited by the blank formulation. The encapsulation efficiency of rhodamine-6G was around 82% and only a 20% of the incorporated amount was released in an aqueous medium after 2 hours of incubation at 37^{0}C under sink conditions (results not shown).

Alexa Fluor 750 was covalently linked to the polymeric shell. The polysaccharide PG was labeled prior to nanocapsules preparation (Alexa Fluor 750-PG) and then used to prepare the fluorescent Alexa Fluor 750-PG nanocapsules. In preliminary experiments, different reaction conditions were assessed by using different proportions of PG:Alexa Fluor 750. We determined that the particle size of the resulting nanostructures was constant regardless this ratio (around 200 nm), but ξ potential was affected by the different proportions (results not shown). Therefore, we could establish the most adequate labeling conditions using the PG:Alexa Fluor 750 mass ratio 25:1. The resulting Alexa Fluor 750-PG nanocapsules preserved the physicochemical properties of blank PG nanocapsules: particle size 222 ± 1 nm; PdI 0.17 ± 0.01; ξ potential +57 ± 1 mV.

Association of particulated (HB) and soluble antigens (HA) to the polymeric surface of immunostimulating nanocapsules.

Both the recombinant hepatitis B surface antigen (HB) and the hemaglutinnin subunit of the influenza virus (HA) were associated to the polymeric surface of PG nanocapsules by electrostatic interactions (**Figure 1**). The HB is a particulated protein which exhibits an intrinsic negative surface charge of -20 mV (15), whereas HA is a soluble protein with an

isoelectric point of 6.69. Hence, under the experimental conditions chosen for the association both proteins were negatively charged and interacted quite efficiently with the cationic polysaccharidic coating (75 and 70% association efficiency, respectively) without altering the particle size distribution (**Table 3**). In addition, despite of the high association efficiency of HB and HA to the nanocapsules, their ζ potential remained highly positive (+60 mV), indicating the prevalent presence of the polysaccharide on their surface.

Table 3: Physicochemical characterization of the different prototypes of PG nanocapsules with different core composition (squalene or squalene+imiquimod) and associating both types of antigens: HB and HA.

Core composition	Ag	Size (nm)	PdI	ζ potential (mV)	Ag A.E. (%)	Imiquimod A.E. (%)
Squalene	--	172 ± 3	< 0.2	+66 ± 1	-	-
	HB	230 ± 13	< 0.2	+60 ± 3	72 ± 8	-
	HA	217 ± 4	< 0.2	+51 ± 2	69 ± 2	-
Squalene + Imiquimod	--	198 ± 5	< 0.2	+63 ± 1		40 ± 2
	HB	299 ± 11	< 0.2	+60 ± 4	78 ± 6	40 ± 2

PdI: polydispersity index; A.E.: association efficiency; Ag: antigen.

Interaction of immunostimulating nanocapsules with macrophages

The effect of PG and imiquimod-PG nanocapsules on APCs was assessed by studying their uptake by macrophages and further cell activation in terms of cytokine secretion. Increasing concentrations of rhodamine-6G PG nanocapsules were incubated with macrophages of the cell line Raw 264.7 for a short period of time (30 minutes). Under the optical microscope, we observed a high density of fluorescent cells which had internalized the nanocapsules. In addition, the uptake of PG nanocapsules

by macrophages increased in a dose-dependent manner (**Figure 3A**). This observation was further confirmed by flow cytometry, which revealed a 100% of internalization of PG nanocapsules for the highest concentration tested (50 μg/mL) (**Figure 3B**). These results confirmed the great capacity of PG nanocapsules to be recognized and taken up by macrophages.

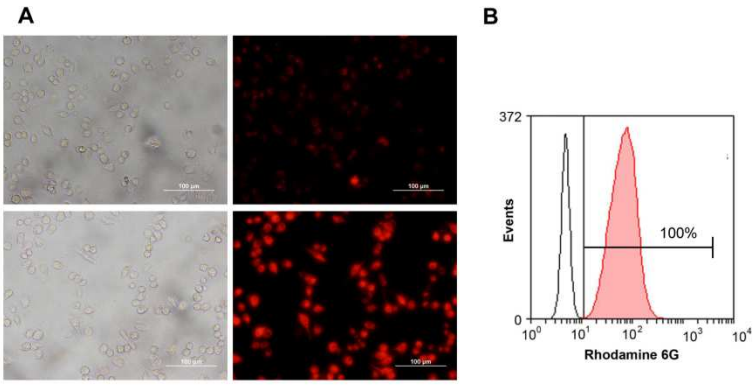

Figure 3: Internalization of fluorescent PG nanocapsules labeled with rhodamine-6G in macrophages measured by optical fluorescence microscopy and flow cytometry. (**A**) Left panels: images acquired in brightfield; right panels: images acquired with fluorescence filters. Upper row: Cells incubated with 10 μg/mL of rhodamine-6G-labeled PG nanocapsules; Lower row: Cells incubated with 50 μg/mL of rhodamine-6G-labeled PG nanocapsules. (**B**) Flow cytometry histogram showing the number of events versus the Rhodamine-6G fluorescence intensity when cells were incubated with 50 μg/mL of rhodamine-6G-labeled PG nanocapsules for 30 minutes.

The activation of murine peritoneal macrophages by PG and imiquimod-PG nanocapsules was also evaluated by measuring the levels of secreted cytokines (IL-1α, IL-6, IL-10 and TNF-α) upon incubation with the nanocapsules for 24 hours at two different concentrations (10 and 100 μg/mL). As observed in **Figure 4**, only imiquimod-PG nanocapsules were able to induce a significant production of all cytokines studied, although their concentration was lower than for the positive control (LPS), except IL-10. The levels of this cytokine and IL-1α increased with the concentration of imiquimod-PG nanocapsules in the medium, whereas IL-6 and TNF-α did not follow a dose-dependent pattern. Regarding PG

nanocapsules only a slight production of the studied cytokines was detected compared to those encapsulating imiquimod and LPS control. In addition, the dose of PG nanocapsules did not affect the levels of cytokines secreted by macrophages.

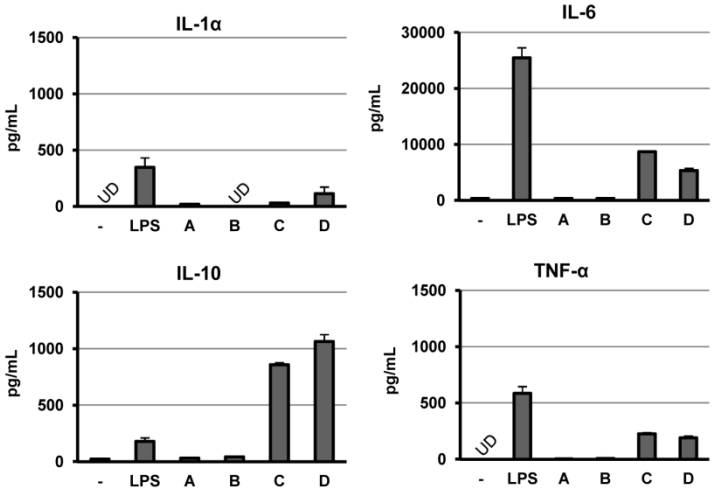

Figure 4: Cytokine production of peritoneal macrophages incubated with blank PG and imiquimod-PG nanocapsules at two different doses (10 and 100 μg/mL) for 24 hours. Negative control was culture medium, and positive control was LPS (1 μg/mL) incubated for 24 hours. Average concentration (pg/mL) of IL-1α, IL-6, IL-10 and TNF-α in culture supernatants, from one representative experiment (performed twice in duplicates). UD: undetectable levels (IL-1α < 15.7 pg/mL; TNF-α < 2.1 pg/mL). Results are presented as mean ± SD.

In vivo fluorescence imaging

PG nanocapsules labeled with Alexa Fluor 750 (NIR dye) and controls fluid Alexa Fluor 750-PG in solution and PBS were intramuscularly injected to FVB mice. The fluorescent signal was monitored during 15 days using the IVIS® Imaging System by acquiring planar images at established time points. According to the images (**Figure 5**), Alexa Fluor 750-PG nanocapsules slowly drained from the injection site. Indeed, it was possible to detect a faint fluorescent signal at the injection site even at day 15, suggesting the formation of a depot which gradually released the nanocapsules over time. The analysis of the images indicated that the

intensity of the signal was similar for both the PG nanocapsules and the free polymer. Around 25% of the injected dose for both interventions was detected by the end of the study (day 15), evidencing minimal differences in the clearance rate from the injection site. This finding suggests that the movement of PG nanocapsules was importantly governed by the polysaccharidic shell. Besides, an intense signal in the abdominal area, which lasted at least 4 hours, was observed for the mice injected with Alexa Fluor 750-PG in solution. A weaker signal lasting up to 2 hours was also observed in mice receiving the nanocapsules. The anatomic localization during necropsy determined that this signal corresponded to the bladder (results not shown) for both interventions.

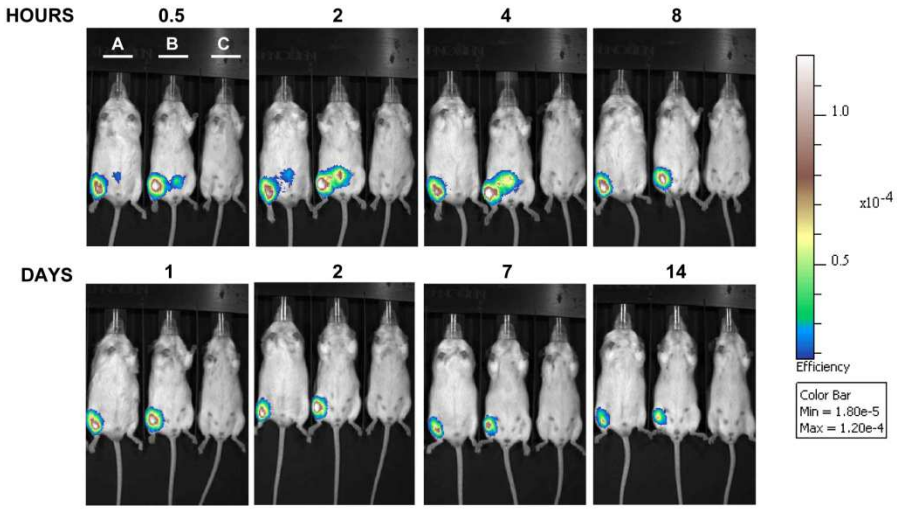

Figura 5: *In vivo* NIR planar images acquired at different time points after intramuscular administration of PG nanocapsules labeled with Alexa Fluor 750 (mouse A), soluble polymer labeled with Alexa Fluor 750 (mouse B) and phosphate buffer saline (mouse C).

Immunization against hepatitis B with immunostimulating nanocapsules

In the present work, we evaluated the potential adjuvant properties of PG and imiquimod-PG nanocapsules associating the HB and their ability to induce immune protection after a single-dose immunization schedule. Hence, 10 µg of HB associated to the nanostructures were intramuscularly

injected to BALB/c mice in a single-shot or following a boost-dose schedule (**Table 1**). As a positive control, 10 μg of alum-adsorbed HB (HB-alum) were administered twice in a 4 week interval.

Single-dose immunization protocol

The potentiating effect of both PG and imiquimod-PG nanocapsules on the specific immune response against HB was observed without significant differences between them all along the time of study. The anti-HB IgG levels remained constant between 100 and 200 mIU/mL regardless the composition of the inner oily core (squalene or squalene+imiquimod), reaching equivalent levels to two doses of HB-alum by the end of the study (weeks 22 and 26) (**Figure 6**). The relevance of these data relies in the ability of both prototypes to raise the specific IgG levels over 100 mIU/mL (protective in humans (16)). Moreover, this protective response was maintained during the six months of study, while two doses of the conventional adjuvant was characterized by a decreasing pattern in serum IgG concentration.

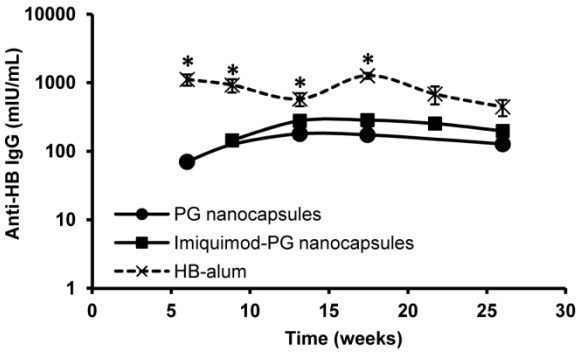

Figure 6: Immune response elicited after a single-shot immunization with PG and imiquimod-PG nanocapsules associating HB (10 μg). The positive control HB-alum (10 μg) was administered at weeks 0 and 4. Results are expressed in mIU/mL of specific anti-HB IgG quantified at different time points post primary immunization (mean +/- SEM). * indicates significant differences ($p<0.05$).

Boost-dose immunization protocol

When PG nanocapsules were administered following a boost-dose immunization regimen, the early immune response was moderate, eliciting lower anti-HB IgG levels than the positive control. However, a pronounced increment was observed from week 17 onwards, achieving significantly higher levels than HB-alum ($p < 0.05$) (**Figure 7**). The kinetics of the immune response was drastically modified when the imiquimod was included in the composition of the nanocapsules. Hence, the response elicited by imiquimod-PG nanocapsules was quick and intense, achieving significantly higher levels than PG nanocapsules and HB-alum at early time points ($p<0.05$). However, serum IgG concentration gradually decreased over time, reaching equivalent levels to those elicited by HB-alum by the end of the study.

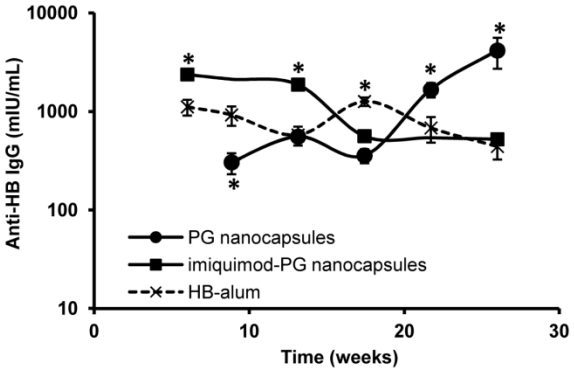

Figura 7: Immune response elicited after two doses (0 and 4 weeks) of PG and imiquimod-PG nanocapsules associating HB, and the positive control HB-alum (10 μg). Results are expressed in mIU/mL of specific anti-HB IgG quantified at different time points post primary immunization (mean +/- SEM). * indicates significant differences ($p<0.05$).

Modulation of the immune response against hepatitis B

The modulation of the immune response against HB by PG and imiquimod-PG nanocapsules was studied by calculating the ratio between the IgG subtypes IgG1 and IgG2a (IgG1/IgG2a). This parameter indicates the main type of immune response, whether it is mediated by Th1 or Th2

lymphocytes. While a predominant Th2 activation induces a humoral response characterized by the main production of IgG1, the presence of IgG2a subtype is related to cellular immune responses mediated by Th1 lymphocytes.

As expected, HB-alum (10 μg at weeks 0 and 4) elicited a strongly biased Th2 immune response (**Figure 8**), inducing higher levels of IgG1 than IgG2a (17). Nanocapsules prototypes behave differently according to their composition and immunization regimen. Following a single-dose schedule, we observed a strong influence of imiquimod in shifting the response to a mixed Th1 and Th2 type (IgG1/IgG2a ratio around 1), whereas PG nanocapsules raised the ratio to a constant value of 2, indicating a predominant Th2 response (**Figure 8A**). Nevertheless, the performance of PG nanocapsules completely changed when a second dose was administered. The IgG1/IgG2 ratio dropped to values around 1, indicating the initiation of a cellular response after the boost dose. In contrast, imiquimod-PG nanocapsules did not modify the profile of the IgG1/IgG2 ratio after the second dose, thus maintaining a mixed Th1/Th2 mediated immune response regardless the immunization schedule.

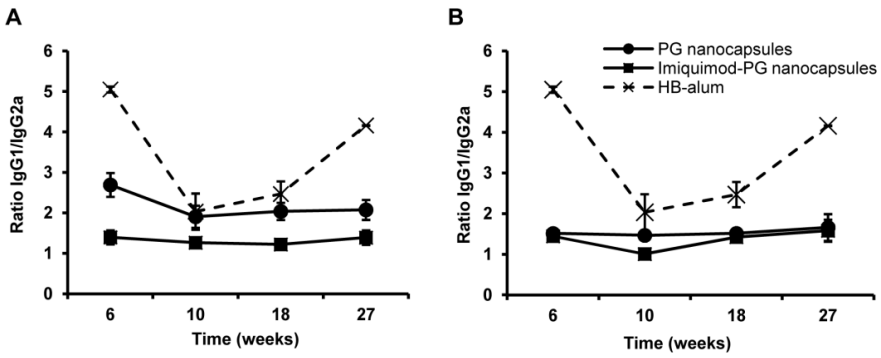

Figura 8: IgG subtypes, IgG1 and IgG2a, against HB elicited after the different immunization protocols for PG and imiquimod-PG nanocapsules associating HB (10 μg) and expressed as the ratio between IgG1 and IgG2a. A) Single dose immunization. B) Boost-dose immunization (0 and 4 weeks). 10 μg HB-alum were administered following the boost-dose immunization regimen. Results are expressed as mean +/- SD.

Immunization against influenza with immunostimulating nanocapsules

The capacity of PG nanocapsules to potentiate the immune response was also evaluated for a different antigen, the hemagglutinin of influenza virus (HA). Two different doses of HA associated to PG nanocapsules (2 and 7.5 μg) were tested in mice. PG nanocapsules were administered subcutaneously in three shots (0, 3 and 5 weeks) and the humoral immune response was monitored during 7 months.

As observed in **Figure 9**, the immune response profile elicited by SqGL was similar to that determined for HB. Moderate specific IgG levels were achieved at early time points, which gradually increased over time. In fact, this immune response was higher than HA-alum and fluid HA on weeks 7 and 28 regardless the antigen dose.

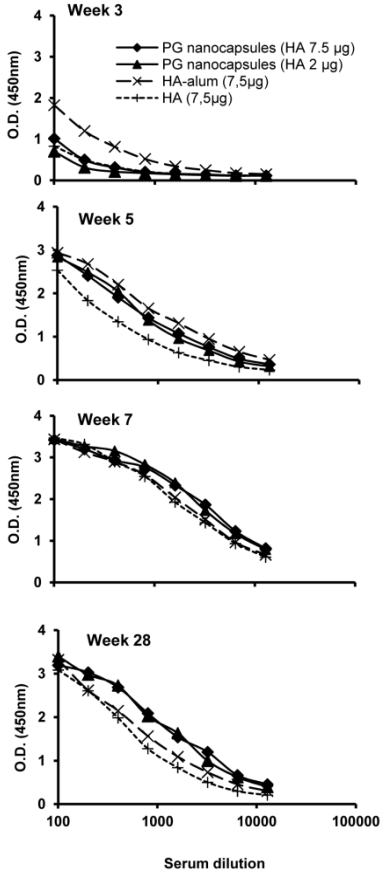

Figure 10: Serum neutralizing antibody levels against HA after three immunizations (0, 3 and 5 weeks) with PG nanocapsules associating two different doses of HA (2 and 7.5 μg) and the two controls (HA-alum and fluid HA, 7.5 μg both). PG nanocapsules HA 7.5 μg (▲), PG nanocapsules HA 2 μg (◆), HA-alum 7.5 μg (X), fluid HA 7.5 μg (+).

DISCUSSION

The widespread use of novel subunit antigens has been mainly hindered by their low immunogenic character. Because of this, these safe antigens require the use of complementary adjuvants and immunopotentiators that could enhance their immunogenicity in order to elicit protective immune responses, modulate them and minimize adverse reactions (3).

Squalene is a linear triterpene molecule naturally present in the organism. It is the first precursor in the biosynthesis of cholesterol and the main component of human sebum. Squalene is also the main oil component of licensed adjuvant emulsions (MF59™ and AS03™ in vaccine formulations against influenza) and it is usually the oil of choice for the development or new vaccine adjuvant emulsions (7). In these emulsion-based vaccine formulations the antigen is usually mixed up with the preformed emulsions. No physical interactions occur between the oil droplets and the antigen, which remains dispersed in the aqueous phase of the emulsion (18). The purpose of this work was to rationally modify the squalene-based emulsions in order to incorporate the different components (oil, surfactants and antigen) within the same nanocarrier. To achieve this aim we proposed the formulation of squalene-based nanocapsules containing a cationic polysaccharidic shell coating. In these core-shell nanostructures the lipid core (squalene oil droplets) has been selected in order to confer the immunostimulant properties to the system, while the polysaccharidic shell (CS or PG) is expected to have a double role, the association of the antigen and its improved presentation to the immune system (**Figure 1**). This combined structure is intended to co-deliver one or more antigens concomitantly immunostimulants with the final goal of promoting and modulating the immune response.

In a first set of experiments we produced CS nanocapsules containing squalene instead of Miglyol® 812 (10) as previously reported. Different proportions of lecithin and CS were tested in order to determine the optimal conditions for the formulation of squalene-based nanocapsules. The resulting nanocapsules exhibited a homogeneous and unimodal

particle size distribution with a mean size in the range of 200-230 nm and a positive surface charge of between +35 and +45 mV, which was indicative of the polymer shell formation around the oily cores (**Figure 2**). However, the colloidal stability of the nanocapsules was highly dependent on the lecithin concentration in the formulation. Namely, low lecithin concentrations (0.4 and 0.5%) were insufficient for preserving the stability of the nanocapsules. In this sense, it has been reported that the minimum amount of lecithin required for the stabilization of microemulsions depends on the equivalent alkane carbon number (EACN) of the oil, which relates to its hydrophobicity (19). The high lipophilic character of squalene (EACN 24 versus 10-12 of Miglyol® 812 previously used in the preparation of CS nanocapsules (10)) would justify the higher proportion of phospholipids required for the stabilization of the nanocapsules. However, when the concentration of lecithin went beyond 0.7% a solid sediment, likely due to the formation of CS-lecithin complexes (14) was observed. From these results, we selected as optimal conditions for the formation of nanocapsules with a squalene core and a PG shell, the CS:lecithin ratios of 1:6 and 1:12.

These conditions were translated into the formulation of squalene-containing PG nanocapsules. The results indicated that PG:lecithin ratio of 1:12, which corresponded to the lowest concentration of PG in the aqueous phase, was the one leading to the smallest particle size (180 nm) and narrowest unimodal distribution (**Table 3**). High concentrated PG solutions increased the viscosity of the aqueous phase, thus hindering the dispersion of the organic solvents to the aqueous medium. Regarding surface charge, the presence of a greater amount of free amino groups in the PG molecule (deacetylation degree of 95.5%), as compared to the CS chains, led to higher positive ξ potential values (+66 mV).

As previously reported for imiquimod-containing CS nanocapsules (20), this lipophilic immunostimulant could be encapsulated within the squalene core of PG nanocapsules (40% association efficiency). On the other hand, while lipophilic molecules were entrapped within the

squalene core of PG nanocapsules, the association of different antigens was accomplished by electrostatic interactions with the cationic polymeric surface. The recombinant hepatitis B surface antigen (HB) and the hemagglutinin subunit of the influenza virus (HA) are different in terms of origin and structure. While HB is a virus-like particle (VLP) composed of several protein subunits embedded in a mixture of lipids forming a 22 nm particle (12), HA is a soluble protein with a molecular weight of 63 kDa (13). The negative ζ potential of HB and negative charge of HA (maintained over its isoelectric point) enabled their association to the PG shell in a high proportion while conserving the physicochemical properties of blank PG nanocapsules, as shown in **Table 3**.

Antigen-presenting cells (APCs) are responsible of recognizing, taking up and processing the antigen to be further presented to T cells and thus, initiating the adaptive immune response. Therefore, the first interaction with these cells is crucial to trigger the immune cascade. In a first instance, the internalization of PG nanocapsules by APCs was assessed using macrophages as cell model. The results obtained by fluorescence microscopy and flow cytometry confirmed a massive capture of PG nanocapsules by macrophages (**Figure 3**). This massive internalization (30 minutes – 100% internalization) may have also been responsible for the important reduction in cell viability. In fact, for the highest concentration tested of both PG and imiquimod-PG nanocapsules (100 µg/mL), around 20% of cells remained viable after 24 hours, although this effect was dose dependent (**Figure 10**). It is known that the particulate nature of the nanocapsules is a key factor for their interaction with APCs, however their composition and surface charge may also affect the intensity of their internalization (21). In general, cationic nanostructures have demonstrated to improve cellular uptake by APCs compared to anionic or neutral systems (22, 23). In fact, chitosan-based nanocarriers, such as nanoparticles (24, 25) and nanocapsules (20) have also demonstrated to be largely taken up by APCs. This surface characteristic

provided by PG shell has been described to promote a strong interaction with the outer membrane of the cells and subsequently, favoring internalization (25).

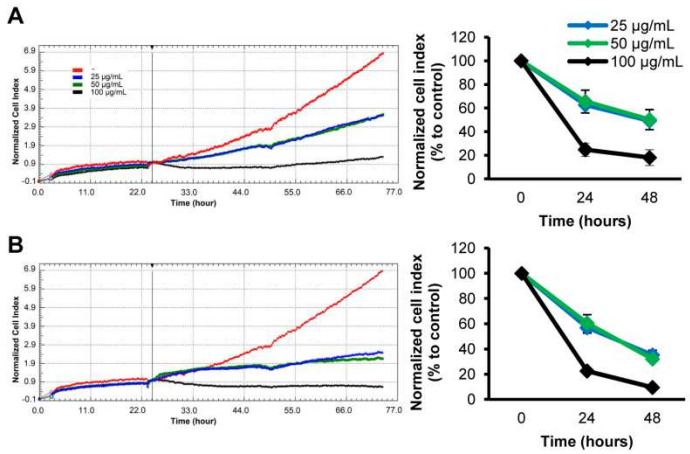

Figure 5: Real-time monitoring of cell growth evaluated by xCELLingence® system. Different concentrations of blank PG and imiquimod-PG nanocapsules (25, 50 and 100 µg/mL – blue, green and black lines repectively) were incubated during 48 hours with Raw 264.7 cells. Upper row: blank PG nanocapsules; lower row: imiquimod-PG nanocapsules. Red line: cells incubated with culture medium (control). Vertical black line indicates the addition of the nanostructures to the cells after 24 hours growing. Results are presented as mean ± SD.

Beyond the high affinity and further internalization of PG nanocapsules by macrophages, their capacity to activate APCs is also a crucial issue in the development and modulation of the adaptive immune response. The low levels of secreted cytokines determined for PG nanocapsules (**Figure 4**) confirmed their non-inflammatory character. This characteristic was also described for other CS-based nanoparticles (26, 27) and CS nanocapsules (20). However, the introduction of imiquimod in the oily core of PG nanocapsules resulted in a significant response in terms of cytokine production. In fact, the slight effect observed for blank PG nanocapsules suggested that imiquimod was the major component of the nanocapsules inducing this cytokine response. Imiquimod is a well-known modifier of the immune response, characterized by promoting the

secretion of different cytokines by APCs upon activation of the intracellular Toll-like receptor 7 (TLR7) (28). The intense production of the pro-inflammatory cytokines IL-1α, IL-6 and TNF-α can be attributed to the effect of imiquimod intracellularly released after internalization of the vehicles. Besides, the production of high levels of IL-10 (higher than LPS) was also observed. This cytokine has been described to importantly contribute to the attenuation of the inflammatory response (29), thus, likely playing a relevant role in regulating the secretion of pro-inflammatory cytokines induced by imiquimod-PG nanocapsules. In fact, this anti-inflammatory cytokine may have contributed to weaken the dose-dependent character previously described for either imiquimod itself (30) or entrapped in a nanocapsular system (20). In addition, the monitorization of cell viability allowed us to determine that the number of viable macrophages importantly decreased within the first 24 hours of study (**Figure 10**). Therefore, we can deduce that the low number of viable cells remaining at 24 hours may have also contributed to impair the increasing response of pro-inflammatory cytokines at the highest concentration of imiquimod-PG nanocapsules tested.

In the present work, *in vivo* optical fluorescence imaging was used to determine the draining rate of the fluorescently labeled nanocapsules from the injection site. The images presented in **Figure 5** show that the fluorescently labeled polymer exhibited the same draining profile as the nanocapsules, thus suggesting that the PG shell might be responsible for the slow draining of the nanocapsules from the injection site. An additional fluorescent spot was identified in the bladder, which was especially noticeable in those mice receiving the free polymer. This could be attributed to faster degradation of the free polymer, as compared to that forming nanocapsules, and the access of the resulting fragments to systemic circulation, followed by their excretion in urine (31). An alternative explanation could be found in a different migration pattern of the nanocapsules and the free polymer. The facilitated uptake of PG nanocapsules by APCs may have promoted their capture at the injection

site and subsequent transport via the lymphatics instead of a direct drainage to the blood stream. However, an in-depth biodistribution study needs to be conducted in order to fully elucidate the mechanism of clearance of the nanocapsules. Irrespective of this, form this study we can conclude that PG nanocapsules were able to form a depot at the injection site allowing a slow drainage of the nanocapsules through the lymphatic system, likely transported by upon APCs.

The efficacy of PG and imiquimod-PG nanocapsules was then evaluated in order to determine the most relevant immunological properties of these nanocarrier-based adjuvants, such as their immunopotentiating effect against different types of antigens, as well as their capacity for reducing the number of immunizations (single-dose) and modulating the immune response.

A single immunization with PG nanocapsules associating HB resulted in protective IgG levels against HB (>100 mIU/mL) all along the study (**Figure 6**). This behavior could be ascribed to the surface composition of the nanocapsules, which, as described above, was found to promote their uptake by macrophages, as well as to determine their biodistribution. Their prolonged retention at the injection site (as determined by NIR imaging) might have allowed their gradual capture by APCs and, thus, their transport to the draining lymph nodes (32) and prolonging antigen presentation over time.

The administration of a second dose of PG nanocapsules led to an enhanced long-term IgG response (**Figure 7**). This boosted response was also observed upon administration of two doses of PG nanocapsules associating HA. In this case, an initial moderate response was followed by increasing IgG levels over time, these levels being higher than those corresponding to the standard alum control (**Figure 9**). In addition, PG nanocapsules were able to induce enhanced and sustained specific immune responses upon administration of low doses of antigen. Indeed, as noted in **Figure 9**, the IgG titers generated by a 2 μg-dose of antigen

were similar than those corresponding to 7.5 μg, thus, confirming the immunopotentiating effect of PG nanocapsules.

The incorporation of imiquimod in the structure of PG nanocapsules had a dose-dependent effect *in vivo*. The response achieved after a single administration of imiquimod-PG nanocapsules was comparable to that of blank PG nanocapsules (**Figure 6**). However, the administration of a second dose led to a sharp boosted immune response (**Figure 7**). The fast and strong response after the boost-dose suggests a different mechanism of action due to the intervention of imiquimod. This is a TLR agonist, which is known to have a strong effect on B cells and particularly, on activated B cells (33). Therefore, the first dose of imiquimod-PG nanocapsules might have firstly activated the B cells, which then responded more efficiently after a second exposure, thus inducing a prompt and intense production of specific IgG Abs.

Besides the immunopotentiating properties of PG and imiquimod-PG nanocapsules against HB, the modulation of the specific immune response has also been studied. Two different behaviors were observed for both prototypes: while imiquimod-PG nanocapsules were able to induce Th1-mediated immune responses regardless the number of doses, the main type of immune response elicited by PG nanocapsules was dependent on the immunization regimen (**Figure 8**). Imiquimod has been extensively described to modulate the immune response by skewing immunity towards a predominant Th1 type (34), as observed when imiquimod-PG nanocapsules were administered even in a single dose. On the other hand, one dose of PG nanocapsules elicited a predominant Th2 response, which shifted to a mixed Th1/Th2 upon the boost-dose. Since these nanocarriers did not contain any immunomodulator drug, their modulating effect must be attributed to their core-corona composition. In this sense CS, has been recognized for its ability to elicit balanced Th1/Th2 responses (10, 35, 36). On the other hand, in the present study we found that the IgG1/IgG2a ratio values were lower than those observed for CS nanocapsules with Miglyol® 812 core administered in a single dose

(IgG1/IgG2a = 2 and 4, respectively for squalene and Miglyol® 812) (10). This finding suggests that the squalene core could have also influenced the balance towards a predominant Th1 response (37).

CONCLUSIONS

Here we report a multifunctional immunoacting nanocarrier having the capacity of incorporating one or more immunostimulants and antigens. Taking advantage of the known success of squalene-based emulsions, this novel nanocarrier has singular advantages associated to its core-corona structure and in particular to its cationic polysaccharidic shell. Overall, this nanocarrier showed the capacity to potentiate and modulate specific immune responses against different antigens, namely HB and HA. Moreover, the composition of the nanocarrier was found to play a crucial role in the kinetics and modulation of the immune response. Therefore, simple modifications of the structure or composition of the nanocapsules could be attempted in order to find the most adequate combination for each antigen. Beyond this, the possibility of associating different antigens and adjuvants to the same nanocarrier provides an unique opportunity in the development of more efficient and multivalent vaccines.

ACKNOWLEDGEMENTS

This work was supported by a grant from the Bill & Melinda Gates Foundation and Consolider Ingenio 2010 (CSD2006-00012; Ministry of Science and Innovation, Spain), Competitive Reference Groups SUDOE-FEDER (SOE1/P1/E014) and Spanish Institute of Health "Carlos III" (PI081444). We would like to thank Shantha Biotechnics Limited (Hyderabad, India) and Algenex S.L. (Madrid, Spain) for providing us rHBsAg and HA, respectively. SV and MP acknowledge a fellowship from Spanish Ministry of Education (FPU predoctoral grants program). The advice from Martin Friede from the World Health Organization, the collaboration of José Vicente González and Edwige Biotteau, and the technical assistance of Rafael Romero, Andrea Hernández and Christian Sánchez Espinel are highly appreciated.

REFERENCES

1. Plotkin SA (2005) Vaccines: Past, present and future. *Nat Med* 11: S5-11.

2. Perrie Y, Mohamed AR, Kirby D, McNeill SE & Bramwell VW (2008) Vaccine adjuvant systems: Enhancing the efficacy of sub-unit protein antigens. *Int J Pharm* 364: 272-280.

3. Vicente S, Prego C, Csaba N & Alonso MJ (2010) From single-dose vaccine delivery systems to nanovaccines. *J Drug Deliv Sci Technol* 20: 267-276.

4. Correia-Pinto JF, Csaba N & Alonso MJ (2013) Vaccine delivery carriers: Insights and future perspectives. *Int J Pharm* 440: 27-38.

5. De Temmerman M, *et al* (2011) Particulate vaccines: On the quest for optimal delivery and immune response. *Drug Discov Today* 16: 569-582.

6. Moon JJ, Huang B & Irvine DJ (2012) Engineering nano- and microparticles to tune immunity. *Adv Mater* 24: 3724-3746.

7. Fox CB (2009) Squalene emulsions for parenteral vaccine and drug delivery. *Molecules* 14: 3286-3312.

8. Vila A, *et al* (2004) Low molecular weight chitosan nanoparticles as new carriers for nasal vaccine delivery in mice. *Eur J Pharm Biopharm* 57: 123-131.

9. Prego C, *et al* (2010) Chitosan-based nanoparticles for improving immunization against hepatitis B infection. *Vaccine* 28: 2607-2614.

10. Vicente S, *et al* (In press) A polymer/oil based nanovaccine as a single-dose immunization approach

11. Atmar RL, *et al* (2011) Norovirus vaccine against experimental human norwalk virus illness. *N Engl J Med* 365: 2178-2187.

12. Grgacic EVL & Anderson DA (2006) Virus-like particles: Passport to immune recognition. *Methods* 40: 60-65.

13. Gomez-Casado E, *et al* (2011) Insect larvae biofactories as a platform for influenza vaccine production. *Protein Expr Purif* 79: 35-43.

14. Prego C, Torres D & Alonso MJ (2006) Chitosan nanocapsules: A new carrier for nasal peptide delivery. *J Drug Deliv Sci Tec* 16: 331-337.

15. Tafaghodi M*, et al* (2012) Hepatitis B surface antigen nanoparticles coated with chitosan and trimethyl chitosan: Impact of formulation on physicochemical and immunological characteristics*. Vaccine* 30: 5341-5348.

16. Shouval D (2003) Hepatitis B vaccines*. J Hepatol* 39: S70-S76.

17. Gupta RK (1998) Aluminum compounds as vaccine adjuvants*. Adv Drug Deliv Rev* 32: 155-172.

18. O'Hagan DT, Ott GS, De Gregorio E & Seubert A (2012) The mechanism of action of MF59 - an innately attractive adjuvant formulation*. Vaccine* 30: 4341-4348.

19. Acosta E, Nguyen T, Witthayapanyanon A, Harwell J & Sabatini D (2005) Linker-based bio-compatible microemulsions*. Environ Sci Technol* 39: 1275-1282.

20. Vicente S*, et al* (In prep.) Co-delivery of viral proteins and TLR7 agonist from polysaccharide nanocapsules: a needle-free vaccination strategy

21. Bachmann MF & Jennings GT (2010) Vaccine delivery: A matter of size, geometry, kinetics and molecular patterns*. Nat Rev Immunol* 10: 787-796.

22. Roser M, Fischer D & Kissel T (1998) Surface-modified biodegradable albumin nano- and microspheres. II: Effect of surface charges on in vitro phagocytosis and biodistribution in rats*. Eur J Pharm Biopharm* 46: 255-263.

23. Foged C, Brodin B, Frokjaer S & Sundblad A (2005) Particle size and surface charge affect particle uptake by human dendritic cells in an in vitro model*. Int J Pharm* 298: 315-322.

24. Zaki NM, Nasti A & Tirelli N (2011) Nanocarriers for cytoplasmic delivery: Cellular uptake and intracellular fate of chitosan and hyaluronic acid-coated chitosan nanoparticles in a phagocytic cell model*. Macromol Biosci* 11: 1747-1760.

25. Bal SM, *et al* (2010) Efficient induction of immune responses through intradermal vaccination with N-trimethyl chitosan containing antigen formulations. *J Control Release* 142: 374-383.

26. Chellat F, *et al* (2005) Metalloproteinase and cytokine production by THP-1 macrophages following exposure to chitosan-DNA nanoparticles. *Biomaterials* 26: 961-970.

27. Liu L, *et al* (2010) The impact of arginine-modified chitosan-DNA nanoparticles on the function of macrophages. *J Nanopart Res* 12: 1637-1644.

28. Stanley MA (2002) Imiquimod and the imidazoquinolones: Mechanism of action and therapeutic potential. *Clin Exp Dermatol* 27: 571.

29. Moore K, Ogarra A, Malefyt R, Vieira P & Mosmann T (1993) Interleukin-10. *Annu Rev Immunol* 11: 165-190.

30. Testerman T, *et al* (1995) Cytokine induction by the immunomodulators imiquimod and S-27609. *J Leukoc Biol* 58: 365-372.

31. Dong W, *et al* (2010) Pharmacokinetics and biodegradation mechanisms of a versatile carboxymethyl derivative of chitosan in rats: *In vivo* and *in vitro* evaluation. *Biomacromolecules* 11: 1527-1533.

32. Henriksen-Lacey M, *et al* (2010) Liposomal cationic charge and antigen adsorption are important properties for the efficient deposition of antigen at the injection site and ability of the vaccine to induce a CMI response. *J Control Release* 145: 102-108.

33. Tomai M, Imbertson L, Stanczak T, Tygrett L & Waldschmidt T (2000) The immune response modifiers imiquimod and R-848 are potent activators of B lymphocytes. *Cell Immunol* 203: 55-65.

34. Wagner T, *et al* (1999) Modulation of Th1 and Th2 cytokine production with the immune response modifiers, R-848 and imiquimod. *Cell Immunol* 191: 10-19.

35. Zaharoff DA, Rogers CJ, Hance KW, Schlom J & Greiner JW (2007) Chitosan solution enhances both humoral and cell-mediated immune responses to subcutaneous vaccination. *Vaccine* 25: 2085-2094.

36. Wen Z, Xu Y, Zou X & Xu Z (2011) Chitosan nanoparticles act as an adjuvant to promote both Th1 and Th2 immune responses induced by ovalbumin in mice. *Marine Drugs* 9: 1038-1055.

37. Fox CB, Baldwin SL, Duthie MS, Reed SG & Vedvick TS (2011) Immunomodulatory and physical effects of oil composition in vaccine adjuvant emulsions. *Vaccine* 29: 9563-9572.

CAPÍTULO 5

CAPÍTULO 5

Biodistribution and lymph node retention of polyglucosamine nanocapsules

Este trabajo ha sido realizado en colaboración con: Beth A. Goins y William T. Phillips.

Radiology Department. University of Texas Health Science Center at San Antonio. 7703 Floyd Curl Dr.; San Antonio, TX 78229-3900; USA.

ABSTRACT

We have previously reported the adjuvant properties of polyglucosamine (PG) nanocapsules using the recombinant hepatitis B surface antigen (rHBsAg) as a model antigen. The aim of this study has been to monitor the biodistribution of PG nanocapsules and their affinity for the draining lymph nodes after subcutaneous (s.c.) injection. The nanocapsules were efficiently radiolabeled with indium-111 (^{111}In) (labeling efficiency of 98%). The stability of the radiolabeled nanocapsules in biological medium was found to be adequate for imaging purposes. The nanometric particle size of blank nanocapsules was preserved after the radiolabeling process and only a 20% of ^{111}In associated to the nanocapsules was released in serum after 48 hours of incubation. The radiolabeled nanocapsules and the control $^{111}InCl_3$ in saline solution (500 μCi in 100 μl) were injected s.c. to New Zealand rabbits. The γ-scintigraphy imaging analysis revealed the slow clearance of the nanocapsules from the injection site and their progressive accumulation in the popliteal lymph node over time (3.8% ± 1.2 ID at 48 hours). Indeed, the clearance rate of the nanocapsules from the injection site was significantly slower than that of the control (free $^{111}InCl_3$), which was rapidly drained into systemic circulation and accumulated mainly in excretion organs (i.e. kidneys). In contrast, the biodistribution of nanocapsules was preferably limited to the lymphatic circulation. These results suggest that the immune potentiating effect previously observed for PG nanocapsules was mainly due to the formation of a depot at the injection site and their slow lymphatic drainage and retention in lymph nodes.

INTRODUCTION

The development of nanocarriers has helped overcoming biopharmaceutical hurdles associated to both conventional drugs and novel therapeutic macromolecules, such as inadequate biodistribution, limited bioavailability upon administration through non-invasive routes or low water solubility (1). In the field of vaccine development, nanotechnology has emerged as a new approach offering a wide range of possibilities for the rational design and engineering of nanovaccines (2). The variety of biomaterials, preparation methods and different nanoassembling structures currently available offer interesting opportunities in the design of nanovaccines. Overall, the specific objectives of this design include (i) promoting migration to the lymph nodes and enhancing the interaction with immune cells, thus improving and modulating antigen-specific immune responses (adjuvant effect); (ii) overcoming mucosal barriers, thus facilitating the access of the antigen to the immunocompetent cells at the submucosa level and generating systemic immune responses (needle-free vaccination) (3-5). These potentialities render nanotechnology a versatile and promising approach in the design of novel vaccine formulations or in the improvement of existing vaccines (6).

In previous reports, we have described an adjuvant system based on polysaccharide/lipid nanocarriers for vaccine delivery. Such nanostructures are composed of a liquid oily core and coated by a polysaccharidic shell (chitosan/polyglucosamine), thus forming a reservoir-type structure called nanocapsules (7-9). These nanocapsules have been shown to allow the association of different antigens to the polymeric surface as well as a lipophilic immunomodulator (imiquimod) within the oily core. In particular, nanocapsules composed of polyglucosamine (PG) and squalene (shell-core, respectively) were recently developed and their efficacy for the delivery of the recombinant hepatitis B surface antigen (rHBsAg) and the hemagglutinin of the influenza virus (HA) was shown (9). Namely, these nanocapsules were

able to improve the immune response of the associated antigens upon intramuscular (i.m.) and subcutaneous (s.c.) immunization and to elicit a protective and sustained specific immune response after a single immunization. This long-lasting response was initially attributed to a prolonged residence time at the injection site, which possibly allowed a slow migration of the nanocarriers to the draining lymph nodes (LN).

In the initiation of the immune response, antigens are delivered to antigen presenting cells (APCs) of peripheral tissues upon administration (usually i.m. or s.c.). These cells capture and process the antigen in order to further present it to T helper cells resident in secondary lymphoid organs, such as the LN. Therefore, the drainage of the injected vaccine towards the LN is a crucial step in the initiation of the adaptive immune response. In general, vaccine delivery systems (liposomes, microspheres, nanoparticles, emulsions) can be easily recognized and phagocyted by APCs thus promoting the uptake of the associated antigen and its subsequent transport to the draining LN (10). In fact, PG nanocapsules have already demonstrated to be quickly and largely internalized by macrophages (9). Therefore the aim of the present work has been to study the biodistribution of the PG nanocapsules after s.c. injection and in particular, their lymphatic migration and retention in draining LN. For this purpose, we have used sensitive scintigraphic imaging techniques, which may provide additional information about *in vivo* fate of PG nanocapsules in real time and correlation with the immune responses previously observed. Hence, in this work, we have developed a simple and stable radiolabeling method of PG nanocapsules with Indium-111 (^{111}In) and studied their biodistribution, in particular, their lymphatic accumulation in rabbits. The study was based upon the analysis of scintigraphic planar images and direct measurements of radioactivity of harvested tissues upon euthanasia.

MATERIALS AND METHODS

Materials

Ultrapure highly deacetylated chitosan in base form (Ultrasan, Mw 276 kDa and deacetylation degree 95.5%) was acquired from Bio Syntech Canada Inc. (Quebec, Canada) and further named as polyglucosamine (GL). The emulsifier soybean L-α-lecithin Epikuron 145V was a gift from Cargill (Barcelona, Spain). Squalene oil (density 0.855 g/mL) was obtained from Merck (Darmstadt, Germany). 1,2-dimyristoyl-sn-glycero-3-phosphoethanolamine-N-diethylenetriaminepentaacetic acid (14:0 DTPA-PE) was purchased from Avanti Polar Lipids, Inc. (Alabaster, AL). Indium-111 chloride ($^{111}InCl_3$) was obtained from Nordion (Ottawa, ON, Canada) and Technitium-99m (^{99m}Tc or Tc-99m) in the chemical form of sodium pertechnetate ($^{99m}TcO_4Na$) was acquired at the local radiopharmacy (GE Healthcare San Antonio, TX). The lipophilic chelator hexamethylpropilenamine oxime (HMPAO) was provided as the commercial kit Ceretec™ (GE Healthcare; Little Chalfont, UK). The organic solvents HPLC grade (2-propanol, chloroform and acetone) were purchased from Fisher Scientific (Pittsburg, PA).

Preparation and radiolabeling of polyglucosamine nanocapsules (PG nanocapsules)

Polyglucosamine nanocapsules (PG nanocapsules) were prepared by the solvent displacement technique, as previously described (9) with slight modifications. Briefly, lecithin (10 mg) and squalene (25 μL) were co-dissolved in 0.5 mL of 2-propanol. This organic phase was poured under constant magnetic stirring upon an aqueous solution of polyglucosamine (0.25 mg/mL in acetic acid solution 0.1%), resulting in the spontaneous formation of PG nanocapsules. The organic solvents were removed under reduced pressure using a rotary evaporator (Büchi, Switzerland) and the final suspension volume was corrected until 5 mL.

PG nanocapsules were radiolabeled following two different protocols:

1) Labeling with Tc-99m

Ceretec™ vial was reconstituted following manufacturer's instructions. Briefly, 4 mL of sodium pertechnetate ($^{99m}TcO^{-}_{4}$) (16 mCi) were injected into the vial and incubated for 5 minutes in order to form the chelation complex ^{99m}Tc-HMPAO. 50, 100 or 200 μL of ^{99m}Tc-HMPAO were immediately added to the acetone phase during the preparation of PG nanocapsules in order to incorporate it within the oily core of PG nanocapsules. Then, the procedure was followed as described above.

Quality controls to test the correct formation of the complex were carried out by paper chromatography as described in the insert of Ceretec™. These controls were performed for the ^{99m}Tc-HMPAO just prepared and once mixed with the organic phase.

2) Labeling with In-111

DTPA-conjugated phosphoethanolamine (DTPA-PE) was dissolved in a mixture 2-propanol:chloroform (60:30) at 10 mg/mL. This solution was incubated with 1 or 2 μL of $^{111}InCl_3$ (0.21 mCi or 5.11 mCi for *in vitro* or animal experiments, repectively) for 30 minutes. Then, 100 μL of ^{111}In-DPTA-PE was incorporated in the organic phase with lecithin and squalene, and the PG nanocapsules preparation procedure was followed as described above.

Physicochemical characterization

Particle size and polydispersity index were measured by photon correlation spectroscopy (PCS) using a ZetaPlus/90Plus (Brookhaven Instruments Corp.; Holtsville, NY). Nanocapsules were adequately diluted in filtered water and each analysis was performed at 25ºC with a detection angle of 90º. ζ potential measurements were performed by laser doppler anemometry (LDA) using the same equipment. Samples were properly diluted in an aqueous solution of KCl 10^{-3} M.

Radiolabeling efficiency

PG nanocapsules radiolabeled with either Tc-99m or In-111 were centrifuged at 21460xg for 90 minutes at 4ºC (Allegra 21R, Beckman-

Coulter; Brea, CA). Surnatant was collected and filtered using Vivaspin 500 MWCO 1,000,000 (Sartorious; Goettingen, Germany) in order to remove any remaining nanocapsules. The activity of each filtered fraction, filter and isolated radiolabeled PG nanocapsules, was measured using a gamma-counter (Packard). The labeling efficiency was calculated as follows: ([activity of isolated PG nanocapsules] + [activity of filters])/total activity.

Assessment of the radiolabeling quality

PG nanocapsules radiolabeled with either Tc-99m or In-111 were incubated with fetal bovine serum (FBS) in a proportion 1:1 (v:v) at 37^{0}C. At indicated time points (baseline, 0.5, 1, 2, 4, 24 and 48 hours) samples were withdrawn and centrifuged in order to separate the free radionuclide. Radioactivity of both separated fractions was counted using a gamma-counter (Packard).

In a different experiment one sample of ^{99m}Tc- or ^{111}In-PG nanocapsules was incubated with FBS (1:1) at 37^{0}C for 30 minutes. The sample was centrifuged and the surnatant collected in order to quantify the free radionuclide. The isolated nanocapsules were then resuspended again with the same volume of FBS and incubated for other 30 minutes. This incubation-separation-resuspension process was repeated for each sample up to 4 times (4 cycles).

Animals

Male New Zealand White rabbits (2.2-2.5 kg) were purchased from Harlan (San Antonio, TX). All the experiments were performed under the National Institutes of Health Animal Use and Care Guidelines and approved by the University of Texas Health Science Center at San Antonio Animal Use Committee. Mice were housed under controlled conditions and provided with food and water *ad libitum*. During imaging procedure, animals were maintained under general anesthesia using inhaled 5% isoflurane/oxygen. Gas anesthesia was continuously provided by an anesthetic machine (Backford Inc.; Wales Center, NY). After each

imaging procedure, animals were left to recover until complete consciousness.

To assess the biodistribution of the nanocapsules after s.c. administration, ^{111}In-labeled PG nanocapsules or $^{111}InCl_3$ in saline (control) were injected in a shaved area on the dorsum of the hind foot over the region of the metatarsals at the midline. After injection, 5 minutes of gentle massage was applied at the injection site (IS).

Images acquisition and analysis

Static scintigraphic images were acquired using a portable planar gamma camera (ERGO, Digirad Corp., Poway, CA) at established time points during 48 hours (baseline, post-massage, 1, 4, 24 and 48 hours). The analysis of the images was performed using the viewer software for medical research images Mango© 2.6 (UTHSCSA, San Antonio, TX).

Biodistribution

Biodistribution studies were performed at 48 hours post-injection. Animals were euthanized and relevant organs were harvested, weighed and counted for radioactivity (Auto-Gamma 5000 Series, Packard Instruments; Downers Grove, IL). Results are shown as percentage of injected dose per gram of tissue (%ID/g).

Statistical analysis

Results are expressed as mean ± standard deviation. The statistical analysis was performed using Statgraphics Centurion XVI.1.15. For comparison between interventions, the analysis of variance (ANOVA) and Fischer LSD post-hoc analysis was employed in order to establish significant differences between groups. Differences were considered significant at a level of $p < 0.05$.

RESULTS

Radiolabeling of polyglucosamine nanocapsules

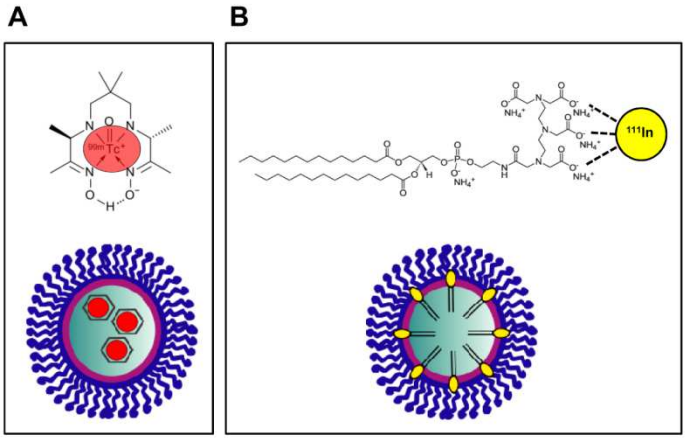

Figure 1: Representation of the different radiolabeling methods for PG nanocapsules. A) Encapsulation of ^{99m}Tc-HPMAO and B) incorporation of ^{111}In-DTPA-PE in the phospholipid layer.

Two different radiolabeling methods were used in order to radiolabel the PG nanocapsules. In a first approach, the lipophilic complex ^{99m}Tc-HPMAO was encapsulated within the oily core of nanocapsules, as depicted in **Figure 1A**. Using this method, a high labeling efficiency was achieved (87%) while maintaining the physicochemical properties of the original formulation (**Table 1**).

Furthermore, another radiolabeling method using ^{111}In was developed. For this purpose, a phospholipid conjugated with DTPA was used (DTPA-PE). The high affinity of ^{111}In for the DTPA molecule enabled the association of the radiotracer to the phospholipid, which was further inserted in the phospholipid phase (lecithin) between the oily core and the polyglucosamine coating (**Figure 1B**). This radiolabeling method was highly efficient (97%) and the radiolabeled PG nanocapsules preserved the physicochemical properties of the original formulation, as indicated in **Table 1**.

Table 1: Physicochemical characterization of PG nanocapsules radiolabeled using different methods.

Radiolabeling method	Size (nm)	PdI	ζ potential (mV)	Labeling efficiency (%)
Blank	242 ± 6	< 0.2	+28 ± 2	--
^{99m}Tc-HPMAO	308 ± 4	< 0.2	+32 ± 4	87 ± 6
^{111}In-DTPA-PE	230 ± 12	< 0.2	+20 ± 4	97 ± 1

Radiolabeling quality assessment

The release of the radiotracer in a biological medium (fetal bovine serum; FBS) was performed in order to assess the quality and stability of the radiolabeling process either with ^{99m}Tc or ^{111}In. Labeled PG nanocapsules were mixed with FBS 1:1 (v:v) and incubated at 37ºC. The release profile was determined by the analysis of the free radionuclide at different time points after separation of the nanocapsules. As observed in **Figure 2**, ^{99m}Tc-PG nanocapsules released a 40% of the radionuclide right after dilution with FBS, but further release of ^{99m}Tc was not observed for the next 4 hours. The weak interaction of ^{99m}Tc with the PG nanocapsules was confirmed upon incubation of the nanocapsules in more drastic conditions. The process of incubating the ^{99m}Tc-PG nanocapsules for 30 minutes at 37ºC, separating the free radionuclide and resuspending the nanocapsules again in FBS, resulted in the progressive leakage of ^{99m}Tc from PG nanocapsules after each cycle (repeated up to four times).

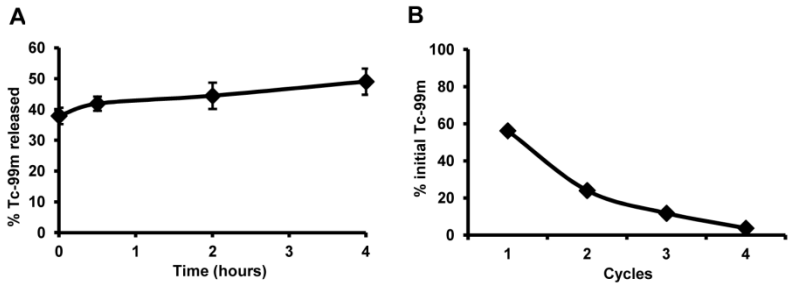

Figure 2: Stability assessment of ^{99m}Tc-PG nanocapsules. (**A**) Release profile of ^{99m}Tc-PG nanocapsules during 4 hours of incubation with FBS at 37ºC. (**B**) Progressive leakage of Tc-99m after consecutive incubation-separation-resuspension cycles in FBS.

In addition, the analysis by paper chromatography was performed in order to determine the stability of the complex ^{99m}Tc-HMPAO. Prior to its formation, ^{99m}Tc must be reduced using $SnCl_2$ (provided in the kit of Ceretec™) in order to fit within the chelator pocket. Any further oxidation into pertechnatate ($^{99m}TcO^-_4$) causes its separation from the HMPAO molecule. We observed that more than 90% of the ^{99m}Tc-HMPAO complex was formed upon incubation of Ceretec™ and $^{99m}TcO^-_4$. However, when it was added to the organic phase during nanocapsules preparation, an 80% of the activity corresponded to free $^{99m}TcO^-_4$. This finding suggests that the ^{99m}Tc oxidized into $^{99m}TcO^-_4$ upon contact with the acetone of the organic phase and likely interact with the cationic shell of PG nanocapsules.

The radiolabeling with ^{111}In-DTPA-PE was more stable than the encapsulation of ^{99m}Tc-HPMAO. In **Figure 3** it is possible to observe a gradual release of the radionuclide over 48 hours, which was not higher than 20% by the end of the study. In addition, after 4 resuspension cycles, only a 40% of the initial activity was lost. Therefore, the structure of the nanocapsules retained more effectively the ^{111}In-DTPA-PE than the ^{99m}Tc-HPMAO, which resulted in a more suitable and stable radiolabeling technique for PG nanocapsules. On the basis of these results, the radiolabeling approach with ^{111}In was selected for further *in vivo* studies.

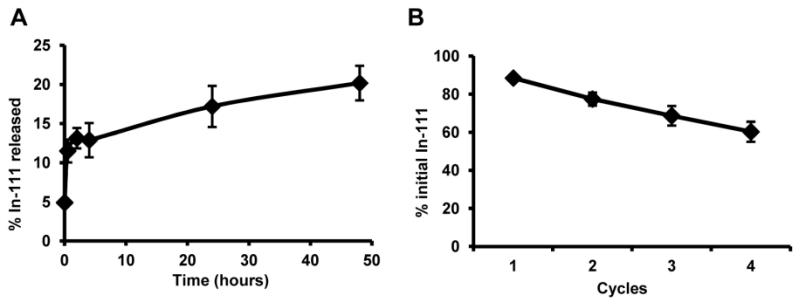

Figure 3: Stability assessment of ^{111}In-PG nanocapsules. (**A**) Release profile of ^{111}In-PG nanocapsules during 48 hours of incubation with FBS at 37^{0}C. (**B**) Progressive leakage of Tc-99m after consecutive incubation-separation-resuspension cycles in FBS.

Image acquisition and analysis after subcutaneous injection of ^{111}In-PG nanocapsules in rabbits.

To study the biodistribution of PG nanocapsules after s.c. injection, ^{111}In-labeled PG nanocapsules were injected in the hind foot of New Zealand White rabbits. As a control, a saline solution of $^{111}InCl_3$ was administered likewise. Using a planar gamma camera, images were acquired at established time points up to 48 hours (**Figure 4**). Different migration patterns were observed for both the ^{111}In-PG nanocapsules and $^{111}InCl_3$, even at early time points.

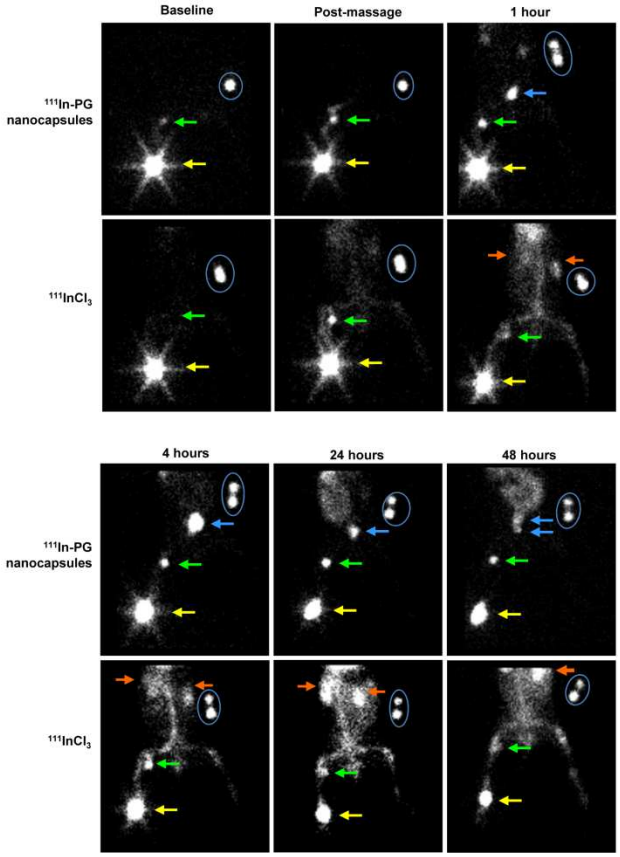

Figure 4: Imaging sequence of the lower body of one representative rabbit from the groups injected with ^{111}In-PG nanocapsules and the control $^{111}InCl_3$. The images were acquired at different time points post-injection for up to 48 hours. Yellow arrow: injection site (rear foot); green arrow: popliteal lymph node; blue arrow: iliac lymph nodes; orange arrows: kidneys; circle: external standard.

In a first instance, PG nanocapsules remained at the injection site (IS) for a long period of time. Although the control could also be detected at 48 hours at the IS, the clearance rate of PG nanocapsules was much slower, thus remaining at higher proportion at longer times, as determined after the analysis of the images (**Figure 5A**). In fact, the differences with the control became statistically significant ($p>0.05$) at 24 and 48 hours.

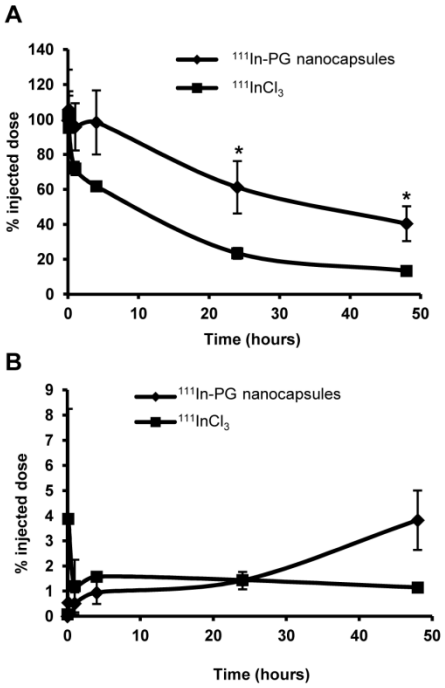

Figure 5: Analysis of the images. Percentage of the injected dose (%ID) retained at the injection site (A) and the popliteal lymph node (B) over time. *Statistically significant differences ($p>0.05$).

A fast drainage to the popliteal lymph node (PLN) was observed for both the ^{111}In-PG nanocapsules and $^{111}InCl_3$, especially after applying gentle massage at the IS. This was especially noticeable for the control, achieving very high levels of activity in the PLN after the massage, which immediately decreased to a constant 1.2% of the injected dose. In contrast, ^{111}In-PG nanocapsules were gradually trapped in the PLN as

noted by the increasing activity levels profile (**Figure 5B**). Nevertheless, this high retention (3% of injected dose) was not significantly higher than that of the control, at least up to 48 hours. In addition, after 1 hour post-injection, ^{111}In-PG nanocapsules also started to reach the iliac LN (ILN). The migration of ^{111}In-PG nanocapsules towards the ILN increased over the time for up to 4 hours. The maximum activity level was followed by a decrease until a constant value of 3% of the injected dose. The presence of PG nanocapsules in both the PLN and ILN was prolonged over time until the end of the study (48 hours) evidencing an important and sustained entrapment of the nanostructures in these lymphatic organs. In contrast, following the administration of the control ($^{111}In^{3+}$) an important clearance into systemic circulation was observed, whereas its presence in the ILN was not detected. This is evident by the high background and widespread distribution of the radioactive signal in the whole body. In fact, the images of the upper body confirm this observation illustrated by the intense signal in highly vascularized organs such as heart, liver and kidneys (**Figure 6**).

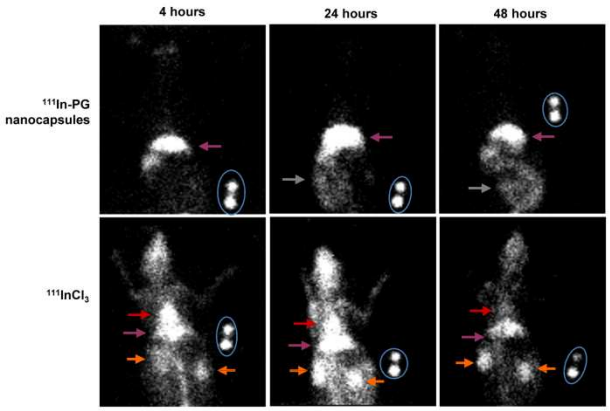

Figure 6: Imaging sequence of the upper body of one representative rabbit from the groups injected with ^{111}In-PG nanocapsules and the control $^{111}InCl_3$. The images were acquired at 4, 24 and 48 hours. Purple arrow: liver; grey arrow: bowel; red arrow: heart; orange arrow: kidneys; circle: external standard.

On the other hand, the early and high accumulation of the tracer in kidneys and liver are indicative of its urinary and hepatic elimination. Differently, from the images, we could infer that the main elimination route of ^{111}In-labeled nanocapsules was through the liver, followed by a pancreatic elimination through the intestine.

Biodistribution

The measurement of the radioactivity in the harvested organs evidenced the spread distribution of the control at the systemic level and the more localized migration of the PG nanocapsules (**Figure 7**). The mean %ID/g (% of injected dose per gram) of the organs extracted from ^{111}In-PG nanocapsules injected rabbits was generally lower than the corresponding values observed in the control injected rabbits. An exception was observed for the mean %ID/g at the IS and in the PLN, where differences were not statistically significant for the control and nanocapsules injected rabbits ($p>0.05$). As previously observed in the scintigraphic planar images the high radioactivity levels observed in the liver confirmed the accumulation of the PG nanocapsules in this organ. These data indicate a regional biodistribution from the IS to the lymphatic system and subsequent excretion through the liver.

Significant differences with the control ($p<0.05$) were found in heart, lung, spleen, kidney and blood, as well as in the contralateral injection site and PLN. The higher levels observed in blood and highly vascularized organs (i.e. lung, spleen) of the control rabbits indicated the important presence of the radiotracer in systemic circulation. In fact, the significantly higher levels of %ID/g in the contralateral foot and PLN were also an indicative of a widespread distribution of the control. Moreover, in agreement with the analysis of the images, the accumulation of the radiotracer in the excretion organs (liver and kidneys) was notable, but in particular, significantly higher levels than ^{111}In-PG nanocapsules were counted in the kidneys.

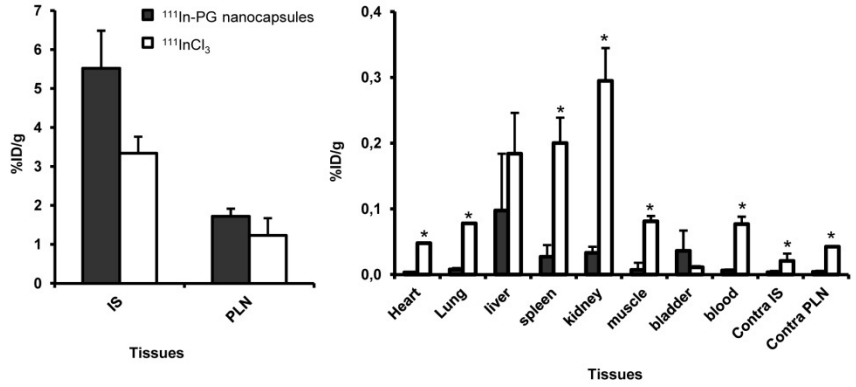

Figure 7: Biodistribution of ^{111}In in the different tissues at 48 hours, comparing the ^{111}In-PG nanocapsules and the solution of $^{111}InCl_3$. IS: injection site; PLN: popliteal lymph node; Contra IS: contralateral injection site; Contra PLN: contralateral popliteal lymph node.

DISCUSSION

PG nanocapsules have shown a potential as vaccine delivery vehicles for different antigens, such as rHBsAg and HA (9). More precisely, these antigen delivery vehicles were found to potentiate the immune response against the associated antigen compared to alum control (conventional adjuvant for these antigens) at the same dose and to elicit a cellular immune response in addition to a humoral response. Furthermore, in the particular case of rHBsAg, the results indicated that a single i.m. administration was sufficient to achieve long-lasting immune protection. One of the hypothetical mechanisms that would explain this long-term response could be the long residence time of the PG nanocapsules at the injection site (IS) and the slow clearance to secondary lymphoid organs. In a previous work (9), using *in vivo* fluorescence imaging we could observe the formation of a depot at the IS, although no information about the biodistribution and elimination of the nanocarriers could be obtained from this preliminary study. Therefore, with the imaging/biodistribution studies based on scintigraphic techniques presented herein, our objective was to study in depth the migration routes of the nanocapsules from the

injection site, as well as their biodistribution pattern and elimination mechanisms.

The first step was the radiolabeling of the PG nanocapsules in order to properly track the emitted radioactive signal. Hence, the aim of this first part of the study has been to develop an efficient and stable radiolabeling method for the PG nanocapsules, which would ensure that the radiolabel remains associated to the nanocarriers under physiological conditions. For this purpose, two different radiolabeling strategies were followed: (a) using ^{99m}Tc and (b) ^{111}In.

For radiolabeling the nanocapsules with ^{99m}Tc, the lipophilic complex formed with oxime or HMPAO was employed (commercially available as Ceretec™). The formation of the complex with HMPAO is only possible using the reduced form of ^{99m}Tc ($^{99m}Tc^{3+}$) and therefore, TcO^{-}_{4} had to be reduced with $SnCl_2$, which was already included in the kit of Ceretec™. Due to the hydrophobic character of this molecule, it was encapsulated within the oily core of PG nanocapsules (**Figure 1A**). This method has been successfully used for radiolabeling liposomes because of the ability of ^{99m}Tc-HMPAO complex to penetrate the lipid bilayer (11). The entrapment of the ^{99m}Tc-HMPAO was very efficient and the physicochemical properties of the PG nanocapsules did not vary with respect to those of the blank formulation. However, the release study in FBS revealed a fast and important leakage (40%) of the radiotracer upon mixing ^{99m}Tc-labeled PG nanocapsules with serum (**Figure 2A**). The amount of ^{99m}Tc initially released did not substantially increase over a period of 4 hours, suggesting that an equilibrium between the free and the encapsulated radiotracer was established. Similar results have been reported for other types of nanocapsules, i.e. polylactic acid-polyethylene glycol (PLA-PEG) nanocapsules (12). However, in our study we decided to further analyze the affinity of ^{99m}Tc–HMPAO for the nanocapsules by performing a series of incubation-separation-resuspension cycles. The results indicated that, a high proportion of the associated radionuclide was progressively lost after each cycle (**Figure 2B**). Besides, the paper

chromatography control of the ^{99m}Tc–HMPAO mixed with the organic solvents confirmed that during preparation a high proportion of ^{99m}Tc forming the HPMAO complex turned into its initial oxidation state ($^{99m}TcO^{-}_{4}$). Thus, we speculated that when the formed complex was added to the organic phase, likely the acetone promoted its oxidation and the anion got attached to the cationic surface of PG nanocapsules. Probably, this feature contributed to the immediate release until establishing an equilibrium with the release medium and moreover, the continuous leakage of the radiotracer after several resuspension cycles. Therefore, in spite of the high radiolabeling efficiency achieved with this method, the quality and stability was poor and it was considered inadequate for further *in vivo* imaging studies because of the high probability of instability of ^{99m}Tc and further release from PG nanocapsules.

The second radiolabeling approach used ^{111}In as radiomarker. To attach the ^{111}In to the structure of PG nanocapsules, a phosphatidylethanolamine (PE 14:0) conjugated with DTPA was employed (DTPA-PE). The ^{111}In and the DTPA chelator form a very stable coordination complex. Moreover, ^{111}In would enable to prolong the time of study due to its longer half life compared to ^{99m}Tc (2.8 days vs. 6 hours). The DTPA-PE was labeled with ^{111}In prior to preparation of PG nanocapsules and then incorporated with the mixture of phospholipids composing the lecithin. Hence, the ^{111}In-DTPA-PE was inserted in the interface oil-water and then coated by PG, as indicated in **Figure 1B**. This method has been previously described to label liposomes, resulting in a highly efficient and stable radiolabeling method (13). In fact, the labeling efficiency of PG nanocapsules was very high (near 100%) and the ^{111}In-labeled PG nanocapsules conserved the original properties of the blank PG nanocapsules (**Table 1**). The labeling quality assessment indicated a strong interaction with the nanostructure, which was evidenced either by determining the released radiotracer in serum over time (no more than 20% after 48 hours) or undergoing harsher conditions of incubation-separation-resuspension (40% released after 4 cycles) (**Figure 3**). This

strong interaction of ^{111}In with DTPA-derivatized lipids composing liposomes was also previously demonstrated (14, 15). Thus, compared to ^{99m}Tc-HMPAO labeling, this method produced highly efficient and stable radiolabeling of the PG nanocapsules while properly conserving their physicochemical properties.

Therefore, PG nanocapsules labeled with ^{111}In-DTPA-PE were administered s.c. to rabbits and their *in vivo* distribution was monitored for up to 48 hours and compared with the control $^{111}InCl_3$ (**Figure 4**). Both formulations followed a lymphatic drainage from the IS as observed by the presence of radioactivity in the PLN at very early time points. In fact, the massage applied in the area of injection promoted the passage to the lymph and further migration to draining LN. However, the main difference relied in the biodistribution patterns. The control was more widespread in the organism whereas ^{111}In-PG nanocapsules distribution was limited to the IS and regional lymphatic circulation. A similar distribution pattern of $^{111}InCl_3$ was previously observed in rabbits by Chinol et al. (16), in which $^{111}InCl_3$ was administered i.v. Despite the different administration route, after 48 hours the visualized organs were kidneys, liver and heart, and also an important presence in the blood pool, as observed in the present study. This similar fate when injected via s.c. or i.v. suggest that after s.c. injection the free radiotracer moved quickly from the IS via the lymphatics towards systemic circulation. In addition, the analysis of the images evidenced that there was not an accumulation of activity in the PLN but a continuous drainage from the IS to the blood. In consequence, free $^{111}In^{3+}$ mainly accumulated in kidneys and liver to be eliminated from the body. To further support these observations, the analysis of the activity of each harvested tissues 48 hours post-injection evidenced the presence of $^{111}In^{3+}$ in the blood, heart, lung, spleen, kidney and contralateral foot and PLN in significantly higher levels than rabbits injected with ^{111}In-PG nanocapsules.

Molecules or delivery systems injected in the subcutaneous cavity can quickly move to the nearest lymph node via the interstitial fluid and

lymph vessels or can be taken up and transported by peripheral APCs, although this latter process may take longer. Regarding delivery systems, this migration can be influenced by their particle size surface charge, composition, shape, etc. (3). As described in literature (3), particles smaller than 200 nm may directly enter the lymph vessels and move towards the first LN. On the other hand, larger particles should be uptaken by specialized APCs, such as macrophages or dendritic cells, in order to transport them to the LN. On the basis of these premises, it could be expected that ^{111}In-PG nanocapsules with a mean particle size of 230 nm migrate from the IS following both mechanisms. In fact, in previous reports, we have determined the high uptake rate of PG nanocapsules by macrophages (9). The very early migration of ^{111}In-PG nanocapsules to the PLN suggests a rapid drainage of the smallest nanocarriers of the population through the subcutaneous insterstitium towards the draining LN, which was further favored by the massage applied at the IS. Additionally, a high proportion of PG nanocapsules started to reach the ILN as early as 1 hour post-injection, indicating that PG nanocapsules moved through the lymphatic system. This pattern continues for up to 4 hours in which the PG nanocapsules getting the ILN achieved a peak of intensity. From the 4th hour onwards, the clearance rate from the IS started to be more pronounced, even though slower than the control, which also coincided with an increment in the gradual accumulation of PG nanocapsules in the PLN. This could be an indicative of the existence of an additional mechanism of migration of PG nanocapsules consisting of their transport by APCs. A similar mechanism has been proposed by other authors who described that particles injected s.c. and transported from peripheral tissues by APCs can reach the draining LN in about 24 hours post-injection (17). In addition, we could also observe an expansion of the PLN size in those rabbits receiving PG nanocapsules indicating a proliferative process or cell recruitment. This hypothesis is suggested by the observation of no significant differences between the %ID/g of the control and PG nanocapsules PLN in the biodistribution analysis (**Figure**

7), since this parameter was corrected with organ weight. On the other hand, the images of the upper body of the rabbits (**Figure 6**) clearly showed an accumulation in the liver since the 4th hour post-injection, evidencing that a small proportion of the injected dose gets to system circulation. This is probably because of a progressive escape from ILN, as suggested by the decreased signal in these organs after the peak at 4 hours. Still, the activity levels of the ^{111}In-PG nanocapsules in the blood pool were undetectable and could not be visualized in the images until higher amounts accumulated in the liver. The images, as well as the activity levels counted in the biodistribution study, indicate that the hepatic is the main excretion route of the particles. The liver is the main organ of lipids metabolism, therefore it is expected that the PG nanocapsules and ^{111}In-DTPA-PE would be mainly metabolized in this organ and subsequently excreted via the gastrointestinal tract.

CONCLUSIONS

The results obtained in the present study suggest that the long-lasting immune potentiating effect previously observed for the PG nanocapsules could be mainly attributed to the formation of a depot at the IS and their continuous lymphatic drainage and further retention in draining LN. Additionally, the slow migration of the PG nanocapsules likely contributed to the long-term LN accumulation, allowing longer interaction with immune cells in these organs and in consequence, prolonging their effect.

ACKNOWLEDGEMENTS

This work was supported by a grant from the Bill & Melinda Gates Foundation and Consolider Ingenio 2010 (CSD2006-00012; Ministry of Science and Innovation, Spain), Competitive Reference Groups SUDOE-FEDER (SOE1/P1/E014) and Spanish Institute of Health "Carlos III" (PI081444). SV acknowledges a fellowship from the Spanish Ministry of Education (FPU predoctoral grants).

REFERENCES

1. Duncan R & Gaspar R (2011) Nanomedicine(s) under the microscope. *Mol Pharm* 8: 2101-2141.

2. Peek LJ, Middaugh CR & Berkland C (2008) Nanotechnology in vaccine delivery. *Adv Drug Deliver Rev* 60: 915-928.

3. Bachmann MF & Jennings GT (2010) Vaccine delivery: A matter of size, geometry, kinetics and molecular patterns. *Nat Rev Immunol* 10: 787-796.

4. Moon JJ, Huang B & Irvine DJ (2012) Engineering nano- and microparticles to tune immunity. *Adv Mater* 24: 3724-3746.

5. Csaba N, Garcia-Fuentes M & Alonso MJ (2009) Nanoparticles for nasal vaccination. *Adv Drug Deliv Rev* 61: 140-157.

6. Vicente S, Prego C, Csaba N & Alonso MJ (2010) From single-dose vaccine delivery systems to nanovaccines. *J Drug Deliv Sci Technol* 20: 267-276.

7. Vicente S, *et al* (In press) A polymer/oil based nanovaccine as a single-dose immunization approach

8. Vicente S, *et al* (In prep.) Co-delivery of viral proteins and TLR7 agonist from polysaccharide nanocapsules: a needle-free vaccination strategy

9. Vicente S, *et al* (In prep.) Highly versatile immunostimulating nanocapsules for specific immune potentiation

10. De Temmerman M, *et al* (2011) Particulate vaccines: On the quest for optimal delivery and immune response. *Drug Discov Today* 16: 569-582.

11. Phillips W, *et al* (1992) A simple method for producing a tc-99m-labeled liposome which is stable invivo. *Nucl Med Biol* 19: 539-&.

12. Pereira MA, *et al* (2008) PLA-PEG nanocapsules radiolabeled with ^{99m}Technetium-HMPAO: Release properties and physicochemical characterization by atomic force microscopy and photon correlation spectroscopy. *Eur J Pharm Sci* 33: 42-51.

13. Maruyama K, Kennel S & Huang L (1990) Lipid-composition is important for highly efficient target binding and retention of immunoliposomes. *Proc Natl Acad Sci U S A* 87: 5744-5748.

14. Mougin-Degraef M, *et al* (2007) Doubly radiolabeled liposomes for pretargeted radioimmunotherapy. *Int J Pharm* 344: 110-117.

15. Helbok A, *et al* (2010) Radiolabeling of lipid-based nanoparticles for diagnostics and therapeutic applications: A comparison using different radiometals. *J Liposome Res* 20: 219-227.

16. Chinol M, Vallabhajosula S, Goldsmith SJ, Paganelli G & Palestro CJ (1996) Evaluation of four radiopharmaceuticals for imaging inflammation in a rabbit model of arthritis. *Ann Nucl Med* 10: 287-291.

17. Manolova V, *et al* (2008) Nanoparticles target distinct dendritic cell populations according to their size. *J Immunol* 38: 1404-1413.

OVERALL DISCUSSION / DISCUSION GENERAL

OVERALL DISCUSSION

Nanocapsules are colloidal structures with a characteristic core-corona architecture, consisting of an oily liquid core surrounded by a polymeric shell, i.e. chitosan (CS) shell. This type of structure has been used for the encapsulation of drugs with the aim of improving their solubility, as well as their transport through mucosal barriers (1). In the present work, the technology and composition of CS nanocapsules was adapted to explore its potential as vaccine adjuvant system and for mucosal antigen delivery. On the aforementioned design, special emphasis has been paid to provide these nanocarriers with a multifunctional character. This characteristic would enable the association of antigens onto the cationic surface and the accommodation lipophilic immunostimulant drugs within the oily core, thus making it feasible the co-delivery of both componenents to the immunocompetent cells.

For the majority of the work, we selected the recombinant hepatitis B surface antigen (rHBsAg) as the model antigen to be associated to the CS surface of the nanocapsules. This was considered to be a challenge as rHBsAg is a viral particle (2) composed of the protein subunits of the virus capsid embedded in lipids acquired from the outer membrane of the infected cell. In subsequent studies, we also evaluated the capacity of the optimized nanocapsules for delivering other types of antigens, such as the hemagglutinin of the influenza virus, which is a soluble protein.

The antigen display on the surface of nanocarriers has been proposed as an approach to mimic the natural structure of pathogens. A example of this approach is the system PeviPRO™, which consists of synthetic virosomes (3). Nowadays, two vaccines based on this system are commercialized: Epaxal® and Inflexal® against hepatitis A and influenza, respectively. The exposure of repetitive copies of the antigenic epitope on the surface of nanoparticles has been shown to enhance the immune response against weakly immunogenic antigens (4). On the other hand, the surface charge of the nanocarriers has also been found to affect their

adjuvant properties (5). Therefore, in a first instance we studied the influence of the surface characteristics of the nanocapsules, i.e. surface composition and antigen organization, on the generation of specific immune responses against hepatitis B.

CS nanocapsules were prepared using Miglyol® 812 and CS (deacetylation degree 85.5%), which constituted the oily core and the outer shell of the nanocapsules, respectively (6). For this purpose, the rHBsAg (HB) was associated to the polymeric shell at different CS:HB (w:w) proportions in order to confer opposite surface charge and composition to the system (CSNC+ and CSNC-) while maintaining the particle size around 250 nm, as shown in **Table 1**. The cationic surface charge of CSNC+ indicated the prevalence of CS on the surface of the nanostructure despite the high antigen association rate. In contrast, the negative charge of CSNC- indicated the predominant exposure of the antigen molecules entrapped in the CS shell towards the external medium (**Figure 1**).

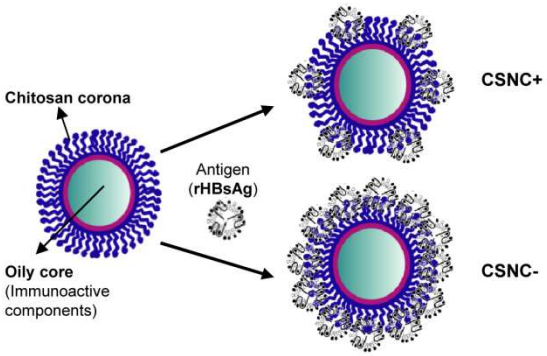

***Figure 1**: Illustration of HB organization on the cationic and anionic prototypes of CSNC (CSNC+ and CSNC-).*

***Table 1**: Physicochemical characterization of the different CS nanocapsules prototypes associating HB. Results are presented as mean ± SD (n=3).*

Formulation	CS:HB ratio	Size (nm)	PdI	ζ potential (mV)	A.E. (%)
Blank	--	196 ± 12	< 0.2	+45 ± 1	-
CSNC-	**1:12.8**	310 ± 34	< 0.2	-23 ± 3	60 ± 3
CSNC+	**1:0.25**	245 ± 53	< 0.2	+41 ± 7	78 ± 3

CSNC: chitosan nanocapsules; HB: recombinant hepatitis B surface antigen; Pdl: polydispersity index; A.E.: association efficiency.

The results of the *in vivo* evaluation of the efficacy of these prototypes showed the superiority of the cationic formulation as compared to the negatively charged one (CSNC-). In addition, CSNC+ formulation was able to significantly improve the specific immune response as compared to the conventional vaccine containing alum (HB-alum) administered intramuscularly (i.m.) at the same dose (10 µg of HB; 0, 4 weeks) (**Figure 2**).

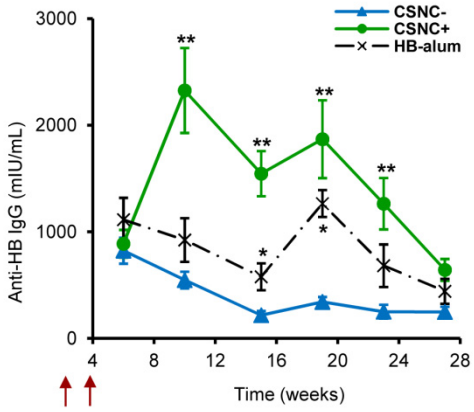

***Figure 2:** Immune response induced by the nanovaccine prototypes (CSNC- and CSNC+) and the positive control (HB-alum) administered to BALB/c mice i.m. at weeks 0 and 4 (10 µg) (arrows) and expressed as IgG anti-HB levels (mIU/ml). CSNC- (blue –▲–); CSNC+ (green –●–) and HB-alum (black –·X·–). Results are presented as mean ± SEM. Statistically significant differences are indicated for *Alum or CSNC+ vs. CSNC- (p < 0.05). ** CSNC+ vs. Alum and CSNC- (p < 0.05). (n=10).*

These results clearly showed the immunostimulatory character of the prototype CSNC+ and the positive effect of its predominant presence on the surface of the antigen-loaded nanocarriers (7-11). This latter characteristic could have importantly contributed to its adequate presentation to the immune system and moreover, to an enhanced activation of antigen presenting cells (APCs) and further development of a strong adaptive immune response. In fact, in an *in vitro* cell study, we observed that CS nanocapsules were recognized and taken up by macrophages up to a great extent (90% after 30 minutes of incubation) (**Figure 3**). This high internalization rate was attributed to their nanostructured cationic presentation. As reported for other cationic nanostructures (12-14), the positive surface charge is indeed relevant in promoting internalization by phagocytic cells. In addition, this massive internalization was observed at very short time points (30 minutes), thus evidencing the fast interaction of CSNC+ with the cells, as occurs for other chitosan-based nanocarriers (12).

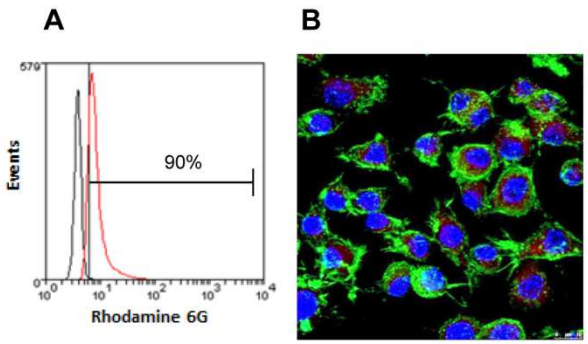

Figure 3: *Internalization of fluorescent CS nanocapsules labeled with rhodamine 6G (50 µg/mL) in macrophages determined by A) flow cytometry and B) confocal microscopy (red channel: fluorescent CS nanocapsules; green channel: Alexa Fluor 488-phalloidin; blue channel: DAPI).*

The adjuvant effect of CSNC+ was also evident after a single immunization, which was sufficient to elicit IgG seroprotective levels (>10mUI/mL for humans (15)) and prolong this specific immune response

during the time of study (six months) (**Figure 4**). This sustained effect could also be attributed to the slow clearance of the cationic nanocarriers from the injection site towards the secondary lymphoid organs (lymph nodes) (16). As a consequence, the continuous stimulation of the immune system at this level can enable a prolongation of their adjuvant effect, as discussed below.

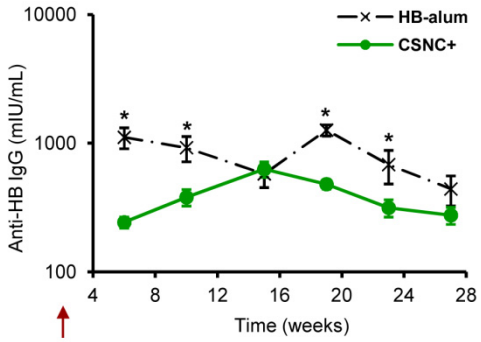

Figure 4: *Immune responses induced by CSNC+ (10 μg; green –●–) administered to BALB/c i.m. in a single-dose (arrow) and the HB-alum (black –·X·–) administered at weeks 0 and 4 (10 μg) and expressed as IgG anti-HB (mIU/ml) levels. Results are presented as mean ± SEM. Statistically significant differences are indicated for *($p < 0.05$) (n=10).*

Furthermore, in additional experiments it was observed that the number of doses of nanovaccine administered affected the immune response pattern. Namely, a single dose of CSNC+ resulted in a predominantly Th2-type response (higher IgG1 levels than IgG2a), whereas both Th1- and Th2-type responses were induced after booster immunization (**Figure 5**). These data agree with previous observations reported for CS aqueous solutions mixed with model antigen (β-galactosidase) (17) and ovalbumin-loaded CS nanoparticles administered subcutaneously (18), thus indicating that CS, either in its fluid or nanostructure form, is able to induce a mixed Th1/Th2 immune response.

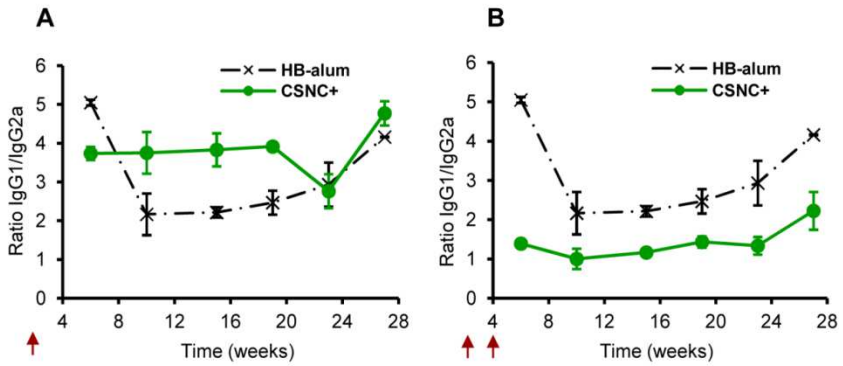

Figure 5: *Ratio of IgG1/IgG2a anti-HB for prototype CSNC+ (10 µg; green –●–) after single (A) or double immunization separated 4 weeks (B) (indicated in arrows) compared to HB-alum (10 µg; black –·X·–) administered to BALB/c mice in two doses (0, 4 weeks). Results are presented as mean ± SD (n=10).*

Overall, the results of these studies evidenced the adjuvant effect of CSNC+ and their ability to provide sustained immune protection following a single-dose immunization strategy. However, taking into account the multifunctional structure of the CS nanocapsules, we have postulated that further improvements of the formulation, i.e. incorporating additional immunostimulants, might be interesting in order to develop a needle-free immunization approach. In order to validate this hypothesis, we have chosen the nasal modality of administration. The nasal mucosa presents several barriers (mucus, epithelial cell layer, enzymatic degradation, mucociliary clearance, etc.) that the antigen has to overcome in order to reach the immunocompetent cells at the submucosa level or at the nose associated lymphoid tissue (NALT). In order to boost the initiation of the immune cascade at the induction sites (submucosa and NALT), our approach was based on the co-delivery of both the antigen and the immunostimulant agent upon their capture by APCs (i.e. dendritic cells, macrophages, etc.). Using this approach, we expected that the immunostimulant drug would work promoting the innate immune response and maximizing the induction of the adaptive immune response, even at low antigen doses. For this purpose, imiquimod

was selected for its incorporation within the oily core of the nanocapsules. Imiquimod is known to work as a modulator of the innate immunity by activating APCs via the intracellular Toll-like receptor 7 (TLR 7). The activation of this receptor results in the production of pro-inflammatory cytokines that can ultimately stimulate and modulate the adaptive immune response through the generation of specific antibodies and T cell mediated responses (19). Due to the high lipophilic character of this drug, it was possible to encapsulate it very efficiently (70%) without altering the original physicochemical properties of blank CS nanocapsules (**Table 1** and **Table 2**). In addition, these characteristics were maintained even when the HB was associated onto the surface of imiquimod loaded-CS nanocapsules (ratio 1:0.25, as CSNC+).

Table 2: *Physicochemical characterization of CS nanocapsules encapsulating imiquimod, associating or not the HB (n=3).*

CS nanocapsules compositions	Size (nm)	PdI	ξ potential (mV)	% HB	% Imiquimod
Imiquimod	199 ± 7	0,22 ± 0,02	+47 ± 1	---	70
Imiquimod/HB	218 ± 9	0,25 ± 0,03	+45 ± 6	70 ± 2	70

The delivery of imiquimod from CS nanocapsules was found to affect the functionality of macrophages, as noted by the increased secretion of pro- and anti-inflammatory cytokines (**Figure 6**). In agreement with previous reports (20, 21), we have observed an important induction of pro-inflammatory cytokines (IL-6 and TNF-α) by imiquimod-loaded CS nanocapsules in a marked dose-dependent manner, while the levels of IL-1α were negligible. On the other hand, this intense stimulation may have triggered a self-regulatory response by inducing the production of IL-10, a non-inflammatory cytokine able to attenuate the effect of the pro-inflammatory cytokines (22).

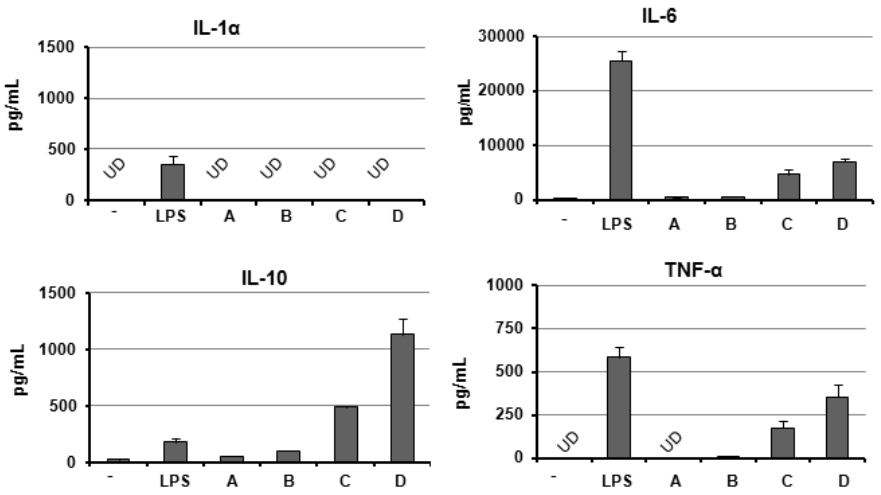

Figure 6: *Cytokines production by peritoneal macrophages incubated with blank and imiquimod-loaded CS nanocapsules at two different doses (10 and 100 μg/mL) during 24 hours. Negative control was culture medium, and positive control was LPS (1 μg/mL). Average concentration (pg/mL) of IL1-α, IL-6, IL-10 and TNF-α in culture supernatants. Data from one representative experiment (performed twice in duplicates). UD: undetectable levels* (IL-1α < 15.7 pg/mL *TNF < 2.1 pg/mL). Blank CS nanocapsules (A: 10 μg/mL; B: 100 μg/mL); imiquimod-loaded CS nanocapsules (C: 10 μg/mL; D: 100 μg/mL).*

The results of the *in vivo* performance of blank and imiquimod-loaded CS nanocapsules upon intranasal vaccination led us to two important observations. One is related to the relevance of the polymeric shell of the nanocapsules to facilitate the transport of the antigen through the nasal mucosa. In fact, a control consisting of the oil nanodroplets without the outer shell of CS (nanoemulsion) was not able to induce any significant response at the same dose of HB (10 μg, weeks 0 and 4) (**Figure 7A**). This observation is in agreement with the capacity of internalization of CS nanocapsules across the nasal mucosa previously reported by Prego et al. (23). The other important finding observed in this study refers to the enhancement of the immune response elicited by the prototype containing imiquimod as compared to blank nanocapsules. Furthermore, this enhanced response was significantly higher at longer time points ($p<0.05$) (**Figure 7A**). Therefore, in agreement with our initial hypothesis,

the co-delivery of the antigen and the immunostimulant drug (both within the same vehicle) resulted in a positive effect on the induction and progression of the specific immune response upon nasal immunization. Nevertheless, this response was much more intense in some animals than in others. A late third dose of this prototype (10 μg of HB at week 28) was administered to this group of mice. We observed that every single animal of the group became totally seroprotected raising the average IgG levels up to 720 mIU/mL (>100 mIU/mL for humans has been considered full protection against HB (15)) (**Figure 7B**). This intense response after a late boost immunization has been associated to the presence of immunologic memory. The immune system may interpret this last immunization as a viral challenge, rapidly responding by rising antibody production. This effect is considered a sign of a proper early immunization, suggesting that the boost dose was not needed to sustain protection due to the strong immunologic memory developed (24).

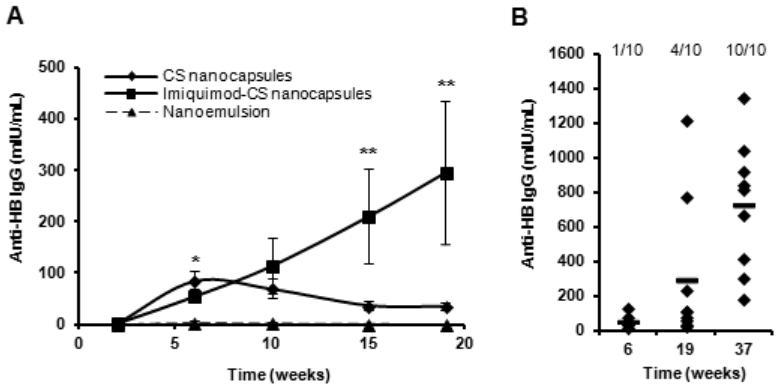

Figure 7: *Systemic immune response after two intranasal immunizations (0, 4 weeks) to BALB/c mice with blank and imiquimod-loaded CS nanocapsules and nanoemulsion (NE) associating HB.* ***A)*** *The plot represents total anti-HB IgG quantified at different time points post primary immunization (mean +/- SEM) (n=10). Statistically significant differences are indicated for * Blank & imiquimod-loaded CS nanocapsules vs NE ($p<0.05$). ** Imiquimod-loaded CS nanocapsules vs blank CS nanocapsules & NE ($p<0.05$).* ***B)*** *Effect of late third nasal dose with imiquimod-loaded CS nanocapsules. Individual IgG concentration in each mouse (diamonds) and mean of ten mice (dash) at early, intermediate and late time points. Fractions represent the number of mice with higher anti-HB IgG than 100 mIU/mL, versus the total number of mice in each group (n=10).*

New modifications of the system were introduced by including a different polymeric corona and oil nanocore. In particular, a more deacetylated form of chitosan (further named as polyglucosamine – PG) and the oil squalene were used. Squalene is a linear triterpene molecule naturally present in the organism. It is the first precursor in the biosynthesis of cholesterol and the main component of human sebum. Squalene is also the main oil component of licensed adjuvant emulsions (MF59™ and AS03™ in vaccine formulations against influenza) and it is usually the oil of choice for the development or new vaccine adjuvant emulsions (25). In these emulsion-based vaccine formulations the antigen is usually mixed up with the preformed emulsions. No physical interactions occur between the oil droplets and the antigen, which remains dispersed in the aqueous phase of the emulsion (26). Therefore, with the incorporation of a PG corona coating the squalene nanodroplets, thus forming a nanocapsular system, we intended to include the different components (oil, surfactants, immunostimulants and antigen) within the same nanocarrier to be simultaneously delivered to APCs.

Table 3: *Physicochemical characterization of the different prototypes of PG nanocapsules associating or not two types of antigens: HB and HA (n=3).*

Core composition	Ag	Size (nm)	PdI	ζ potential (mV)	Ag A.E. (%)	Imiquimod A.E. (%)
Squalene	--	172 ± 3	< 0.2	+66 ± 1	-	-
	HB	230 ± 13	< 0.2	+60 ± 3	72 ± 8	-
	HA	217 ± 4	< 0.2	+51 ± 2	69 ± 2	-
Squalene + Imiquimod	--	198 ± 5	< 0.2	+63 ± 1		40 ± 2
	HB	299 ± 11	< 0.2	+60 ± 4	78 ± 6	40 ± 2

PdI: polydispersity index; Ag: antigen; A.E.: association efficiency.

The developed PG nanocapsules were able to efficiently associate two different antigens: (i) the HB, representative of a virus-like particle (VLP) (27), and (ii) the hemagglutinin subunit of influenza virus (HA), which is a soluble protein antigen (28). As well, the incorporation of the immunomodulatory agent imiquimod within the oily core was also achieved without compromising their nanometric particle size and highly positive surface charge (**Table 3**).

The potential adjuvant properties of PG nanocapsules associating the HB, as well as their ability to induce immune protection after a single-dose immunization schedule, were evaluated in BALB/c mice. In these studies we could further assess the effect of the composition of the nanocarriers on the kinetics and modulation of the immune response.

After a single immunization (10μg), the anti-HB IgG levels elicited by both prototypes were above those considered to be seroprotective in humans (100-200 mIU/mL). Although the mean IgG levels elicited by PG nanocapsules containing imiquimod were slightly higher, no specific benefits could be ascribed to the encapsulated imiquimod after a single injection (**Figure 8**). As previously discussed, this sustained effect was mainly attributed to their direct effect on the immune system (high uptake and activation of APCs), and their prolonged residence time at the injection site. This last characteristic was further explored using different imaging techniques. The optical *in vivo* fluorescence imaging suggested that PG nanocapsules were able to form a depot at the injection site for long periods of time, and then slowly drained over time. Further studies using γ-scintigraphy provided us with specific detail of the nanocapsules migration pattern.

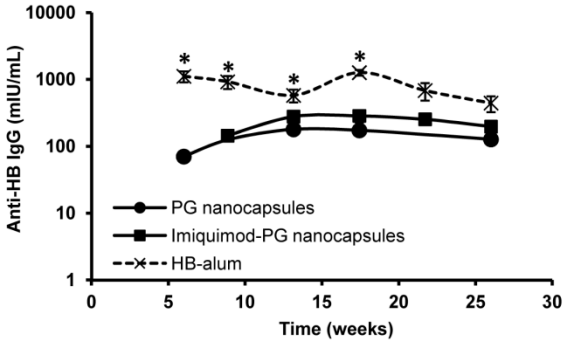

Figure 8: *Immune response elicited after a single-shot immunization with blank and imiquimod-loaded PG nanocapsules (10 μg) to BALB/c mice. The positive control HB-alum (10 μg) was administered at weeks 0 and 4. Results are expressed in mIU/mL of specific anti-HB IgG quantified at different time points post primary immunization (mean +/- SEM) (n=10). Statistically significant differences are indicated for * ($p<0.05$).*

PG nanocapsules were adequately labeled with Indium-111 (^{111}In) in order to track them after *in vivo* administration using a gamma camera. In this study, we could observe that PG nanocapsules administered subcutaneously to New Zealand White rabbits formed a depot at the injection site and then follow a slow lymphatic drainage. Then, they gradually accumulated in the popliteal lymph node (PLN) (**Figure 9**)and later, at one hour post-injection, PG nanocapsules also started to reach the iliac lymph nodes (ILN) following the normal lymphatic circulation. Hence, according to this study, the long-lasting immunopotentiating effect of PG nanocapsules could be mainly attributed to two main factors: (i) their continuous lymphatic drainage from the injection site and further retention in draining lymph nodes, and (ii) the long residence time at the injection site, which would allow a continuous interaction of PG nanocapsules with peripheral APCs thus promoting their uptake and transport to the draining lymph node.

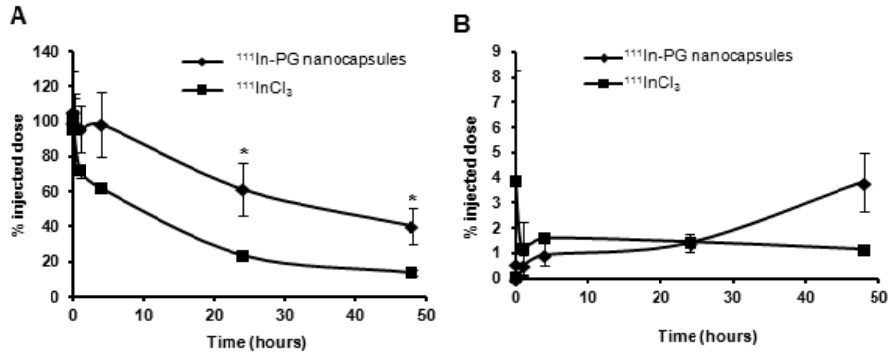

Figure 9: *Analysis of the images of rabbits injected with ^{111}In-labeled PG nanocapsules acquired at different time points using a gamma camera. Percentage of the injected dose (%ID) retained at the injection site (A) and at the popliteal lymph node (B) over time. *Statistically significant differences (p>0.05) (n=3).*

Although no differences in the elicited immune response between blank and imiquimod-loaded PG nanocapsules were found after a single immunization, a second dose with the prototypes containing HB evidenced important differences in terms of kinetics and modulation of the immune response. The increasing IgG levels achieved over time for PG nanocapsules indicate a dose-accumulating effect, which finally resulted in a significant delayed boosted response (**Figure 10**) and, thus, to a long-lasting response. This effect was also observed when the antigen HA was administered associated to PG nanocapsules. In fact, the moderate initial response notably increased over time, achieving higher IgG titers than the controls (alum-HA and plain HA), as occurred for HB (**Figure 11**). In addition, PG nanocapsules were able to induce an enhanced and sustained specific immune response even upon administration of low doses of antigen. Interestingly, very similar IgG titers were elicited when two different doses of HA were tested (2 and 7.5 μg).

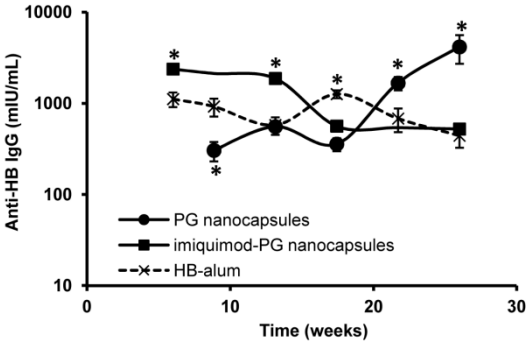

Figura 10: *Immune response elicited after two doses (0 and 4 weeks) of blank and imiquimod-loaded PG nanocapsules associating HB, and the positive control HB-alum (10 µg) to BALB/c mice. Results are expressed in mIU/mL of specific anti-HB IgG quantified at different time points post primary immunization (mean +/- SEM) (n=10). Statistically significant differences are indicated for * (p<0.05).*

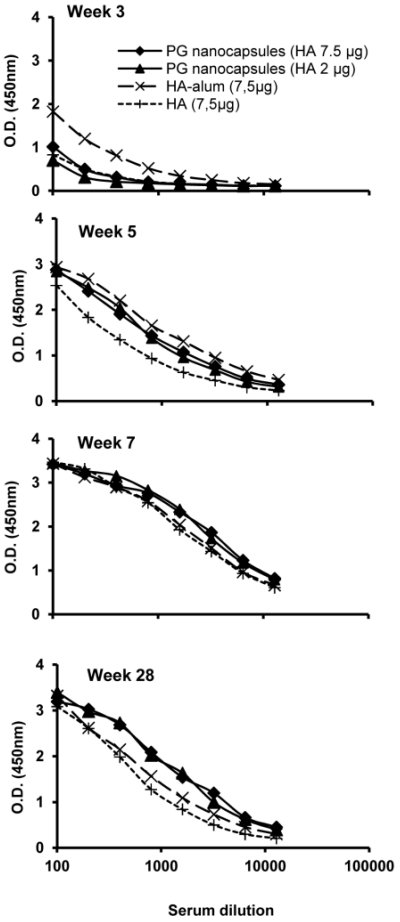

Figure 11: *Serum neutralizing antibody levels against HA after three immunization to BALB/c mice (0, 3 and 5 weeks) with PG nanocapsules associating two different doses of HA (2 and 7.5 µg) and the two controls (HA-alum and fluid HA, 7.5 µg both). PG nanocapsules 2 µg (■);PG nanocapsules 7.5 µg (◆); fluid HA 7.5 µg (●), HA-alum 7.5 µg (▲).*

On the other hand, the incorporation of imiquimod into PG nanocapsules had a dose-dependent effect *in vivo*. As discussed above, a single dose of imiquimod-loaded PG nanocapsules did not increase the response observed for imiquimod-free PG nanocapsules (**Figure 8**). However, the impact of the encapsulated imiquimod was great after the administration of a second dose, as noted by the rapid boosted response (**Figure 10**). This strong response after the boost-dose suggests a different immunostimulation mechanism as compared to that of imiquimod-free PG nanocapsules. Imidazolquinolines have been described as potent activators of B cells. In particular, imiquimod was reported to be more efficient in activated B cells than in naïve B cells (29). Therefore, in the actual scenario, the first dose of PG nanocapsules containing imiquimod may have activated the B cells, which then responded more efficiently after a second exposure, thus inducing a prompt and intense production of specific IgG antibodies.

The effect of the composition of the nanocapsules was also observed on the type of immune response elicited by each prototype. While PG nanocapsules encapsulating imiquimod were able to induce Th1-mediated immune responses regardless the number of doses, the main type of immune response elicited by imiquimod-free PG nanocapsules was dependent on the immunization regimen (**Figure 12**). Imiquimod has been extensively described to modulate the immune response by skewing immunity towards a predominant Th1 type (30), as indeed observed when this prototype was administered even in a single dose. Besides, one dose of PG nanocapsules elicited a predominant Th2 response, which shifted to a mixed Th1/Th2 upon the boost-dose, as also occurred for chitosan nanocapules (CSNC+) described above. However, in the present study we found that the IgG1/IgG2a ratio values were lower than those observed for CSNC+ with Miglyol® 812 core administered in a single dose (IgG1/IgG2a = 2 and 4, respectively for squalene and Miglyol® 812). This finding suggests that the squalene core could have also influenced the balance Th1/Th2 (31).

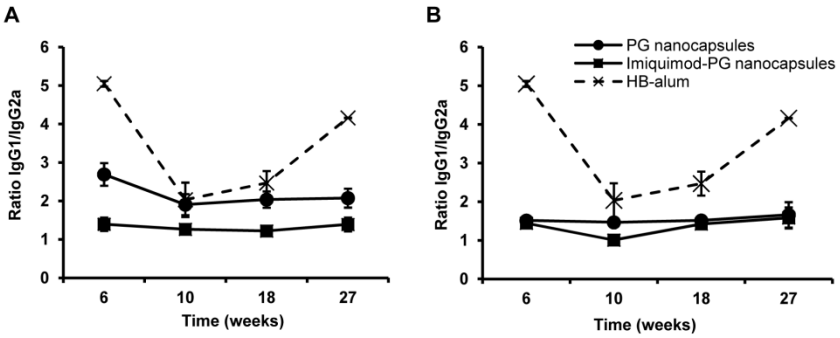

Figura 12: *IgG subtypes, IgG1 and IgG2a, against HB elicited after the different immunization protocols for blank and imiquimod-loaded PG nanocapsules associating HB (10 μg) and expressed as the ratio between IgG1 and IgG2a. A) Single dose immunization. B) Boost-dose immunization (0 and 4 weeks). 10 μg HB-alum were administered following the boost-dose immunization regimen. Results are expressed as mean +/- SD (n=10).*

Finally, as a general conclusion, the core-corona structure of these polysaccharide-lipid nanocarriers conferred a high versatility to the system, which enabled the association of immunoactive compounds and different types of antigens as part of the same structure, while preserving nanometric particle size and cationic surface charge. In addition, the *in vivo* studies showed that these novel antigen nanocarrier have the capacity to potentiate and modulate specific immune responses. More precisely, we have observed that the composition of the nanocapsules played a crucial role in the kinetics and modulation of the immune response. Therefore, on the basis of these results it seems plausible to envisage that specific immunization strategies could be achieved by a judicious definition of the combination of antigens, immunomodulators and immunization regimens. In addition, such strategies could be also intended to induce systemic immune responses using a needle-free or non-invasive administration route, such as the intranasal, as herein shown.

DISCUSIÓN GENERAL

Las nanocápsulas son estructuras coloidales que presentan una arquitectura característica tipo núcleo-corona, la cual consiste en un núcleo líquido oleoso rodeado por una capa polimérica, por ejemplo de quitosano (CS). Este tipo de estructura ha sido utilizada para la encapsulación de fármacos con la finalidad de aumentar su solubilidad, así como su transporte a través de barreras mucosas (1). En el presente trabajo, la tecnología y la composición de las nanocápsulas de CS han sido adaptadas para explorar su potencial como sistema adyuvante de vacunas y para la liberación de antígenos a través de las mucosas. En el diseño del sistema anteriormente mencionado, se ha puesto un énfasis especial en dotar a estas nanoestructuras de un carácter multifuncional. Esta multifuncionalidad permitiría la asociación de antígenos a la superficie catiónica y la encapsulación de fármacos inmunoestimulantes en el núcleo oleoso, haciendo posible de esta forma la co-liberación de ambos componentes a las células del sistema inmune.

Para la mayor parte del trabajo, hemos seleccionado el antígeno recombinante de la hepatitis B (rHBsAg) como modelo antigénico para ser asociado a la superficie de CS de las nanocápsulas. Esto se ha considerado un reto ya que el rHBsAg es en si mismo una partícula viral (2), compuesta por subunidades proteicas de la cápside del virus integradas en lípidos adquiridos de la membrana celular de la célula infectada. En estudios posteriores también hemos evaluado la capacidad de las nanocápsulas optimizadas para liberar otro tipo de antígenos, como la hemaglutinina del virus de influenza, que es una proteína soluble.

La presentación del antígeno sobre la superficie de las nanocápsulas se ha propuesto como una estrategia para mimetizar la estructura natural de los patógenos, como la utilizada en el sistema PeviPRO™, consistente en virosomas sintéticos, y del cual ya se encuentran comercializadas una vacuna de hepatitis A (Epaxal®) y otra de influenza (Inflexal®) (3). Esta disposición de copias repetitivas del epitopo antigénico sobre la superficie

de las nanopartículas, se ha determinado que puede aumentar la respuesta inmune frente a antígenos de baja inmunogenicidad (4). Por otra parte, también se ha visto que la carga superficial de las nanoestructuras afecta a sus propiedades adyuvantes (5). Por tanto, en primer lugar, hemos estudiado la influencia de las características superficiales de las nanocápsulas, como la composición y la organización del antígeno en la superficie, en la generación de respuestas inmunes específicas frente a la hepatitis B.

Las CS nanocápsulas se prepararon utilizando Miglyol® 812 y CS (grado de deacetilación 85.5%), que constituían respectivamente el núcleo oleoso y la cubierta externa de las nanocápsulas (6). Posteriormente, el rHBsAg (a partir de ahora HB) se asoció a la cubierta polimérica en distintas proporciones CS:HB (w:w) para conferirle al sistema una carga superficial y composición opuestas (formulaciones CSNC+ y CSNC-), mientras que el tamaño de partícula se mantiene en torno a los 250 nm, tal y como se muestra en la **Tabla 1**. La superficie catiónica de CSNC+ indica la prevalencia del CS en la superficie de la nanoestructura, a pesar de la elevada eficacia de asociación del antígeno. Por el contrario, la carga de negativa de CSNC- indica la exposición predominante de las moléculas del antígeno atrapado en la cubierta de CS hacia el medio externo (**Figura 1**).

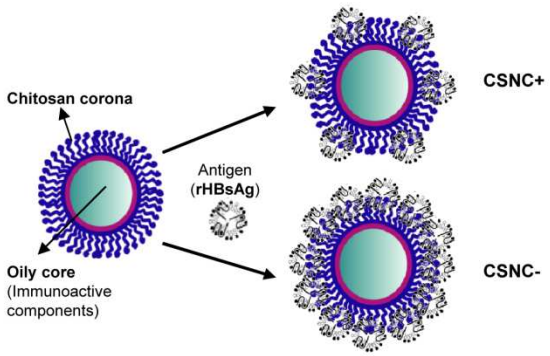

***Figure 1**: Ilustración de la organización de HB en los prototipos catiónico y aniónico de las CSNC (CSNC+ y CSNC-).*

***Tabla 1**: Caracterización físico-química de los diferentes prototipos de CSNC asociando el HB. Resultados presentados como media ± SD (n=3).*

Formulación	CS:HB ratio	Tamaño (nm)	PdI	Potential ζ (mV)	A.E. (%)
Blancas	--	196 ± 12	< 0.2	+45 ± 1	-
CSNC-	**1:12.8**	310 ± 34	< 0.2	-23 ± 3	60 ± 3
CSNC+	**1:0.25**	245 ± 53	< 0.2	+41 ± 7	78 ± 3

CSNC: CS nanocápsulas; HB: antígeno recombinante de superficie de la hepatitis B; Pdl: índice de polidispersión; A.E.: eficacia de asociación.

Los resultados de la evaluación de la eficacia *in vivo* de estos prototipos evidencian la superioridad de la formulación catiónica (CSNC+) con respecto a la cargada negativamente (CSNC-). Además, la formulación CSNC+ fue capaz de mejorar significativamente la respuesta inmune alcanzada por la vacuna convencional con álum (HB-alum), administrada a la misma dosis por vía intramuscular (i.m.) (10 μg de HB; 0, 4 semanas) (**Figura 2**).

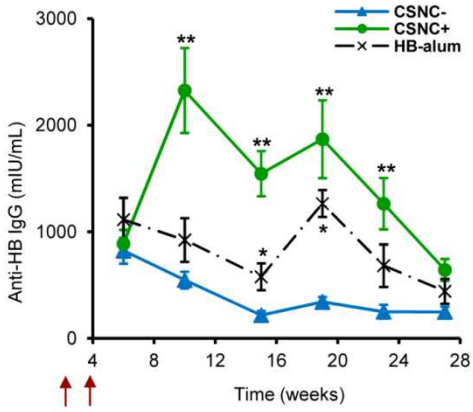

***Figura 2:** Respuesta immune inducida por los prototipos de nanovacuna (CSNC- y CSNC+) y el control positivo (HB-alum) administrados a ratones BALB/c en las semanas 0 y 4 (10 μg) (flechas) y expresada como niveles de IgG anti-HB (mIU/ml). CSNC- (azul –▲–); CSNC+ (verde –●–) and HB-alum (negro –·X·–). Los resultados se presentan como media ± SEM. Las diferencias significativas se indican como: *Alum o CSNC+ vs. CSNC- ($p < 0.05$). ** CSNC+ vs. Alum y CSNC- ($p < 0.05$). (n=10).*

Estos resultados demuestran claramente el carácter inmunestimulador del prototipo CSNC+ y el efecto positivo de la presencia predominante del CS sobre la superficie de las nanocápsulas asociando el antígeno (7-11). Esta última característica podría haber contribuido de forma importante a su adecuada presentación al sistema inmune y, además, a una mayor activación de las células presentadoras de antígeno (APCs) y al posterior desarrollo de una respuesta adaptada robusta. De hecho, en un estudio celular *in vitro*, observamos que las CS nanocápsulas son ampliamente reconocidas y captadas por los macrófagos (90% después de 30 minutos de incubación) (**Figura 3**). Esta elevada internalización se atribuye a su presentación como nanoestructura catiónica. Tal y como se ha descrito para otras nanoestructuras catiónicas (12-14), la carga superficie positiva es relevante para favorecer la internalización por las células fagocíticas. Además, esta internalización masiva se ha visto a tiempos muy cortos (30 minutos), de forma que se pone en evidencia una rápida interacción de CSNC+ con las células, al igual que ocurre con otras nanoestructuras basadas en CS (12).

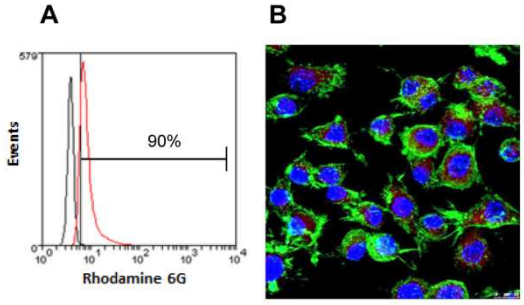

Figure 3: *Internalización de CS nanocápsulas fluorescentes marcadas con rodamina-6G (50 µg/mL) en macrófagos determinado por A) citometría de flujo y B) microscopía confocal (canal rojo: CS nancápsulas fluorescentes; canal verde: Alexa Fluor 488-faloidina; canal azul: DAPI).*

El efecto adyuvante de CSNC+ también se observó después de una inmunización única, la cual fue suficiente para alcanzar niveles de IgG seroprotectores (>10mUI/mL para humanos (15)) que se prolongaron durante el tiempo de estudio (seis meses) (**Figura 4**). Este efecto sostenido

podría ser atribuido a un aclaramiento lento de las nanocápsulas catiónicas desde el lugar de inyección hacia los órganos linfoides secundarios (ganglios linfáticos) (16). En consecuencia, la estimulación continua del sistema inmune a este nivel puede llegar a prolongar el efecto adyuvante de las nanocápsulas, como se explicará más adelante.

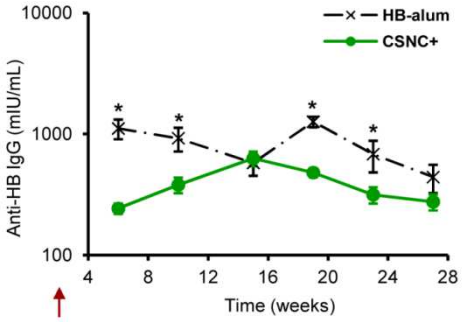

Figure 4: *Respuesta immune inducida por CSNC+ (10 µg; verde –●–) administradas a ratones BALB/c i.m. en una dosis única (flecha) y el HB-alum (black –·X·–) administrado a las semanas 0 y 4 (10 µg) y expresado como niveles de IgG anti-HB (mIU/ml). Los resultados se presentan como media ± SEM. Las diferencias estadísticamente significativas se indican como *(p < 0.05) (n=10).*

En experimentos adicionales, se observó que el número de dosis de nanovacuna administrada afectaba al patrón de la respuesta inmune. Así, una dosis única de CSNC+ dio lugar a una respuesta predominantemente del tipo Th2 (mayores niveles de IgG1 que IgG2a), mientras que tras una inmunización en dos dosis se inducen ambos tipos de respuesta, Th1 y Th2 (**Figura 5**). Estos resultados concuerdan con observaciones descritas previamente para soluciones acuosas de CS con un antígeno modelo (β-galactosidasa) (17) y nanopartículas de CS encapsulando ovalbúmina (18), ambos administrados por vía subcutánea, lo cual indica que el CS, tanto en su forma fluida como en forma nanoparticulada, es capaz de inducir respuestas inmune mixtas Th1/Th2.

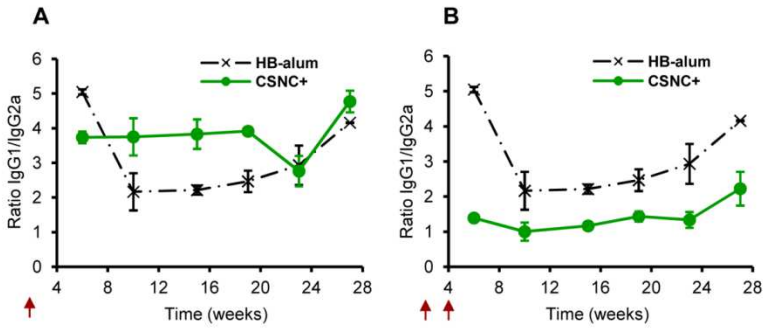

Figure 5: *Relación entre los niveles de IgG1 e IgG2a anti-HB (IgG1/IgG2a) para el prototipo CSNC+ (10 µg; verde –●–) después de una inmunización única (A) ó doble (B) (indicado con flechas) y comparado con dos dosis de HB-alum (10 µg; negro –·X·–) (0, 4 semanas). Los resultados se presentan como la media ± SD (n=10).*

En general, los resultados de estos estudios evidencian el efecto adyuvante de CSNC+ y su capacidad para generar protección inmunológica sostenida tras la administración de una dosis única. Sin embargo, teniendo en cuenta la estructura multifunctional de las CS nanocápsulas, hemos postulado que una mejora en la formulación, por ejemplo incorporando un inmunoestimulante en núcleo oleoso, podría ser interesante para el desarrollo de un sistema de liberación sin agujas o "needle-free". Para validar esta hipótesis, hemos elegido la vía nasal como vía de administración. La mucosa nasal presenta varias barreras (el moco, la capa de células epiteliales, la degradación enzimática, el aclaramiento mucociliar, etc.) que el antígeno debe superar para llegar a las células inmunocompetentes de la submucosa o del tejido linfoide asociado a mucosas (NALT). Con la finalidad de potenciar el inicio de los eventos que finalmente den lugar a la respuesta inmune específica, nuestra estrategia se basa en la co-liberación del antígeno junto al agente inmunoestimulante, una vez que las nanocápsulas transportadoras sean captadas por las APCs (células dendríticas, macrófagos, etc.). Utilizando este sistema, esperamos que el fármaco inmunoestimulante promueva la respuesta inmune innata y así se maximice la inducción de la respuesta inmune adaptada, incluso a dosis bajas del antígeno. Para ello, se

seleccionó el imiquimod para ser incorporado en el núcleo oleoso de las nanocápsulas. El imiquimod es conocido por actuar como modulador del sistema inmune innato mediante la activación de las APCs a través del receptor intracelular "Toll-like receptor 7" (TLR 7). La activación de este receptor tiene como resultado la producción de citocinas proinflamatorias que pueden, en último término, estimular y modular la respuesta inmune adaptada a través de la producción de anticuerpos específicos y respuestas mediadas por células T (19). Debido al importante carácter lipofílico del imiquimod, ha sido posible encapsularlo muy eficientemente (70%) sin alterar las propiedades físico-químicas de las nanocápsulas blancas (**Tabla 1** y **Tabla 2**). Además estas características se mantienen incluso cuando se asocia el HB a la superficie de las nanocápsulas cargadas con el imiquimod (ratio 1:0.25, como en CSNC+).

Tabla 2: *Caracterización físico-química de las CS nanocápsulas encapsulando imiquimod y asociando o no el HB (n=3).*

Composición de CS nanocápsulas	Tamaño (nm)	PdI	Potencial ξ (mV)	% HB	% Imiquimod
Imiquimod	199 ± 7	0,22 ± 0,02	+47 ± 1	---	70
Imiquimod/HB	218 ± 9	0,25 ± 0,03	+45 ± 6	70 ± 2	70

Se ha determinado que la liberación del imiquimod desde las CS nanocápsulas afecta a la funcionalidad de los macrófagos, induciéndolos a secretar citocinas pro- y anti-inflamatorias (**Figura 6**). De acuerdo con trabajos anteriores (20, 21), hemos observado una importante inducción de citocinas pro-inflamatorias (IL-6 and TNF-α) en un modo fuertemente dosis-dependiente, mientras que los niveles de IL-1α fueron casi inapreciables. Por otro lado, esta intensa estimulación pudo haber provocado una respuesta reguladora mediante la inducción de IL-10, una citocina no inflamatoria capaz de atenuar el efecto de las citocinas pro-inflamatorias (22).

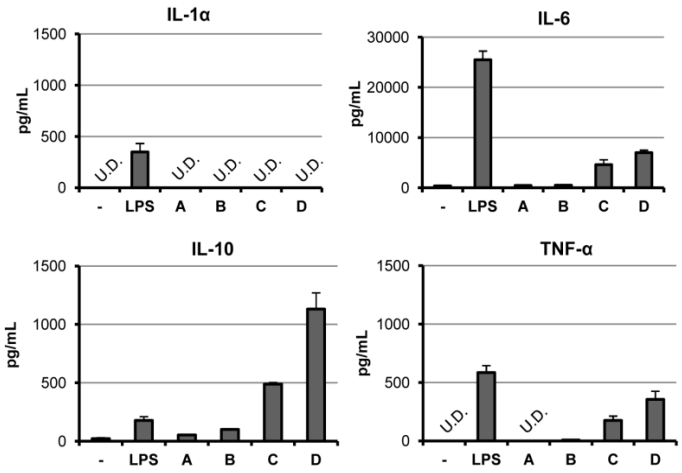

Figura 6: *Producción de citocinas por macrófagos peritoneales incubados con CS nanocápsulas blancas o cargadas con imiquimod a dos dosis distintas (10 and 100 μg/mL) durante 24 horas. El control negativo fue medio de cultivo y el positivo fue LPS (1 μg/mL). La concentración media (pg/mL) de IL1-α, IL-6, IL-10 and TNF-α en el sobrenadante del medio de cultivo se ha calculado a partir un experimento representativo realizado dos veces y en duplicado. UD: niveles no detectables* (IL-1α < 15.7 pg/mL *TNF < 2.1 pg/mL). CS nanocápsulas blancas (A: 10 μg/mL; B: 100 μg/mL); CS nanocápsulas cargadas con imiquimod (C: 10 μg/mL; D: 100 μg/mL).*

Los resultados obtenidos tras administración nasal de las CS nanocápsulas blancas y cargadas con imiquimod han puesto de manifiesto dos aspectos importantes. Uno tiene que ver con la relevancia de la cubierta polimérica de las nanocápsulas a la hora de facilitar el transporte del antígeno a través de la mucosa nasal. De hecho, el control de la nanoemulsión, es decir, las gotas de aceite sin la cubierta de CS, no fue capaz de inducir una respuesta significativa a la misma dosis de HB (10 μg, semanas 0 y 4) (**Figura 7A**). Este resultado concuerda con la capacidad de internalización de las CS nanocápsulas a través de la mucosa nasal previamente descrito por Prego y col. (23). Otro resultado importante en este estudio se refiere al aumento de la respuesta inmune inducido por el prototipo que contiene imiquimod en comparación con las nanocápsulas blancas. Además, esta mayor respuesta fue significativamente mayor a tiempos más largos ($p<0.05$) (**Figura 7A**). Por tanto, de acuerdo con nuestra hipótesis inicial,

la co-liberación del antígeno y el inmunoestimulante (ambos incluidos en el mismo nanovehículo) da lugar un efecto positivo en la inducción y progresión de la respuesta inmune específica tras la inmunización nasal. Sin embargo, esta respuesta fue mucho más intensa en algunos animales que en otros. Posteriormente, se administró en este grupo de ratones una tercera dosis tardía con este prototipo (10 μg de HB en la semana 28).

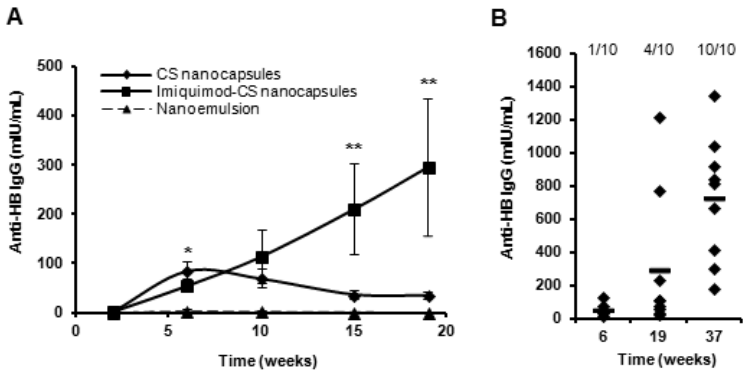

Figura 7: *Respuesta immune sistémica después de dos inmunización intranasales (semanas 0 y 4) a ratones BALB/c con CS nanocápsulas blancas o cargadas con imiquimod y la nanoemulsión asociando HB. A) El gráfico representa los niveles de anti-HB IgG medidos a diferentes tiempos tras la primera inmunización (media +/- SEM) (n=10). Las diferencias estadísticamente significativas se indican como: * CS nanocápsulas blancas y cargadas con imiquimod vs. nanoemulsión (p<0.05). ** CS nanocápsulas cargadas con imiquimod vs. CS nanocápsulas blancas y nanoemulsión (p<0.05). B) El efecto de la tercera dosis tardía con CS nanocápsulas cargadas con imiquimod. Se representan los niveles individuals de IgG en cada ratón (diamantes) y la media de diez ratones (raya) a un tiempo corto, intermedio y tardío. Las fracciones representan el número de ratones con niveles de anti-HB IgG mayores de 100 mIU/mL, versus el número total de ratones (n=10).*

Observamos que los niveles de IgG en cada uno de los animales del grupo sobrepasaban los niveles de seroprotección (media 720 mIU/mL; >100 mIU/mL para humanos se consideran protección total frente a HB (15)) (**Figura 7B**). Esta respuesta tan intensa obtenida tras la administración de la tercera dosis se ha asociado a la existencia de memoria inmunológica. Así, el sistema inmune es capaz de interpretar esta última inmunización como una exposición al virus, de forma que responde rápidamente elevando la producción de anticuerpos. Este efecto se considera un signo

de una inmunización temprana adecuada (con las 2 primeras dosis), sugiriendo que la dosis de recuerdo no sería necesaria para sostener la protección debido al desarrollo de dicha memoria inmunológica (24).

Posteriormente, se introdujeron nuevas modificaciones en el sistema consistentes en la incorporación de una cubierta polimérica diferente y otro núcleo oleoso. En concreto se utilizó, respectivamente, una forma más desacetilada del CS (denominada a partir de aquí poliglucosamina – PG) y el aceite escualeno. El escualeno es un triterpeno lineal que está presente de forma natural en el organismo. Es el primer precursor en la biosíntesis del colesterol y el principal componente del sebo en humanos. El escualeno es además el componente oleoso mayoritario de las emulsiones adyuvantes ya aprobadas para su uso en humanos (MF59™ and AS03™ en formulaciones de vacunas frente a influenza) y es normalmente el aceite de elección para el desarrollo de nuevas emulsiones adyuvantes para vacunas (25). En estas emulsiones, normalmente el antígeno se mezcla con la emulsión preformada sin que ocurra ningún tipo de interacción entre el antígeno y las gotículas de aceite, de forma que éste se queda disperso en la fase acuosa de la emulsión (26). Por tanto, con la incorporación de la corona de PG cubriendo las vesículas de escualeno, formando así un sistema nanocapsular, pretendemos incluir los distintos componentes (aceite, tensoactivos, inmunoestimulantes y antígeno) dentro del mismo nanovehículo para ser liberados simultáneamente a las APCs.

Las PG nanocápsulas desarrolladas fueron capaces de asociar eficazmente dos antígenos diferentes: (i) el HB, representante de una partícula viral (VLP) (27), y (ii) la hemaglutinina del virus de influenza (HA), que es una proteína soluble (28). Así mismo, también se consiguió la incorporación del imiquimod en el núcleo oleoso, sin comprometer el tamaño nanométrico del sistema y su carga superficial positiva (**Tabla 3**).

Tabla 3: *Caracterización físico-química de los diferente prototipos de PG nanocápsulas asociando (o no) los dos tipos de antígenos: HB y HA (n=3).*

Composición del núcleo	Ag	Tamaño (nm)	PdI	Potential ζ (mV)	Ag A.E. (%)	Imiquimod A.E. (%)
Escualeno	--	172 ± 3	< 0.2	+66 ± 1	-	-
	HB	230 ± 13	< 0.2	+60 ± 3	72 ± 8	-
	HA	217 ± 4	< 0.2	+51 ± 2	69 ± 2	-
Escualeno + Imiquimod	--	198 ± 5	< 0.2	+63 ± 1		40 ± 2
	HB	299 ± 11	< 0.2	+60 ± 4	78 ± 6	40 ± 2

PdI: índice de polidispersión; Ag: antígeno; A.E.: eficacia de asociación.

Las potenciales propiedades adyuvantes de las PG nanocápsulas asociando el HB, así como su capacidad para inducir protección inmunológica tras una única inmunización, se evaluaron en ratones BALB/c. En estos estudios hemos podido valorar además, el efecto de la composición de las nanocápsulas en la cinética y modulación de la respuesta inmune.

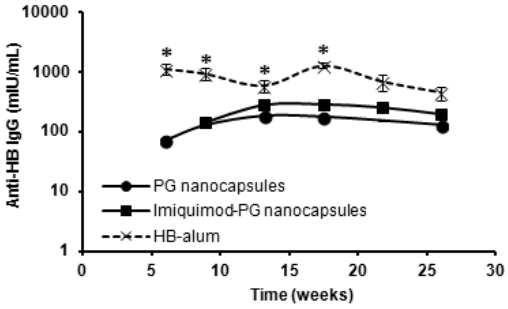

Figure 8: *Respuesta immune alcanzada tras una inmunización única con PG nanocápsulas blancas o cargadas con imiquimod (HB 10 µg) en ratones BALB/c. El control positivo HB-alum (10 µg) se administró en las semanas 0 y 4. Los resultados están expresados como niveles de anti-HB IgG (mIU/mL) medidos a distintos tiempos tras la primera inmunización (media +/- SEM) (n=10). Las diferencias significativas se indican con * (p<0.05).*

Tras una única inmunización (10μg), los niveles de anti-HB IgG alcanzados por ambos prototipos (PG nanocápsulas conteniendo imiquimod o no) se situaron por encima de los niveles considerados seroprotectores en humanos (100-200 mIU/mL). Aunque los niveles medios fueron ligeramente mayores para la formulación con imiquimod, estos no fueron significativamente mayores que los obtenidos para la formulación sin inmunoestimulante (**Figura 8**).

Tal y como se argumentó previamente, este efecto sostenido se atribuye a un efecto directo sobre el sistema inmune (alta captación y activación de APCs), y al tiempo de residencia prolongado en el lugar de inyección. Esta última característica, fue explorada más a fondo utilizando distintas técnicas de imagen. La técnica de imagen óptica de fluorescencia *in vivo* (IVIS) sugería que las PG nanocápsulas formaban un depot en el lugar de inyección durante un período de tiempo largo, para luego drenar lentamente desde allí. Otros estudios basados en técnicas de imagen por gammagrafía, nos han permitido profundizar en detalle en el patrón de migración de las nanocápsulas. Para ello, las PG nanocápsulas se marcaron con Indio-111 (^{111}In) para poder seguirlas tras su administración *in vivo* utilizando una gamma-cámara. En este estudio, hemos podido observar que la PG nanocápsulas administradas por vía subcutánea a conejos New Zealand White, formaban un depot en el lugar de inyección y posteriormente drenaban a través del sistema linfático. A continuación, observamos que las nanocápsulas comenzaban a acumularse gradualmente en el ganglio linfático popliteal (PLN) (**Figura 9**) y más tarde, tras una hora post-inyección, también comenzaban a llegar a los ganglios ilíacos (ILN) siguiendo la circulación linfática normal. De acuerdo con este estudio, el efecto inmunopotenciador de las nanocápsulas a largo plazo podría ser debido a dos factores principales: (i) el drenaje linfático continuo desde el lugar de inyección y su posterior retención en los ganglios linfático, y (ii) el tiempo de residencia prolongado en el lugar de inyección, el cual permitiría una interacción continua de las PG

nanocápsulas con las APCs periféricas, de forma que se favorecería su captación y transporte hacia el ganglio linfático.

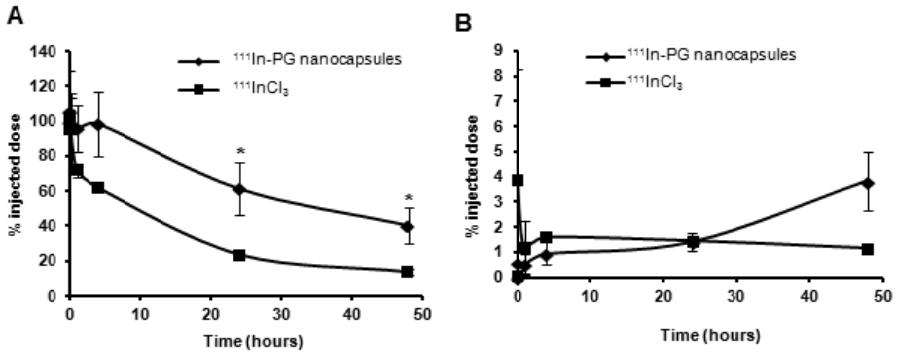

Figura 9: *Análisis de las imágenes obtenidas mediante gammagrafía a distintos tiempos de los conejos inyectados con PG nanocápsulas marcadas con ^{111}In. Porcentaje de la dosis inyectada retenida en el lugar de inyección (A) y en el ganglio linfático (B). * Diferencias estadísticamente significativas (p>0.05) (n=3).*

Aunque no existan diferencias significativas entre las respuestas alcanzadas por las PG nanocápsulas con y sin imiquimod tras una inmunización única, la segunda dosis con estos prototipos asociando HB sí que puso en evidencia diferencias importantes en cuanto a la cinética y a la modulación de la respuesta inmune. Los elevados niveles IgG alcanzados a largo plazo por las PG nanocápsulas indican un efecto acumulado de las dosis administradas, el cual finalmente da lugar a una respuesta potenciada tardía (**Figura 10**) y, por tanto, a una respuesta de larga duración. Este efecto también se ha observado en el caso del antígeno HA asociado a PG nanocápsulas. De hecho, la respuesta inicial moderada se incrementa de forma notable con el tiempo, alcanzando niveles de IgG más altos que los controles (HA-alum y HA solo) (**Figura 11**), como ocurría con el HB. Además, las PG nanocápsulas fueron capaces de inducir una respuesta inmune específica elevada y sostenida en el tiempo, incluso utilizando dosis de antígeno bajas. De hecho, los títulos de IgG fueron muy parecidos para las dos dosis de HA ensayadas (2 y 7.5 μg).

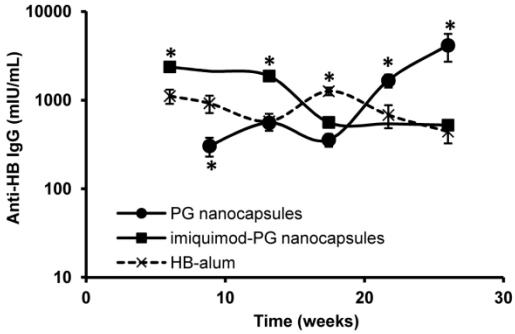

Figura 10: *Respuesta immune alcanzada tras dos dosis (10 µg, 0 y 4 semanas) de PG nanocápsulas encapsulando imiquimod o no con HB, y el contro positivo HB-alum (10 µg) a ratones BALB/c. Los resultados se expresan como mIU/mL de anti-HB IgG medidas a diferentes tiempos tras la primera inmunización (media +/- SEM) (n=10). Las diferencias estadísticamente significativas se indican como * (p<0.05).*

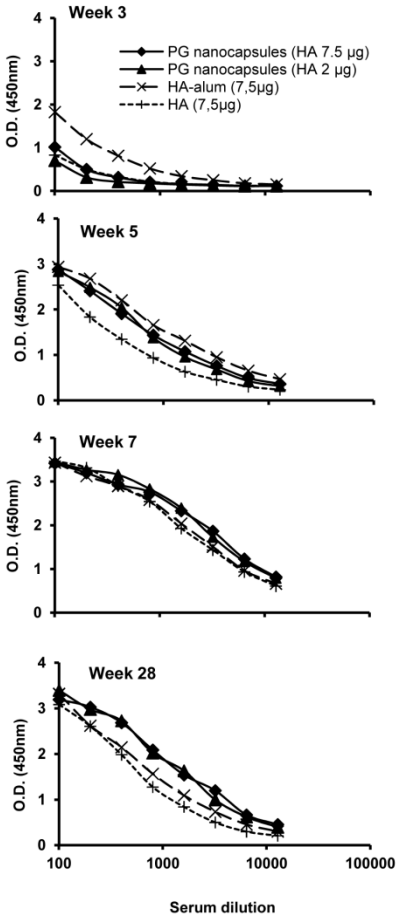

Figura 11: *Niveles de anticuerpos neutralizantes frente a HA tras tres inmunizaciones a ratones BALB/c (0, 3 and 5 semanas) con PG nanocápsulas asociando dos dosis distintas de HA (2 y 7.5 µg) y los dos controles (HA-alum y HA solo, 7.5 µg cada uno). PG nanocápsulas 2 µg (■); PG nanocápsulas 7.5 µg (◆); HA 7.5 µg (●), HA-alum 7.5 µg (▲).*

Por otro lado, la incorporación de imiquimod en las PG nanocápsulas produjo un efecto dosis-dependiente *in vivo*. Tal y como se ha descrito anteriormente, una dosis única de las PG nanocápsulas con imiquimod no aumentan la respuesta con respecto a las PG nanocápsulas sin el inmunoestimulante (**Figura 8**). Sin embargo, el impacto del imiquimod encapsulado fue mayor tras la administración de la segunda dosis, tal y como se puede apreciar por la respuesta tan pronunciada alcanzada inmediatamente tras la segunda inmunización (**Figura 10**). Esta fuerte respuesta sugiere un mecanismo diferente de estimulación del sistema inmune en comparación con las PG nanocápsulas sin imiquimod. Se ha descrito que las imidazolquinolinas son potentes activadores de las células B. En concreto, se ha determinado que el imiquimod actúa más eficazmente en células B ya previamente activadas que en células B inmaduras (29). Por ello, en este caso las PG nanocápsulas que contienen imiquimod han podido activar a las células B tras la primera inmunización, las cuales responderían más eficazmente tras la segunda exposición de forma que la producción de IgG específicos sea más rápida e intensa.

El efecto de la composición de las nanocápsulas también afecta al tipo de respuesta inmune alcanzada por cada prototipo. Mientras que las PG nanocápsulas con imiquimod son capaces de inducir una respuesta mediada principalmente por linfocitos Th1 independientemente del número de dosis administradas, el tipo de respuesta inmune alcanzada con las PG nanocápsulas sin imiquimod fue dependiente del régimen de inmunización (**Figura 12**). El imiquimod se caracteriza por modular la respuesta inmune predominantemente hacia el tipo Th1 (30), tal y como se ha visto cuando el prototipo con imiquimod se administra incluso a una dosis única. Por otro lado, una dosis de PG nanocápsulas dio lugar una respuesta del tipo Th2 predominantemente, la cual cambia hacia una respuesta mixta Th1/Th2 tras la segunda inmunización, como también ocurría con las CS nanocápsulas (CSNC+) descritas anteriormente. Sin embargo, en este estudio se ha puesto de manifiesto que los valores de la

proporción IgG1/IgG2a fueron más bajos que para CSNC+ (con núcleo de Miglyol® 812) tras la inmunización única (IgG1/IgG2a = 2 y 4, respectivamente para escualeno y Miglyol® 812). Este resultado sugiere que el escualeno también podría haber influido en el balance ~~balance~~ Th1/Th2 (31).

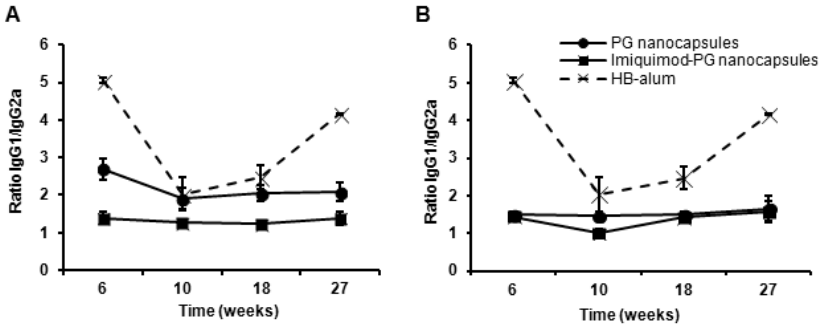

Figura 12: *Subtipos de IgG, IgG1 e IgG2a, frente a HB generados tras la administración de PG nanocápsulas con y sin imiquimod encapsulado (HB 10 µg), siguiendo distintos protocolos de inmunización. Los resultados se expresan como la relación entre IgG1 e IgG2a. A) Inmunización en dosis única. B) Inmunización en dos dosis separadas 4 semanas. El control HB-alum se administró en dos dosis de 10 µg separadas 4 semanas. Los resultados son la media de 10 ratones +/- SD.*

Finalmente como conclusión general, la estructura de núcleo-corona de estos nanovehículos compuestos por polisacáridos y lípidos confiere una gran versatilidad al sistema, ya que permite la asociación de compuestos inmunoactivos y distintos tipos de antígenos formando parte de una misma estructura, conservando al mismo tiempo un tamaño nanométrico y una carga superficial catiónica. Además, los estudios *in vivo* han servido para demostrar que estas nanocápsulas tienen la capacidad de potenciar y modular la respuesta inmune específica. Más concretamente, hemos observado que la composición de las nanocápsulas juega un papel crucial en la cinética y modulación de la respuesta inmune. Por tanto, en base a estos resultados, parece plausible que se puedan llegar a plantear diversas estrategias de inmunización específicas, a través de la acertada combinación de antígeno, inmunomoduladores y regímenes de

inmunización. Además, dichas estrategias podrían también ser concebidas, para generar respuestas inmunes sistémicas utilizando un sistema "needle-free" o a través de una vía de administración no invasiva, como puede ser la nasal, como aquí se presenta.

REFERENCES / REFERENCIAS

1. Oyarzun-Ampuero FA, Garcia-Fuentes M, Torres D & Alonso MJ (2010) Chitosan-coated lipid nanocarriers for therapeutic applications. *J Drug Deliv Sci Tec* 20(4): 259-265.

2. Gavilanes F, *et al* (1990) Hepatitis B surface antigen. role of lipids in maintaining the structural and antigenic properties of protein components. *Biochem J* 265: 857-864.

3. Moser C, Metcalfe IC & Viret J (2003) Virosomal adjuvanted antigen delivery systems. *Expert Rev Vaccines* 2(2): 189-196.

4. Schroeder U, *et al* (2009) Peptide nanoparticles serve as a powerful platform for the immunogenic display of poorly antigenic actin determinants. *J Mol Biol* 386(5): 1368-1381.

5. He C, Hu Y, Yin L, Tang C & Yin C (2010) Effects of particle size and surface charge on cellular uptake and biodistribution of polymeric nanoparticles. *Biomaterials* 31(13): 3657-3666.

6. Prego C, Torres D & Alonso MJ (2006) Chitosan nanocapsules as carriers for oral peptide delivery: Effect of chitosan molecular weight and type of salt on the in vitro behaviour and in vivo effectiveness. *J Nanosci Nanotechnol* 6(9-10): 2921-2928.

7. Prego C, *et al* (2010) Chitosan-based nanoparticles for improving immunization against hepatitis B infection. *Vaccine* 28(14): 2607-2614.

8. Slutter B, *et al* (2010) Conjugation of ovalbumin to trimethyl chitosan improves immunogenicity of the antigen. *J Control Release* 143(2): 207-214.

9. Borges O, *et al* (2008) Alginate coated chitosan nanoparticles are an effective subcutaneous adjuvant for hepatitis B surface antigen. *Int Immunopharmacol* 8(13–14): 1773-1780.

10. Zhao K, *et al* (2011) Preparation and immunological effectiveness of a swine influenza DNA vaccine encapsulated in chitosan nanoparticles. *Vaccine* 29(47): 8549-8556.

11. Jiang L, *et al* (2007) Novel chitosan derivative nanopartictes enhance the immunogenicity of a DNA vaccine encoding hepatitis B virus core antigen in mice. *J Gene Med* 9(4): 253-264.

12. Zaki NM, Nasti A & Tirelli N (2011) Nanocarriers for cytoplasmic delivery: Cellular uptake and intracellular fate of chitosan and hyaluronic acid-coated chitosan nanoparticles in a phagocytic cell model. *Macromol Biosci* 11(12): 1747-1760.

13. Foged C, Brodin B, Frokjaer S & Sundblad A (2005) Particle size and surface charge affect particle uptake by human dendritic cells in an in vitro model. *Int J Pharm* 298(2): 315-322.

14. Zwiorek K, *et al* (2008) Delivery of cationic gelatin nanoparticles strongly increases the immunostimulatory effects of CpG oligonucleotides. *Pharm Research* 25(3): 551-562.

15. Shouval D (2003) Hepatitis B vaccines. *J Hepatol* 39: S70-S76.

16. Henriksen-Lacey M, *et al* (2010) Liposomal cationic charge and antigen adsorption are important properties for the efficient deposition of antigen at the injection site and ability of the vaccine to induce a CMI response. *J Control Release* 145(2): 102-108.

17. Zaharoff DA, Rogers CJ, Hance KW, Schlom J & Greiner JW (2007) Chitosan solution enhances both humoral and cell-mediated immune responses to subcutaneous vaccination. *Vaccine* 25(11): 2085-2094.

18. Wen Z, Xu Y, Zou X & Xu Z (2011) Chitosan nanoparticles act as an adjuvant to promote both Th1 and Th2 immune responses induced by ovalbumin in mice. *Marine Drugs* 9(6): 1038-1055.

19. Stanley MA (2002) Imiquimod and the imidazoquinolones: Mechanism of action and therapeutic potential. *Clin Exp Dermatol* 27: 571.

20. Weeks C & Gibson S (1994) Induction of interferon and other cytokines by imiquimod and its hydroxylated metabolite R-842 in human blood-cells in-vitro. *J Interferon Res* 14(2): 81-85.

21. Testerman T, *et al* (1995) Cytokine induction by the immunomodulators imiquimod and S-27609. *J Leukoc Biol* 58(3): 365-372.

22. Moore K, Ogarra A, Malefyt R, Vieira P & Mosmann T (1993) Interleukin-10. *Annu Rev Immunol* 11: 165-190.

23. Prego C, Torres D & Alonso MJ (2006) Chitosan nanocapsules: A new carrier for nasal peptide delivery. *J Drug Deliv Sci Tec* 16(5): 331-337.

24. Banatvala J, *et al* (2000) Are booster immunisations needed for lifelong hepatitis B immunity? *Lancet* 355(9203): 561-565.

25. Fox CB (2009) Squalene emulsions for parenteral vaccine and drug delivery. *Molecules* 14(9): 3286-3312.

26. O'Hagan DT, Ott GS, De Gregorio E & Seubert A (2012) The mechanism of action of MF59 - an innately attractive adjuvant formulation. *Vaccine* 30(29): 4341-4348.

27. Grgacic EVL & Anderson DA (2006) Virus-like particles: Passport to immune recognition. *Methods* 40(1): 60-65.

28. Gomez-Casado E, *et al* (2011) Insect larvae biofactories as a platform for influenza vaccine production. *Protein Expr Purif* 79(1): 35-43.

29. Tomai M, Imbertson L, Stanczak T, Tygrett L & Waldschmidt T (2000) The immune response modifiers imiquimod and R-848 are potent activators of B lymphocytes. *Cell Immunol* 203(1): 55-65.

30. Schoen MP & Schoen M (2007) Imiquimod: Mode of action. *Br J Dermatol* 157: 8-13.

31. Fox CB, Baldwin SL, Duthie MS, Reed SG & Vedvick TS (2011) Immunomodulatory and physical effects of oil composition in vaccine adjuvant emulsions. *Vaccine* 29(51): 9563-9572.

CONCLUSIONES / CONCLUSIONS

CONCLUSIONES

El trabajo experimental recogido en la presente memoria se ha dirigido al desarrollo de un sistema adyuvante de vacunas basado en nanocápsulas de quitosano, capaz de potenciar y modular respuestas inmunes específicas cuando se administre por vía parenteral ó a través de una vía no invasiva, como es la nasal.

1. Utilizando como antígeno modelo el antígeno recombinante de superficie de la hepatitis B (rHBsAg), se han establecido las propiedades óptimas del sistema para conseguir una potenciación de la respuesta inmune con respecto al adyuvante de referencia (álum) y alcanzar niveles protectores de IgG durante largos períodos de tiempo tras una única administración intramuscular. Dicho sistema, compuesto por nanocápsulas de quitosano con núcleo de Miglyol® 812, son capaces de asociar eficazmente el rHBsAg (75%), manteniendo un tamaño de partícula en torno a 250 nm, poblaciones monodispersas y elevado potencial ζ positivo (+40 mV).

2. La modificación de los componentes de la cubierta y el núcleo oleoso se realizó utilizando un derivado más catiónico del quitosano (poliglucosamina) y un aceite con propiedades adyuvantes, como es el escualeno. Las nanocápsulas resultantes permitieron la asociación a su superficie distintos tipos de antígenos (rHBsAg y la hemaglutinina del virus de influenza – HA) así como la encapsulación del fármaco inmunomodulador imiquimod, manteniendo el tamaño nanométrico (˜200 nm) y un fuerte potencial ζ positivo (+60 mV).

3. Las nanocápsulas formadas por quitosano ó poliglucosamina como cubierta externa, y Miglyol® 812 ó escualeno como núcleo oleoso, son altamente captadas e internalizadas por macrófagos *in vitro* y son capaces de liberar el imiquimod encapsulado dando lugar a una fuerte respuesta de producción de citocinas.

4. La incorporación de imiquimod a las nanocápsulas favorece significativamente la generación de una respuesta inmune sistémica tras la administración nasal.

5. Tras su administración parenteral, las nanocápsulas compuestas por poliglucosamina y escualeno dan lugar a una potenciación de la respuesta inmune frente a los dos tipos de antígenos estudiados (rHBsAg y HA) a largo plazo, generando mayores niveles de IgG que el álum a la misma dosis. La asociación de imiquimod a estas nanocápsulas da lugar a una respuesta inmune más rápida y pronunciada, además polarizándola hacia un tipo predominantemente Th1 (celular).

6. La administración en una dosis única de las nanocápsulas compuestas por poliglucosamina y escualeno, en ausencia de imiquimod, induce una respuesta protectora frente al rHBsAg que se mantiene a lo largo del tiempo.

7. El análisis de la biodistribución de las nanocápsulas mediante técnicas de imagen sugiere que la importante respuesta inmune generada por éstas, así como su duración, puede ser debida a la permanencia en el lugar de inyección por tiempos más prolongados y posterior retención en los ganglios linfáticos drenantes.

CONCLUSIONS

The experimental work enclosed in this manuscript has been aimed at developing a vaccine adjuvant system based on chitosan nanocapsules, which is able to potentiate and modulate specific immune responses upon either nasal or parenteral administration.

1. Using the recombinant hepatitis B surface antigen (rHBsAg) as a model antigen, we have identified the optimal properties of the system in order to achieve immune potentiation and elicit protective IgG levels for long periods of time upon a single-dose intramuscular administration. Such a system, consisting of chitosan nanocapsules with a Miglyol®812 core, were able to effectively associate the rHBsAg on their surface (75%), while maintaining a particle size around 250 nm and highly positive ζ potential (+40 mV).

2. The modification of the components of the shell and oily core was performed using a more cationic derivative of chitosan (polyglucosamine) and an oil with adjuvant properties, such as the squalene. The resulting nanocapsules were able to associate on their surface different types of antigens (rHBsAg and the hemmaglutinin of influenza virus – HA), as well as to encapsulate the immunomodulator drug, imiquimod, while maintaining the nanometric particle size (~200 nm) and a strong positive ζ potential (+60 mV).

3. Nanocapsules consisting of chitosan or polyglucosamine as the outer shell, and Miglyol® 812 or squalene as the oily core, were highly captured and internalized by macrophages *in vitro*, where they are able to release the encapsulated imiquimod and induce a strong cytokine response.

4. The incorporation of imiquimod to the nanocapsules was found to have a significant impact on the generation of a protective systemic immune response upon nasal administration.

5. Following intramuscular administration, the nanocapsules composed of polyglucosamine and squalene induced a long-term boosted immune response (higher than that corresponding to alum) against the two types of antigens herein studied (rHBsAg y HA). The association of imiquimod resulted in a fast response and biased towards a predominant Th1 type (cellular).

6. A single dose administration of polyglucosamine/squalene nanocapsules, containing or not imiquimod, elicited a protective immune response against rHBsAg which persisted for a long period of time.

7. The analysis of the biodistribution of the nanocapsules by imaging techniques suggested that the important immune response generated, as well as the duration, could be due to the long residence time at the injection site and subsequent retention in the draining lymph nodes.

ANEXOS

Vaccine 28 (2010) 2607–2614

Contents lists available at ScienceDirect

Vaccine

journal homepage: www.elsevier.com/locate/vaccine

Chitosan-based nanoparticles for improving immunization against hepatitis B infection

Cecilia Prego[a], Patrizia Paolicelli[a], Belen Díaz[b], Sara Vicente[a], Alejandro Sánchez[a], África González-Fernández[b], María José Alonso[a,*]

[a] Nanobiofar Group, Department of Pharmacy and Pharmaceutical Technology, University of Santiago de Compostela, 15782 Santiago de Compostela, Spain
[b] Immunology Area, Faculty of Biology, University of Vigo, Campus Lagoas Marcosende, 36310 Vigo, Pontevedra, Spain

ARTICLE INFO

Article history:
Received 2 April 2009
Received in revised form
21 December 2009
Accepted 11 January 2010
Available online 20 January 2010

Keywords:
Chitosan-based nanoparticles
Subunit antigens
Adjuvant

ABSTRACT

The design of effective vaccine delivery vehicles is opening up new possibilities for making immunization more equitable, safe and efficient. In this work, we purpose polysaccharidic-based nanoparticles as delivery structures for virus-like particle antigens, using recombinant hepatitis B surface antigen (rHBsAg) as a model.

Polysaccharidic-based nanoparticles were prepared using a very mild ionic gelation technique, by cross-linking the polysaccharide chitosan (CS) with a counter ion. The resulting nanoparticles could be easily isolated with a size in the nanometric range (160–200 nm) and positive surface charge (+6 to +10 mV). More importantly, CS-based nanoparticles allowed the efficient association of the antigen (>60%) while maintaining the antigenic epitope intact, as determined by ELISA and Western blot. The entrapped antigen was further released *in vitro* from the nanoparticles in a sustained manner without compromising its antigenicity. In addition, loaded CS-based nanoparticles were stable, and protected the associated antigen during storage, either as an aqueous suspension under different temperature conditions (+4 °C and −20 °C), or as a dried form after freeze-drying the nanoparticles. Finally, immunization studies showed the induction of important seroprotection rates after intramuscular administration of the nanoparticles, indicating their adjuvant capacity. In fact, CS-based nanoparticles were able to induce anti-HBsAg IgG levels up to 5500 mIU/ml, values 9-fold the conventional alum-adsorbed vaccine.

In conclusion, we report here a polysaccharidic nanocarrier which exhibits a number of *in vitro* and *in vivo* features that make it a promising adjuvant for vaccine delivery of subunit antigens.

1. Introduction

Vaccination is considered one of the greatest achievements of biomedical science and public health. Routine immunization had led to the control and significant reduction of many infectious diseases. However, the benefit of immunization is severely limited to most of the population in need [1]. The important disparity in vaccination coverage between industrialized and developing countries entails millions of deaths from preventable diseases, which could be averted by improving immunization technologies.

The development of strategies to reduce the inequities in vaccination from preventable infectious diseases represents a grand challenge in global health. Indeed, there is a commitment from numerous philanthropic associations from the public and private sectors, such as the Global Alliance for Vaccines and Immunization (GAVI) and the Bill & Melinda Gates Foundation, among others, to bring technologies which could solve the problems related to the vaccination failure in developing countries [2]. Within this frame, the technological approaches are expected to be focused on improving the vaccine thermostability, decreasing the number of shots and, when possible, avoiding injections with a needle-free vaccination approach [3].

First of all, to ensure the optimal efficacy of vaccines, particular attention is needed during their storage, distribution or handling. In the case of alum-adsorbed vaccines, a loss of potency occurs when frozen due to a destruction of the particular gel structure of the adjuvant [4], and after exposure to elevated temperatures due to changes on the properties of the solution such as ionic strength and pH, among others. So far, strategies addressed to obtain a stable-dried formulation while maintaining the immunogenicity, were based on the use of spray-freeze-drying or spray coating techniques [5,6].

Secondly, to induce a full protective antibody response against the target disease, a multiple-dose vaccination schedule is usu-

* Corresponding author at: Department of Pharmacy and Pharmaceutical Technology, School of Pharmacy, University of Santiago de Compostela, 15782 Santiago de Compostela, Spain. Tel.: +34 981 563100; fax: +34 981 547148.
E-mail address: mariaj.alonso@usc.es (M.J. Alonso).

0264-410X/$ – see front matter © 2010 Elsevier Ltd. All rights reserved.
doi:10.1016/j.vaccine.2010.01.011

http://www.sciencedirect.com/science/article/pii/S0264410X10000423

J. DRUG DEL. SCI. TECH., 20 (4) 267-276 2010

From single-dose vaccine delivery systems to nanovaccines

S. Vicente, C. Prego, N. Csaba, M.J. Alonso*

Departamento de Farmacia y Tecnología Farmacéutica, Facultad de Farmacia, Universidad de Santiago de Compostela, 15782-Santiago de Compostela, Spain
*Correspondence: mariaj.alonso@usc.es

The application of micro- and nanotechnologies to the development of vaccine delivery systems started in the 70s. From that time onwards, significant advances in this field have opened up opportunities in the research of new adjuvants and the design of safer and more effective vaccines. The versatility of vaccine delivery vehicles represents an important feature in vaccine development. Indeed, the modulation of the composition, particle size and/or surface properties, offers a wide range of possibilities for overcoming natural barriers and controlling antigen release. Thus, it is currently accepted that besides their ability to enhance the low immunogenicity of new subunit and DNA vaccines, these delivery carriers represent a promising strategy for needle-free and single-dose vaccination. In this review article we aim to present the historical advances made in the field of vaccine delivery, particularly the progress made in the last two decades, describing our specific contribution, ranging from the idea of single-dose vaccination to the current concept of nanovaccines. Overall, this review illustrates the potential of nanosciences and nanotechnologies to solve the current problems of vaccination and, thus, to expand the immunization coverage worldwide.

Key words: Vaccine delivery – Antigen delivery – Microparticles – Nanoparticles – Adjuvants – Nanocarriers – Single-dose vaccination – Nanovaccines.

I. INTRODUCTION

1. A brief history of vaccine development

Vaccines have been successfully used in medicine since the first vaccine against smallpox was administered to humans by Edward Jenner in the XVIIIth century. This vaccine was an intuitive approach to protect population against smallpox, which consisted of the cowpox bacteria that caused a much milder illness than smallpox but generated protection against the human disease. At that time, the first basis of the "attenuated vaccines" concept was established and the first step for smallpox eradication worldwide was taken [1].

A critical action in vaccine evolution after Jenner's first approach was attributed to Louis Pasteur in the XIXth century. His contribution relied on isolating and attenuating the disease-causing microorganism that subsequently offered immune protection after inoculation. Following this initial discovery, his team generated new live-attenuated vaccines against chicken cholera, rabies and anthrax. Despite these great advances, important drawbacks related to microorganism reactivation and anaphylactic reactions were identified in the course of these developments, which raised important concerns about the safety and public confidence of vaccines [1]. From this moment on, vaccinology science started to focus on producing safer vaccines while bearing in mind the importance of preserving the protective efficacy of those live-attenuated vaccines. Many efforts oriented to this aim have been focused on the search for new antigenic markers, adequate adjuvants and the application of new technologies for improving antigen administration [2].

Significant advances in vaccine safety have been associated with the development of new antigenic agents by different strategies, such as i) exhaustive purification of attenuated or deactivated vaccines, ii) improvement of the attenuation techniques by rational genetic mutations to avoid microorganisms reactivation, iii) the search and production of new subunit antigens and iv) the design of antigen-encoding plasmids using the most advanced genetic engineering tools [3]. Although most of the commercialized vaccines are still based on live-attenuated or inactivated microorganisms, several subunit vaccines have been successfully introduced in the clinic, such as the diphtheria and tetanus toxoids, and *Haemophilus influenza* vaccine (Hib). The efforts oriented towards developing recombinant subunit antigens employing innovative recombinant DNA techniques have been particularly relevant. In fact, the launch of the recombinant hepatitis B vaccine in 1986, and more recently human papilloma virus (HPV) vaccine in 2006, meant a new advance towards the introduction of recombinant vaccines in the immunization schedules. A different approach obtained by recombinant DNA techniques is the generation of nucleic acid vaccines. This immunization strategy is based on the design of DNA plasmids with a genetic sequence encoding the protein antigen. Mimicking the natural pathways of the viral infection mechanisms, once internalized in the host cell, the DNA-vaccine would be expressed by the natural intracellular expression mechanisms and the antigen could be processed by antigen presenting cells (APCs) and presented via the major histocompatibility complex molecule (MHC) [4]. Moreover, recent advances associated with genome sequencing, i.e. identifying sequences in the genome of virus, bacteria or parasites that could potentially encode pathogenicity factors or secreted and membrane-associated proteins [5], are expected to greatly contribute to the development of new subunit vaccines.

Although subunit vaccines, such as hepatitis B or human papilloma vaccine, have been successfully introduced clinically, the use of this new type of vaccines has not yet become widespread. The further development of these vaccines has been limited due to their low immunogenic character and potency that make the use of complementary adjuvants necessary. Therefore, as the development of these new vaccines advances, there is an increasing need to produce safe and efficient adjuvants.

Nevertheless, the need for adequate adjuvants to enhance the immunogenicity of subunit antigens is only one of the challenges currently faced in vaccine development. In a global scenario, there exist other limitations that hinder adequate immunization coverage worldwide and remain a challenge which still needs to be addressed, i.e. deficient thermostability and improper administration by injection. Therefore, the identification and knowledge of such drawbacks can guide vaccine development towards the generation of effective, accessible and safe vaccines to global population.

2. The need to improve immunization coverage with existing antigens

The low immunization coverage against some critical diseases for which there already exists an effective vaccine is a critical problem,

(19) OFICINA ESPAÑOLA DE PATENTES Y MARCAS

ESPAÑA

(11) Número de publicación: **2 366 255**

(21) Número de solicitud: 201131074

(51) Int. CI.:

A61K 9/51	(2006.01)
A61K 47/48	(2006.01)
A61K 39/12	(2006.01)
C08B 37/08	(2006.01)
B82Y 5/00	(2011.01)

(12) PATENTE DE INVENCIÓN CON EXAMEN PREVIO B2

(22) Fecha de presentación: **27.06.2011**

(43) Fecha de publicación de la solicitud: **18.10.2011**

Fecha de la concesión: **27.07.2012**

(45) Fecha de anuncio de la concesión: **08.08.2012**

(45) Fecha de publicación del folleto de la patente: **08.08.2012**

(73) Titular/es:
Universidade de Santiago de Compostela
Edificio Emprendia, Campus Vida
15782 Santiago de Compostela, A Coruña, ES

(72) Inventor/es:
ALONSO FERNÁNDEZ, María José;
SÁNCHEZ BARREIRO, Alejandro y
VICENTE OZORES, Sara

(74) Agente/Representante:
Torrente Vilasánchez, Susana

(54) Título: **NANOCOMPOSICIONES SACARÍDICAS PARA LA LIBERACIÓN DE VACUNAS.**

(57) Resumen:
Nanocomposiciones sacarídicas para la liberación de vacunas. La presente invención se refiere a un sistema para la administración de antígenos, que comprende un sistema de nanocápsulas de un tamaño medio inferior a 1 micrómetro, que comprenden a su vez: a) poli-D-glucosamina; b) al menos un aceite adyuvante seleccionado de entre el grupo constituido por isoprenoides, terpenoides y terpenos; c) al menos un tensioactivo, preferiblemente de tipo aniónico o de tipo no iónico; d) al menos un antígeno, preferiblemente de tipo viral; y opcionalmente e) una molécula bioactiva con propiedades inmunoestimulantes o inmunomoduladoras; caracterizadas porque presentan una estructura característica tipo reservorio donde los componentes lipídicos forman un núcleo oleoso que se encuentra recubierto por al menos un polisacárido catiónico. Adicionalmente, la invención se refiere a composiciones farmacéuticas que comprenden dicho sistema de nanocápsulas así como a procedimientos para su preparación y usos del mismo.

Figura 7

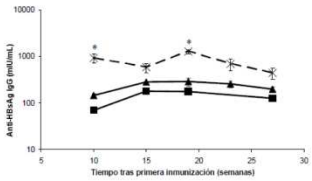

ES 2 366 255 B2

http://goo.gl/7k9J5 (article from http://worldwide.espacenet.com/)